UNCLASSIFIED

AD 420575

DEFENSE DOCUMENTATION CENTER

FOR

SCIENTIFIC AND TECHNICAL INFORMATION

CAMERON STATION, ALEXANDRIA, VIRGINIA
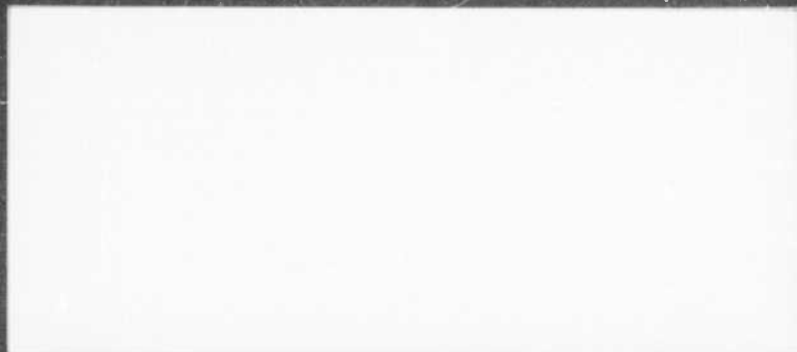
UNCLASSIFIED

SUBIC

Submarine Integrated Control
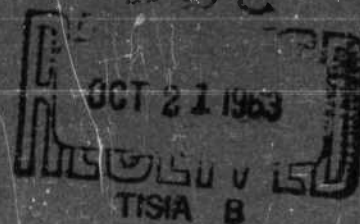
GENERAL DYNAMICS/ELECTRIC BOAT
Research and Development Department
Groton, Connecticut

PROCESSING OF DATA FROM SONAR

SYSTEMS

by

R.A. McDonald
P.M. Schultheiss
F.B. Tuteur
T. Usher, Jr.

Dunham Laboratory
Yale University

Examined: *C.R. DeVoe*

C.R. DeVoe
Head, Information Processing Section

Approved: *A. J. van Woerkom*

Dr. A. J. van Woerkom
Chief Scientist

U417-63-045
September 1, 1963

FOREWORD

The work described in this report was accomplished by members of the
Dunham Laboratory, Yale University under subcontract to the SUBIC
program (contract NOnr 2512(00)) for which the Office of Naval Re-
search is the sponsor and General Dynamics/Electric Boat the prime
contractor. Cdr F. R. Haselton, Jr., USN, is Project Officer for
ONR; Dr. A. J. van Woerkom is Project Coordinator for Electric Boat
and Chief Scientist of the Applied Sciences Department.

The SUBIC program encompasses all aspects of submarine system analysis.
This report is one of a series dealing with acoustic signal processing.

TABLE OF CONTENTS

iii

ABSTRACT

This report describes work concerned with the detection of a single target in an isotropic noise field. In each case studied, the data source was assumed to be a given array of omnidirectional hydrophones, but many different schemes for processing the various hydrophone outputs were considered. The problems investigated involved comparison of optimum detectors with standard detectors and comparison of detectors operating on clipped and unclipped hydrophone data, or, more generally, hydrophone data that have been operated upon by an arbitrary non-linear device. The results of these comparisons are described in detail.

Department of Engineering and Applied Science
Yale University

General Dynamics/Electric Boat Research

PROCESSING OF DATA FROM SONAR SYSTEMS

(Report on Work Performed under Contract 53-00-10-0231
January 21, 1963 to July 1, 1963)

by

R. A. McDonald
P. M. Schultheiss
F. B. Tuteur
T. Usher, Jr.

The following is a summary of work performed under contract 53-00-10-0231 between Yale University and the Electric Boat Company during the period 21 January 1963 to 1 July 1963. Detailed results and supporting arguments for the various conclusions are contained in a series of seven progress reports that are appended.

With minor exceptions the work reported on was all concerned with the detection of a single target in an isotropic noise field. In each case the data source was assumed to be a given array of omnidirectional hydrophones, but many different schemes for processing the various hydrophone outputs were considered. The basic assumptions concerning the properties of noise and target signal fell into one of two general categories:

A. Both signal and noise are independent stationary Gaussian random variables; the signal is directional, the noise isotropic. In this case the statistical properties of signal and noise are completely specified by a statement of total power and spectral properties.

B. Signal and noise have one component satisfying condition A. In addition each may contain one or more periodic components in the low frequency band $0 \leq f \leq W_1$ cps. Furthermore the random component of the signal in the high frequency band $W_1 \leq f \leq W_2$ cps may be modulated in amplitude by one of the periodic low frequency components of the signal.

Assumption A clearly constitutes a minimal description of signal and noise and therefore leads to detection schemes of only moderate efficiency. On the other hand, knowledge of power and spectral properties may be very nearly all that is available; in fact, even this knowledge may be quite imperfect.

1

.The best detection scheme under assumption A therefore sets realistic bounds on attainable detectability in many situations of practical interest.

Assumption B represents an attempt to obtain more refined detection procedures by specifying additional signal properties that do occur in important practical cases. The signal emitted by a moving ship contains periodic or quasi-periodic low frequency components generated by the propeller and other mechanical components. Amplitude modulation of the high frequency range at the propeller frequency is also a commonly observed phenomenon in such situations. Periodic or quasi-periodic noise components are often generated by moving machinery on the observing ship.

The problems investigated may also be divided into two broad classes:

a) Comparison of optimum detectors with standard detectors. The term "optimum detector" is interpreted as a likelihood ratio detector operating on the outputs of an array of hydrophones mechanically or electrically steered "on target." The "standard detector" operates on the output of the same hydrophone array by adding, squaring and then smoothing by means of a low pass filter. A block diagram of a standard detector is shown in Fig. 1 of Progress Report No. 3.

b) Comparison of detectors operating on clipped and unclipped hydrophone data, or, more generally, hydrophone data that have been operated upon by an arbitrary nonlinear device. Where no remarks to the contrary appear, comparisons are always based on rms or mean square signal to noise ratio at the detector output. The input signal to noise ratio at each hydrophone is assumed to be small.

2

Results

1) Comparison of optimum and standard detector under assumption A.

This forms the subject matter of Progress Report No. 3. Using results given by Bryn[1] the figure of merit (rms signal to noise ratio) of the optimum detector for reasonably long observation times can be written in the form

$$\sqrt{\frac{T}{2\pi}} \sqrt{\int_{\omega_1}^{\omega_2} \left[\frac{S(\omega)}{N(\omega)} G(\omega)\right]^2 d\omega}$$

T is the observation time in seconds, ω_1 and ω_2 are the lower and upper endpoints of the processed frequency interval in rad/sec. $S(\omega)$ and $N(\omega)$ are the input signal and noise spectra at each hydrophone. $G(\omega)$ is the array gain, a quantity introduced by Bryn and defined as the ratio of the contributions of signal and noise to the average detector output normalized with respect to the input signal to noise ratio at each hydrophone.

Several features of the above expression are significant. The factor $\sqrt{T}$ indicates the usual dependence of statistical fluctuation on sample size. The fact that the integrand is non-negative shows that the detector should utilize all frequencies where $S(\omega)$ does not vanish identically. In cases of great practical interest $G(\omega)$ varies only slowly and over a moderate total range. Hence the greatest contribution to the integral is made by frequency ranges where the input signal to noise ratio is relatively large. It is clear that changes in signal or noise spectra are important only to the extent that they affect the integral. Thus knowledge of the detailed structure of signal and noise spectra is of limited value

---

[1] F. Bryn, "Optimal Signal Processing by Three-Dimensional Arrays Operating on Gaussian Signals and Noise," J. Acoust. Soc. Am., vol. 34, no. 3, March 1962 pp. 289-297,

in detection. Even the knowledge that the signal contains a very narrow-band component, so that $S(\omega)/N(\omega)$ is large over a narrow band, contributes little to the solution of the detection problem unless the narrow-band component contains a significant fraction of the total signal power (or the noise power level happens to be exceptionally low in the frequency range of the narrow-band signal).

The array gain $G(\omega)$ is larger for the optimum detector than for the standard detector using the same set of hydrophones, particularly at low frequencies. This effect may be attributed qualitatively to the circumstance that the optimum detector tends to reduce the effect of noise correlation between different hydrophones. The phenomenon is clearly most pronounced at low frequencies.[1] Thus the optimum detector is superior to the standard detector in two respects: 1) It can combat noise correlation between hydrophones and 2) it can utilize variations in input signal to noise ratio over the processed frequency band.[2] Significant differences in performance between the two types of detectors will arise only when one or both of these factors are important.

If signal and noise spectra are both flat over a frequency band $0 \le \omega \le \omega_a$ and vanish for $\omega > \omega_a$, and if ω_a is sufficiently large so that the noise correlation between hydrophones is negligible, neither one of the above factors is operative and the performance of optimum and standard detectors is identical. [Report No. 3, Eq. (55)]. If the noise

---

[1] At high frequencies, where there is no noise correlation between hydrophones, the array gain simply equals the number of elements in the array.

[2] The standard detector is sensitive primarily to total power. Spectral properties affect its design only to the extent that they determine what frequency range should be processed.

has the specified properties but the signal deviates from the flat spectrum, the optimum detector is better by an amount depending on the extent of the deviation $\left[\text{Eq. (58)} \right]$.

If signal and noise spectra are not bandlimited, the figure of merit of the optimal detector can have a peculiar property. Consider for example the case (quite closely approximated in situations of practical interest) of signal and noise spectra identical in shape. Since $G(\omega)$ approaches a constant equal to the number of hydrophones as $\omega \to \infty$, the figure of merit clearly approaches infinity as $\omega_2 \to \infty$. This says that detection can be accomplished to an arbitrary degree of certainty in any finite time. The statement becomes reasonable as soon as one recognizes that the assumptions imply equal input signal to noise ratio in every frequency band. Thus the optimum detector can in principle extract as much useful information by observing a 100 cps band at extremely high frequencies, where signal and noise power are both negligible, as by observing a comparable band near zero frequency where both signal and noise power are substantial.

This example illustrates a common danger in the use of optimal procedures: Assumptions that appear at first glance quite innocuous may have exceedingly far-reaching consequences. In important practical problems the signal and noise spectra are in fact closely similar over the frequency range where most of their power is concentrated. At high frequencies, however, the signal spectrum inevitably falls off faster than the noise spectrum, if only because of white noise locally generated in the circuitry, and this effect becomes crucial when one works with optimal techniques.

In order to obtain realistic comparisons one must therefore restrict the optimum detector to the frequency range over which the postulated spectra may be expected to describe the actual state of affairs with reasonable accuracy. Specific calculations were carried out under the assumption that signal and noise spectra both fall off with the second power of frequency above 1500 cps. When the frequency range processed by the optimum detector extends to 5000 cps its figure of merit then has a value 2.6 times that of the standard detector. When the processed frequency range extends to 10,000 cps the corresponding figure is 3.8. (Report No. 3, pages 28-29).

In order to avoid the somewhat arbitrary assignment of an upper frequency limit, a second approach was also taken. By using a model of the transmission characteristics of sea water proposed by Eckart (Report No. 3, p. 29, footnote 2) one can obtain a modification of the high frequency characteristics of the signal spectrum that removes the basic difficulty and leads to a finite result, even when an infinite frequency range is processed. The ratio of performance indices of the optimum and standard detector is now range dependent $\left[\text{Eq. } (94) \right]$ but varies only from a value somewhat less than 2 to about 8 for the variations of range for which the analytical assumptions are likely to be valid. Thus the two lines of analysis lead to quite comparable results, and one comes to the conclusion that improvements of this order of magnitude cannot be exceeded unless signal and noise spectra differ drastically from the assumed form.

The foregoing comments should not be construed to infer that improvements by factors of 2 to 8 are unimportant. If they were realizable by even moderately simple instrumentations, they would be quite significant.

6

However, in interpreting these figures it is necessary to keep in mind two factors: a) The larger improvement figures correspond to conditions such as extremely close range or identical shape of signal and noise spectra over a very wide frequency band, conditions that are either of limited interest or unlikely to be satisfied in practice. b) The optimal instrumentation is likely to be very complicated. In practice, therefore, one is likely to pay a very high price in complexity of instrumentation for only limited gain in performance.

2) Comparison of optimum and standard detector under assumption B.

The effort to exploit the presence in the target signal of low frequency periodic functions and amplitude modulation, by one of these, of the high frequency range has taken two distinct directions.

a) A study was made of the optimum scheme for detecting a Gaussian signal amplitude modulated by a sinusoid in the usual isotropic Gaussian noise background. This is very nearly equivalent to an optimum detector processing only the frequency range $W_1 \leq f \leq W_2$ of assumption B. In practice the frequency W_1 would be sufficiently low so that the power of the random signal component in $0 \leq f \leq W_1$ would be a small fraction of the total signal power. However, the periodic low frequency components of the signal, which could well be important to the detection process, are ignored. The reason for considering a detection process neglecting such important information is that the frequencies of the periodic signal components are not known a priori and that the self noise generated near the receiver is likely to contain very strong periodic components in the same frequency range so that the filtering problem would be very formidable.

7

b) An attempt was made to utilize the low frequency periodic signal components as well as the high frequency amplitude modulation without requiring either knowledge of the frequencies of the periodic components or identification and removal of the periodic self noise. The analyzed system is not optimal, but it has at least some of the features that one would expect to find in an optimal system.

The approach described under a) is covered in detail by Progress Report No. 5. The following specific cases are considered:

i) Noise and unmodulated signal both have the properties of white noise limited to the same band. The receiving array consists of a single hydrophone.

ii) Signal and noise have the same properties as in i). There are K hydrophones spaced sufficiently far apart so that the noise correlation between different hydrophones is negligible.

iii) The noise and array properties are the same as in ii) but the unmodulated signal spectrum falls off with the second power of frequency above a certain point.

iv) The unmodulated signal has the properties of i) but the noise spectrum falls off with the second power of frequency above a certain point. The receiving array consists of a single hydrophone.

In cases i), ii), and iv) the ratio of the figure of merit of the optimum detector to that of an optimum detector operating on the unmodulated signal in the same noise background is approximately $1 + \frac{1}{2} b^2$, $\left[\text{Progress Report No. 5, Eqs. (30), (39) and (54)} \right]$. The symbol b is the

8

modulation index, a number certainly less than unity and in most practical
cases substantially less than unity. Thus only a very limited improvement
in detectability results from use of the knowledge that the signal is
periodically amplitude modulated. In case iii) the improvement ratio is
even smaller $\left[\text{Eq. }(44)\right]$. More complicated cases have not been analyzed,
but there is no reason to expect significantly different conclusions.

The result appears even more decisive if one considers that the
analysis assumed purely sinusoidal modulation of known amplitude, frequency
and phase. In practice the phase and amplitude would certainly be unknown
and the frequency would most likely be known only to lie between certain
limits. The effect of these uncertainties would be a further degradation
in the detectability index. Thus one is forced to the conclusion that the
existence of periodic amplitude modulation of the random target signal is,
by itself at least, of little value in target detection.

The reason for this phenomenon becomes clearer if one considers the
instrumentation required for optimum detection. For case i) it is given
by the simple configuration shown in Fig. 1 of Progress Report No. 5
(p. 11). The circuit evidently consists of a standard power detector
followed by an arrangement for coherent detection of the envelope. Thus
the basic detection scheme is incoherent and the slight gain over a
simple power detector results only from the secondary coherent detection
operation on the envelope. The latter would obviously be degraded by lack
of knowledge of envelope amplitude, phase or frequency.

Progress Report No. 7 deals with the second approach (b) to the
problem of utilizing the added information supplied by assumption B.
It postulates the specific instrumentation shown in Fig. 1 of the report.

9

The outputs of the various array elements are added and the resulting signal is split into the two frequency ranges $0 \leq f \leq W_1$ and $W_1 \leq f \leq W_2$. The high frequency range, with its sinusoidal amplitude modulation, is processed by a standard power detector. The output of this detector contains the modulating signal in addition to fluctuating components. It is used to multiply the signal carried by the low frequency channel, which contains a sinusoidal component at the modulation frequency. Thus the high frequency channel is used to generate a sinusoidal "reference" for the coherent demodulation of the sinusoidal low frequency component of the signal. The attractive feature of this scheme is that the low frequency sinusoid and the "reference" automatically assume the same frequency. It is not necessary to have a priori knowledge about this frequency, and the presence of sinusoidal noise components in the low frequency range presents only a secondary problem, as long as they do not coincide too closely with the signal sinusoid. Only the assumption that low frequency sinusoid and modulation envelope are in phase may be somewhat artificial. The weakness of the proposed scheme is the low amplitude of the reference sinusoid, particularly when the modulation index is small, and the presence in the "reference" channel of large non-sinusoidal fluctuations, all of which are "noise" to the proposed instrumentation. Detailed analysis shows that this defect outweighs the advantages of more complete utilization of assumption B. Under typical operating conditions the performance index of the proposed instrumentation is substantially lower than that of a simple power detector operating on the high frequency band alone $\left[\text{Eq. } (24) \right]$. One must, of course, keep in mind that the proposed detector is not optimal. One could, for instance, use it to supplement a

10

simple power detector and thus presumably obtain a performance somewhat better than that of the power (standard) detector. However, the results of the report raise some doubts whether, even with optimal procedures, detectability under assumptions B is significantly greater than under assumptions A. For the present this question must still be regarded as unresolved.

The conclusions from 1) and 2) concerning possible improvements over the standard detection scheme (Fig. 1 of Progress Report No. 3) may be summarized as follows:

a) If signal and noise are characterized only by total power and spectral properties and the spectral properties do not differ drastically, the performance index of the standard detector is not greatly inferior to that of the optimum detector. One must also keep in mind that the instrumentation required to realize the optimum detector is apt to be complicated. Unless simple modifications of the standard detector can be found that make it optimal, the attainable improvement would not appear to justify the increased complexity of equipment in most practical cases.

b) Knowledge that the random signal is periodically amplitude modulated is of little value in detection.

c) It appears that large improvements in performance relative to the standard detector can be made only under one of the following two conditions:

  i) An effective scheme, different from the one discussed in Progress Report No. 7, can be found for detecting low

11

frequency periodic signal components in the presence of strong periodic components of self noise. This requires continuous monitoring and careful processing of self noise data.

ii) It is possible to give a more detailed characterization of the signal than is implied by assumptions A or B. In particular it would be valuable to have a description of the typical waveshape of the signal, with as few random parameters as possible. This would open the way to use of genuine coherent detection schemes.

3) Effect of clipping and other nonlinear operations on target detectability. Assumptions A. Same noise power at each hydrophone.

The procedure of clipping the basic hydrophone data before further processing has certain practical advantages, particularly when digital data handling techniques are used. Theoretical studies were therefore undertaken to determine the effect of data clipping on target detectability and to see whether nonlinear operations more general than clipping might lead to more advantageous results. The problem was approached by two rather different routes.

a) Progress Report No. 4 considers the standard (power) detector as the basic instrumentation but allows an arbitrary, odd function, zero memory nonlinear device to be inserted at the output of each hydrophone. (See Fig. 1 of Progress Report No. 4. Note that the linear processor and the clipper are special examples of such a device.) The analysis is carried out under the assumption that signal and noise spectra are identical in shape and that noise correlation between different hydrophones is negligible. The

12

result is stated in terms of the usual output signal to noise ratio[1]
and also in terms of a second figure of merit, defined as the
difference between on target and off target average output divided
by off target average output. In each case $\left[\text{Eqs. (58) and (40)} \right]$
it is demonstrated that the best performance is achieved with a
linear processor. However, the dependence of the figure of merit,
particularly the output signal to noise ratio, on the specific
nature of the processor is not at all critical if the processor
does not contain dead band. The signal to noise ratio for the
clipped instrumentation falls below the optimum by a factor of
only 0.89. (Fig. 3).

Progress Report No. 4 also considers modifications in the
basic detector characteristic. The processors are now taken to
be linear but the conventional square law device is replaced by a
general even power device. It is shown that maximum output signal
to noise ratio[1] occurs when the detector is a square law device,
but once again the index of performance varies only slowly with
modifications in the detector characteristic. The second figure
of merit, the normalized difference of on and off target average
output, can exhibit a very different behavior. If the detector
has a dead band, for instance, the performance index grows
monotonically with the size of the dead band and approaches
infinity in the limit $\left[\text{Eq. (112)} \right]$. The reason for this peculiar

---

[1]Note a slight difference in definitions between Progress Report No. 4
and the reports discussed earlier: In Report No. 4 the average signal
component at the output is defined as the difference between average output
on and off target. In the reports mentioned earlier it is the increase in
average output which occurs when a signal appears that was previously absent,
the array being steered "on target" at all times.

13

phenomenon is, of course, that the off target average output tends to zero more rapidly than the on target average output. This observation is not entirely of academic interest, for substantial reductions in off target average output can be achieved for values of dead band that cause only minor degradation in output signal to noise ratio (Figures 8 and 9). Thus the "off target plateau" of the directivity pattern can be reduced materially without significant sacrifice of output signal to noise ratio.

b) The second approach to the problem of nonlinear data processing was an attempt to assess the inherent "cost of clipping" by comparing the output signal to noise ratio of optimum detectors operating on clipped and unclipped data.[1] This analysis is contained in Progress Report No. 6. Results were obtained only under the following special assumptions: Signal and noise both have the properties of Gaussian white noise band-limited to $0 \leq f \leq W$ cps. The hydrophone outputs are sampled at regular intervals of $\frac{1}{2W}$ seconds and there is no correlation between noise outputs of different hydrophones. Under these conditions the rms output signal to noise ratio of the detector operating on clipped samples is $\frac{2}{\pi}\sqrt{1 - \frac{1}{M^2}}$ times as large as that of the detector operating on unclipped samples, where M is the number of hydrophones in the array. It is probably realistic to consider this as the actual cost (in terms of detectability) of clipping sampled data. One must keep in mind, however, that part of the information loss

---

[1] When the detection scheme is optimal it is only necessary to consider information destroying nonlinear operation (such as clipping) on the basic data. A one to one nonlinearity could always be removed by an inverse operation in the optimal detector.

14

might be due to sampling rather than to clipping. For while the assumed sampling rate is sufficient to avoid information loss from sampling in the unclipped case, the spectrum of the clipped signal is not bandlimited, so that no finite sampling rate can guarantee complete reconstructability of the continuous signal from the samples. It is interesting to observe that evaluation of Eq. (58) of Progress Report No. 4 for the white noise spectra postulated in Progress Report No. 6 leads to a value very close to $\frac{2}{\pi}$ for the degradation in output signal to noise ratio. This at least suggests - although it certainly does not prove - that the figure $\frac{2}{\pi}$ is indeed a good estimate of the "cost of clipping" for reasonably large arrays. It further suggests that the optimum detector for processing clipped data derived from spectra with the white noise properties assumed in Report No. 6 does not differ greatly from the standard (power) detector.

4) Effect of clipping on target detectability. Assumptions A. Noise power may vary from hydrophone to hydrophone.

One of the primary reasons for clipping hydrophone data prior to further processing is the possibility that the noise power may vary sharply from hydrophone to hydrophone. Due to malfunction or special operating conditions one hydrophone, or a group of hydrophones, may contribute far more noise than the rest. When this is a serious possibility, it appears reasonable to clip all hydrophone outputs, incur the small loss of information discussed in 3), but prevent a large contribution to the output noise from a few faulty hydrophones. This type of consideration is in fact one of the primary reasons for the use of clipping in practical instrumentations.

15

The theoretical background of this problem is explored in Progress Report No. 2. The basic instrumentation investigated was that of the standard detector with and without clippers. $\left[\text{Fig. 1} \right]$ The analysis assumed signal and noise spectra of identical shape and the absence of noise correlation between different hydrophone outputs.

Output signal to noise ratios for the clipped and unclipped instrumentations were compared under several sets of assumptions concerning noise power at different hydrophones.

a) The probability density of noise power N_i for the ith hydrophone is uniform on a logarithmic scale over $N_L \leq N_i \leq N_H$ and vanishes elsewhere. $\left[\text{Eq. (14)} \right]$

b) The probability density of N_i is uniform on a linear scale over $N_L \leq N_i \leq N_H$ and vanishes elsewhere. $\left[\text{Eq. (26)} \right]$

c) The probability density of N_i varies as $\frac{1}{N_i^2}$ over $N_L \leq N_i \leq N_H$ and vanishes elsewhere. $\left[\text{Eq. (29)} \right]$

d) The noise power at each hydrophone can assume only the values N_L and N_H and does so with probabilities p and $(1 - p)$ respectively. $\left[\text{Eq. (15)} \right]$

In each instance the noise powers at different hydrophones were assumed to be statistically independent.

Comparisons were made primarily on the basis of a figure of merit defined as the difference between on target and off target average output divided by off target average output (as in Report No. 4). The output signal to noise ratio was also considered and found to have identical properties except for a multiplying constant.

16

The results show the expected trend in each case. When there is little or no variation in noise power, the unclipped instrumentation is superior by a small margin. When large variations in noise power can occur, the clipped instrumentation becomes superior. The exact extent of this superiority depends rather critically on the probability distribution of the noise. In cases b) and c) the ratio of clipped to unclipped performance indices is close to unity for physically reasonable values of N_L and N_H. In case a) and particularly in case d) (when approximately half of the hydrophones are in the high noise state) very substantial improvements in performance are made possible by clipping.

The results of sections 3) and 4) may be summarized as follows:

a) The clipping of hydrophone data never causes a large decrease in signal detectability. It may result in substantial improvement if large variations in noise power from hydrophone to hydrophone are likely.

b) Signal detectability is not at all critically dependent on the specific properties of nonlinear processors operating on the basic hydrophone data unless the processors have a significant amount of dead band. Neither is the precise nature of the nonlinearity used in detection critically important. Since some properties of the bearing response pattern are more critically dependent on these parameters, it appears possible to improve the bearing response pattern without seriously affecting detectability.

17

Progress Report No. 1 has not been mentioned in this discussion. It deals with the correlation between noise output at different hydrophones and provides computational results in this area that serve as background for several of the other reports. In particular it shows under what conditions one can make the very convenient assumption that the noise correlation between different hydrophone outputs is negligible.

General Dynamics/Electric Boat Research
(53-00-10-0231)

Progress Report No. 1

by

Theron Usher, Jr.

and

Peter M. Schultheiss

Dunham Laboratory
Yale University
New Haven, Connecticut
February, 1963

Department of Engineering and Applied Science
Yale University

General Dynamics/Electric Boat Research
(53-00-10-0231)

SPACE-TIME CORRELATION IN ISOTROPIC NOISE FIELDS

by

Theron Usher, Jr.

and

Peter M. Schultheiss

February, 1963

SPACE-TIME CORRELATION IN ISOTROPIC NOISE FIELDS

I. Introduction

Several investigations have been made in order to determine the cross-correlation between signals produced by two omnidirectional transducers located in a field of many scattered noise sources.[1,2,3] Knowledge of the noise cross-correlation is often necessary in determining the performance capabilities of arrays of such transducers which are used to determine the direction of a signal source located in the field of the scattered noise sources.

In this report, an attempt is made to expand and simplify the interpretation of the results given in the references listed. Three-dimensional and two-dimensional isotropic noise fields will be considered. The field is considered isotropic in that the power received from any direction is constant.

An infinite number of noise sources distributed uniformly on the surface of a sphere of infinite radius from the local transducers is used to simulate the three-dimensional isotropic field.

For the two-dimensional field, an infinite number of noise sources are distributed uniformly along a circle of infinite radius in the plane of signal propagation.

In addition, the noise produced by each source is assumed to be stationary and statistically independent of that produced by every other source, and each noise source is described by the same autocorrelation function.

II.   Cross-Correlation with Time Delay

Figure 1 describes the geometry for the spherical noise field.

Fig. 1

Geometry of Spherical
Noise Field
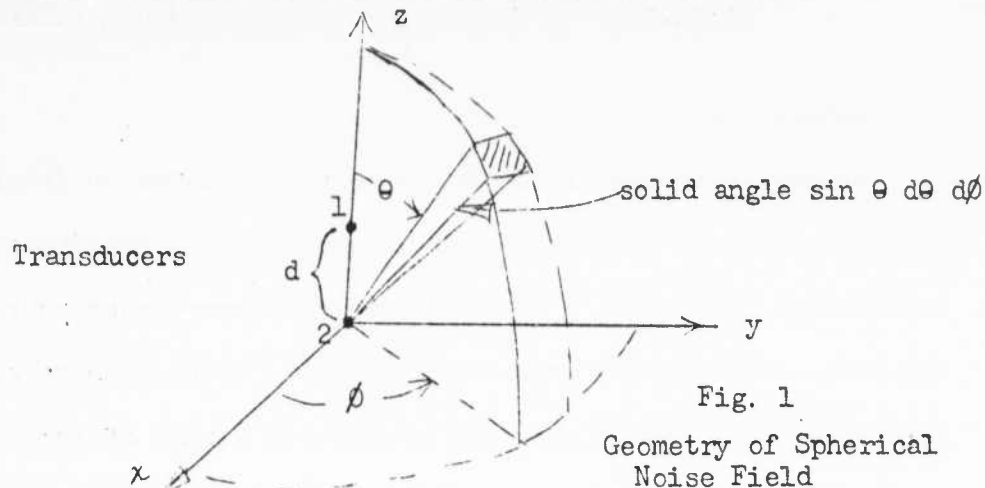
It has been shown[1] that the normalized cross-correlation function for the delayed output of transducer 1 with the output of transducer 2 is given by Equation (1).

$$\rho(\frac{d}{c}, \tau) \; = \; \frac{\langle v_1(t - \tau)\, v_2(t)\rangle}{\langle v_1{}^2(t)\rangle} \; = \; \int_0^{2\pi} d\phi \int_0^{\pi} \rho'(\tau + \frac{d}{c}\cos\Theta)\, \frac{1}{4\pi}\, \sin\Theta\, d\Theta$$

$$= \int_0^{\pi} \rho'(\tau + \frac{d}{c}\cos\Theta)\, \frac{\sin\Theta}{2}\, d\Theta \tag{1}$$

In Equation (1), $\frac{d}{c}$ is the time required for the signal to travel the distance between the two transducers, and $\rho'(\tau)$ is the normalized autocorrelation function for each noise source. A change of variables

$$\tau' = \tau + \tau_s \cos\Theta \qquad \frac{d}{c} = \tau_s \tag{2}$$

results in Equation (3)

A1-2

$$\rho(\tau_s, \tau) = \frac{1}{2\tau_s} \int_{-\tau_s + \tau}^{\tau_s + \tau} \rho'(\tau') \, d\tau' \tag{3}$$

Equation (3) simply represents the average value of $\rho'(\tau')$ over an interval $2\tau_s$ in length, centered at $\tau' = \tau$. Figure 2 depicts this interpretation graphically.
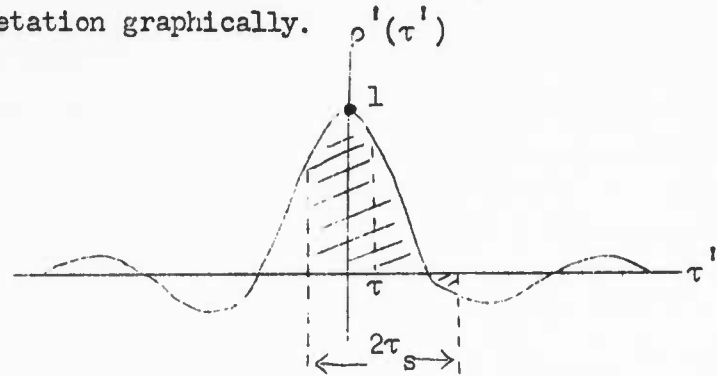
Fig. 2
Graphical Interpretation of $\rho(\tau_s, \tau)$

For the circular noise field, the cross-correlation function has been shown to be[1]

$$\rho(\tau_s, \tau) = \int_0^{\pi} \rho'(\tau + \tau_s \cos \Theta) \frac{1}{\pi} \, d\Theta \tag{4}$$

With the variable transformation in Equation (2), Equation (4) becomes

$$\rho(\tau_s, \tau) = \frac{1}{2\tau_s} \int_{-\tau_s + \tau}^{\tau_s + \tau} \frac{2}{\pi} \frac{\rho'(\tau')}{\left[1 - \left| \frac{\tau' - \tau}{\tau_s} \right|^2 \right]^{1/2}} \, d\tau' \tag{5}$$

Equation (5) represents a weighted average of $\rho'(\tau)$ over an interval $2\tau_s$ centered at $\tau' = \tau$. The weighting function is shown in Figure 3. It can be seen that the values of $\rho'(\tau')$ at the ends of the interval are weighted very heavily.

$$f(\tau') = \frac{2}{\pi}\left[1 - \left(\frac{\tau' - \tau}{\tau_s}\right)^2 \right]^{-\frac{1}{2}}$$

Fig. 3
Weighting Function for $\rho'(\tau')$
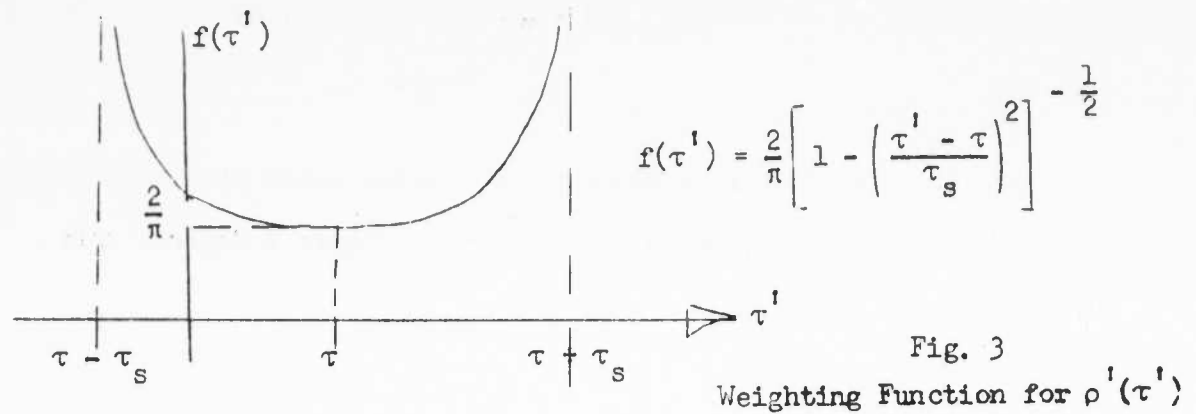
Note also that the average value of the weighting function expressed in Equation (6) is unity.

$$\frac{1}{2\tau_s} \int_{-\tau_s + \tau}^{\tau_s + \tau} \frac{2}{\pi}\left[1 - \left(\frac{\tau' - \tau}{\tau_s}\right)^2 \right]^{-1/2} d\tau' = 1 \qquad (6)$$

A comparison of the results in Equations (3) and (5) reveals that the evaluation of the cross-correlation function for the three-dimensional noise field is considerably simpler than that for the two-dimensional case   For each pair of transducers in an electronically steered array, the observation is also made that the maximum relative electrical delay necessary to steer the directional response of the array is never greater than the wave propagation time between the pair of transducers in question. In terms of the symbols used previously, the following is always true for the determination of bearing response patterns.

$$\tau \leq \tau_s \qquad (7)$$

An examination of Figures 2 and 3 indicates that the cross-correlation function for a two-dimensional field is less than that for a three-dimensional field for values of τ near zero. Identical well-damped auto-correlation functions are assumed in both cases. In the two-dimensional case, the small values of $\rho'(\tau')$ near $\tau' = \pm \tau_s$ are weighted more heavily than the same values in the three-dimensional case. However, for values of τ near τ_s, $\rho(\tau_s, \tau)$ for the two-dimensional field should be greater than that for the three-dimensional field since the large value of $\rho'(\tau')$ near $\tau' = 0$ receives infinite weighting in the former case.

Evaluation of $\rho(\tau_s, \tau)$ for two simple forms of $\rho'(\tau')$ follows.

III. Evaluation of Cross-Correlation Function - Case A

The function $\rho(\tau_s, \tau)$ is first evaluated for the simple exponential autocorrelation function given in Equation (8)

$$\rho'(\tau') = \varepsilon^{-\omega_0|\tau'|} \tag{8}$$

The corresponding spectral density is

$$S(\omega) = \frac{2}{\pi\omega_0} \frac{1}{1 + \left(\frac{\omega}{\omega_0}\right)^2} \tag{9}$$

The integral for $\rho(\tau_s, \tau)$ must be performed in two parts because of the term $|\tau'|$ appearing in the expression for $\rho'(\tau')$. For the three-dimensional noise field:

$$\rho(\tau_s, \tau) = \frac{1}{2\tau_s}\left[\int_{-\tau_s+\tau}^{0} \varepsilon^{\omega_0\tau'} d\tau' + \int_{0}^{\tau_s+\tau} \varepsilon^{-\omega_0\tau'} d\tau'\right]$$

$$= \frac{1 - \varepsilon^{-\omega_0\tau_s} \cosh \omega_0\tau}{\omega_0\tau_s} \qquad \tau < \tau_s \tag{10}$$

If $\tau = \tau_s$, the maximum electrical delay necessary, Equation (10) reduces to

$$\rho(\tau_s, \tau_s) = \frac{1 - \varepsilon^{-2\omega_o \tau_s}}{2\omega_o \tau_s} \tag{11}$$

Furthermore, if $\omega\tau_s \gg 1$ and $\tau = 0$,

$$\rho(\tau_s, 0) \cong \frac{1}{\omega_o \tau_s} \tag{12}$$

Equation (12) also places an upper bound on $\rho(\tau_s, \tau)$ for any τ and τ_s.

If the separation is defined in terms of wavelengths of the half-power frequency of the individual noise spectra, the relation with the parameter $\omega_o \tau_s$ is

$$\frac{d}{\lambda_o} = d \frac{f_o}{c} = \frac{d}{c} \cdot \frac{\omega_o}{2\pi} = \frac{\omega_o \tau_s}{2\pi} \tag{13}$$

The upper bound for $\rho(\tau_s, \tau)$ is

$$\rho(\tau_s, \tau) \leq \frac{1}{2\pi \left(\substack{\text{transducer separation in wavelengths} \\ \text{of upper half power frequency}}\right)} \tag{14}$$

For the two-dimensional noise field, Equation (4) may be used with several approximations to evaluate $\rho(\tau_s, \tau)$. Equation (15) is obtained after appropriate substitutions are made.

$$\rho(\tau_s, \tau) = \frac{1}{\pi} \int_0^\pi \varepsilon^{-\omega_o |\tau + \tau_s \cos \theta|} d\theta$$

$$= \frac{1}{\pi} \left[\int_0^{\theta_o} \varepsilon^{-\omega_o(\tau + \tau_s \cos \theta)} d\theta + \int_{\theta_o}^\pi \varepsilon^{\omega_o(\tau + \tau_s \cos \theta)} d\theta \right] \tag{15}$$

where
$$\Theta_o = \cos^{-1}\left(-\frac{\tau}{\tau_s}\right) \qquad (16)$$

If $\omega_o\tau_s$ is large, the integrand has negligible value except in the vicinity of $\Theta = \Theta_o$. The exponent of the integrand may be approximated by the first three terms in the Taylor series expansion around $\Theta = \Theta_o$:

$$\omega_o(\tau + \tau_s \cos\Theta) \cong 0 - \omega_o\tau_s \sin\Theta_o(\Theta - \Theta_o) - \omega_o\tau_s \cos\Theta_o \frac{(\Theta - \Theta_o)^2}{2}$$

$$\cong 0 - \omega_o\sqrt{\tau_s^2 - \tau^2}\;(\Theta - \Theta_o) + \omega_o\tau \frac{(\Theta - \Theta_o)^2}{2} \qquad (17)$$

If $a = \omega_o\sqrt{\tau_s^2 - \tau^2}$ and $b = \omega_o\tau$, then Equation (15) becomes

$$\rho(\tau_s, \tau) \cong \frac{1}{\pi}\left[\int_0^{\Theta_o} \varepsilon^{\,a(\Theta-\Theta_o) - \frac{b}{2}(\Theta-\Theta_o)^2}\,d\Theta + \int_{\Theta_o}^{\pi} \varepsilon^{\,-a(\Theta-\Theta_o) + \frac{b}{2}(\Theta-\Theta)^2}\,d\Theta\right] \qquad (18)$$

Before Equation (18) is evaluated for the general case, $0 < \tau < \tau_s$, several special cases will be evaluated. For $\tau = 0$, $b = 0$, $a = \omega_o\tau_s$, and $\Theta_o = \frac{\pi}{2}$. Then Equation (18) becomes

$$\rho(\tau_s, 0) \cong \frac{2}{\pi}\int_0^{\frac{\pi}{2}} \varepsilon^{\,\omega_o\tau_s(\Theta - \frac{\pi}{2})}\,d\Theta \cong \frac{2/\pi}{\omega_o\tau_s} \qquad (19)$$

For $\tau = \tau_s$, $a = 0$, $b = \omega_o\tau_s$, and $\Theta_o = \pi$. The second integral in Equation (18) disappears, and the result is

$$\rho(\tau_s, \tau_s) \cong \frac{1}{\pi}\int_0^{\pi} \varepsilon^{\,-\frac{1}{2}\omega_o\tau_s(\Theta - \pi)^2}\,d\Theta \cong \frac{1}{\sqrt{2\pi\,\omega_o\tau_s}} \qquad (20)$$

A1-7

The results in Equations (19) and (20) are valid only if $\omega_o \tau_s >> 1$.

For values of τ near zero, such that the quadratic portion of the exponent may be neglected, the result in Equation (21) applies.

$$\rho(\tau_s, \tau) \cong \frac{1}{\pi}\left[\int_0^{\Theta_o} \varepsilon^{\omega_o\sqrt{\tau_s^2 - \tau^2}\,(\Theta - \Theta_o)}\, d\Theta + \int_{\Theta_o}^{\pi} \varepsilon^{-\omega_o\sqrt{\tau_s^2 - \tau^2}\,(\Theta - \Theta_o)}\, d\Theta\right]$$

$$\cong \frac{2/\pi}{\omega_o\sqrt{\tau_s^2 - \tau^2}} \tag{21}$$

Finally, the integrals in Equation (18) are evaluated by completing the squares in the exponents, and by letting $\Theta' = \Theta - \Theta_o$, and $\Theta'' = \Theta_o - \Theta$.

$$\rho(\tau_s, \tau) \cong \frac{1}{\pi}\left[\varepsilon^{\frac{a^2}{2b}}\int_0^{\Theta_o} \varepsilon^{-\frac{(\sqrt{b}\Theta' - a/\sqrt{b})^2}{2}}\, d\Theta' + \varepsilon^{\frac{a^2}{2b}}\int_0^{\pi-\Theta_o} \varepsilon^{-\frac{(\sqrt{b}\Theta'' - a/\sqrt{b})^2}{2}}\, d\Theta''\right]$$

$$\tag{22}$$

Additional variable substitutions found in Equations (23) and (24) and the definition of tabulated functions[4,5] in Equations (25) and (26) allow the final result to be written in Equation (27).

$$x = \frac{\sqrt{b}\Theta' + \frac{a}{\sqrt{b}}}{\sqrt{2}} \tag{23}$$

$$y = \frac{\sqrt{b}\Theta'' - \frac{a}{\sqrt{b}}}{\sqrt{2}} \tag{24}$$

$$\text{erf}(\alpha) = \frac{2}{\sqrt{\pi}}\int_0^{\alpha} \varepsilon^{-t^2}\, dt \tag{25}$$

$$F(\beta) = \int_0^\beta \varepsilon^{t^2}\, dt \tag{26}$$

Then

$$\rho(\tau_s, \tau) = \frac{1}{\pi}\left\{ \varepsilon^{\frac{a^2}{2b}}\sqrt{\frac{\pi}{2b}}\left[\operatorname{erf}\left(\sqrt{\frac{b}{2}}\,\theta_o + \frac{a}{\sqrt{2b}}\right) - \operatorname{erf}\left(\frac{a}{\sqrt{2b}}\right)\right]\right.$$
$$\left. + \varepsilon^{-\frac{a^2}{2b}}\sqrt{\frac{2}{b}}\left[F\left(\frac{a}{\sqrt{2b}}\right) - F\left(\frac{a}{\sqrt{2b}} - \sqrt{\frac{b}{2}}(\pi - \theta_o)\right)\right]\right\} \tag{27}$$

The result in Equation (10) for the three-dimensional noise field is plotted in Figure 4 for two values of $\omega_c\tau_s$ as a function of τ/τ_s and compared to similar results in Equations (19), (20), (21), and (27) for the two-dimensional field. Previous quantitative conclusions concerning the relative size of $\rho(\tau_s, \tau)$ for the two types of noise fields are seen to be substantiated in Figure 4.

IV. Evaluation of Cross-Correlation Function – Case B

The normalized auto correlation function found in Equation (28) is considered next.

$$\rho'(\tau') = \frac{1}{2}\left[\left(1 - \frac{\zeta}{\sqrt{\zeta^2 - 1}}\right)\varepsilon^{(-\zeta + \sqrt{\zeta^2 - 1})\omega_o|\tau'|} + \right.$$
$$\left. \left(1 + \frac{\zeta}{\sqrt{\zeta^2 - 1}}\right)\varepsilon^{(-\zeta - \sqrt{\zeta^2 - 1})\omega_o|\tau'|}\right] \tag{28}$$

If $\zeta < 1$, Equation (28) may be put into the form

$$\rho'(\tau') = \frac{1}{\sqrt{1 - \zeta^2}}\,\varepsilon^{-\zeta\omega_o|\tau'|}\cos\left(\sqrt{1 - \zeta^2}\,\omega_o|\tau'| + \cos^{-1}\sqrt{1 - \zeta^2}\right) \tag{29}$$

The corresponding spectral density for $\rho'(\tau')$ is the simple narrow band spectrum which follows.

A1-9

FIG 4.

$\rho(\tau_s, \tau)$ vs. τ/τ_s FOR TWO VALUES OF $\omega_0 \tau_s$

THREE DIM.

TWO DIM.

$\rho(\tau_s, \tau)$

$\omega_0 \tau_s = 3$

$\omega_0 \tau_s = 3$

$\omega_0 \tau_s = 10$

$\omega_0 \tau_s = 10$

$\dfrac{\tau}{\tau_s}$

A1-10

$$S(\omega) = \frac{1}{\pi \zeta \omega_o} \frac{4\zeta^2 \left|\frac{\omega}{\omega_o}\right|^2}{\left[1 - \left|\frac{\omega}{\omega_o}\right|^2\right]^2 + 4\zeta^2 \left|\frac{\omega}{\omega_o}\right|^2} \tag{30}$$
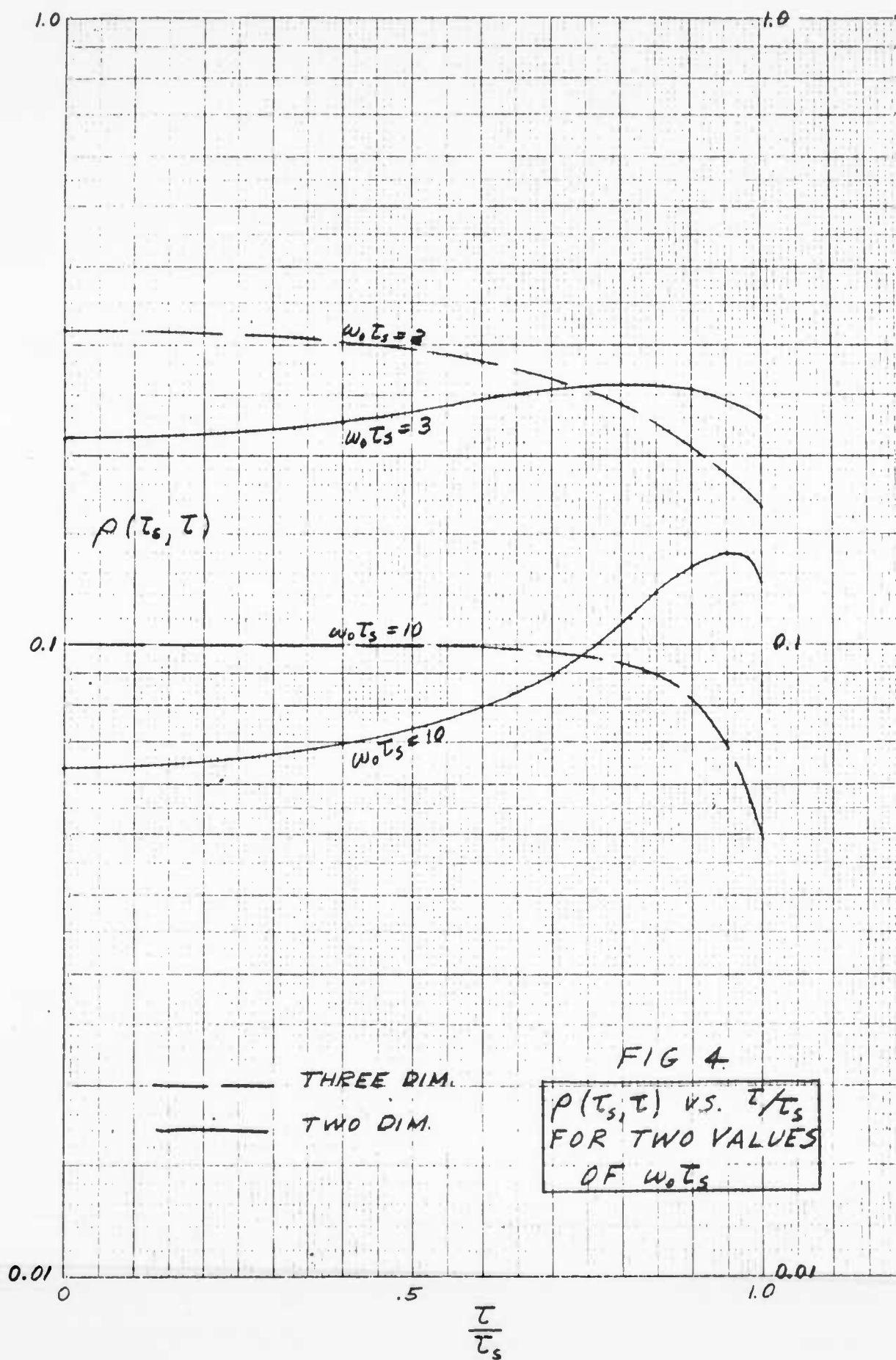
In Equation (30), ω_o is the center frequency, and $2\zeta\omega_o$ is the bandwidth between half power points.

In order to find $\rho(\tau_s, \tau)$ for the three-dimensional field, Equation (28) is substituted into Equation (3). One step in the integration process yields

$$\rho(\tau_s, \tau) = \frac{1}{4\sqrt{\zeta^2 - 1} \, \omega_o \tau_s} \left\{ \left[-\varepsilon^{(\zeta - \sqrt{\zeta^2 - 1}) \omega_o \tau'} + \varepsilon^{(\zeta + \sqrt{\zeta^2 - 1}) \omega_o \tau'} \right]_{-\tau_s + \tau}^{0} \right.$$

$$\left. + \left[\varepsilon^{(-\zeta + \sqrt{\zeta^2 - 1}) \omega_o \tau'} - \varepsilon^{(-\zeta - \sqrt{\zeta^2 - 1}) \omega_o \tau'} \right]_{0}^{\tau_s + \tau} \right\} \tag{31}$$

Evaluation at the limits indicated in Equation (31) and simplification of terms results in Equation (32).

$$\rho(\tau_s, \tau) = \frac{\varepsilon^{-\zeta\omega_o\tau_s}}{\sqrt{1 - \zeta^2} \, \omega_o \tau_s} \left[\sin(\sqrt{1 - \zeta^2} \, \omega_o \tau_s) \cos(\sqrt{1 - \zeta^2} \omega_o \tau) \cosh(\zeta\omega_o\tau) \right.$$

$$\left. \cdot \cos(\sqrt{1 - \zeta^2} \, \omega_o \tau_s) \sin(\sqrt{1 - \zeta^2} \, \omega_o \tau) \sinh(\zeta\omega_o\tau) \right] \tag{32}$$

Combination of the terms inside the brackets of Equation (32) yields Equation (33):

$$\rho(\tau_s, \tau) = \frac{\epsilon^{-\int \omega_o \tau_s}}{\sqrt{1 - \zeta^2}\, \omega_o \tau_s} \left(\cosh^2 \zeta \omega_o \tau - \sin^2 \sqrt{1 - \zeta^2}\, \omega_o \tau\right)^{1/2}$$

$$\times \sin\left[\sqrt{1 - \zeta^2}\, \omega_o \tau_s - \tan^{-1}(\tan \sqrt{1 - \zeta^2}\, \omega_o \tau \tanh \zeta \omega_o \tau)\right] \tag{33}$$

Special cases for $\tau = 0$, and $\tau = \tau_s$ are found in Equations (34) and (35) respectively.

$$\rho(\tau_s, 0) = \epsilon^{-\int \omega_o \tau_s} \frac{\sin \sqrt{1 - \zeta^2}\, \omega_o \tau_s}{\sqrt{1 - \zeta^2}\, \omega_o \tau_s} \tag{34}$$

$$\rho(\tau_s, \tau_s) = \epsilon^{-2 \int \omega_o \tau_s} \frac{\sin 2\sqrt{1 - \zeta^2}\, \omega_o \tau_s}{2\sqrt{1 - \zeta^2}\, \omega_o \tau_s} \tag{35}$$

Interesting behavior of $\rho(\tau_s, \tau)$ is also apparent, if ζ is small, for values of τ_s in Equation (36)

$$\tau_s = \tau + \frac{n\pi}{2\omega_o \alpha} \qquad\qquad n = 0,1,2,3,\dots \tag{36}$$

$$\alpha = \sqrt{1 - \zeta^2} \simeq 1$$

With the substitution of the relation in Equation (36), Equation (33) becomes

$$\rho\left(\tau + \frac{n\pi}{2\alpha\omega_o}, \tau\right) = \frac{\epsilon^{-\zeta \omega_o \tau}\, \epsilon^{-\frac{n\pi \zeta}{2\alpha}}}{\alpha\omega_o \tau + \frac{n\pi}{2}} \left(\cosh^2 \zeta \omega_o \tau - \sin^2 \alpha\omega_o \tau\right)^{1/2}$$

$$\times \sin\left[\alpha\omega_o \tau + \frac{n\pi}{2} - \tan^{-1}(\tan \alpha\omega_o \tau \tanh \zeta \omega_o \tau)\right] \tag{37}$$

Examination of the arctan function in Equation (37) reveals that

$$\tan^{-1}(\tan \alpha\omega_o \tau \tanh \zeta \omega_o \tau) \begin{cases} = \alpha\omega_o \tau & \text{when } \alpha\omega_o \tau = \frac{n\pi}{2} \\[2mm] \cong \alpha\omega_o \tau & \text{when } \zeta \omega_o \tau > 1 \end{cases} \tag{38}$$

A1-12

Thus

$$\rho\left(\tau + \frac{n\pi}{2\alpha\omega_0}, \tau\right) \approx \frac{\varepsilon^{-\omega_0\tau} \, \varepsilon^{-\frac{n\pi\varphi}{2\alpha}}}{\alpha\omega_0\tau + \frac{n\pi}{2}} \left(\cosh^2 \varphi \, \omega_0\tau - \sin^2 \alpha\omega_0\tau\right)^{1/2} \sin\frac{n\pi}{2}$$

$$(39)$$

Sufficient computation with Equation (32) or (33) would result in a contour map of $\rho(\tau_s, \tau)$, similar to that in Reference 2. However, Equation (39) gives some important details about such a map, without resorting to detailed computation procedures. The loci described by Equation (36) are plotted in Figure 5. The axes are appropriately normalized.
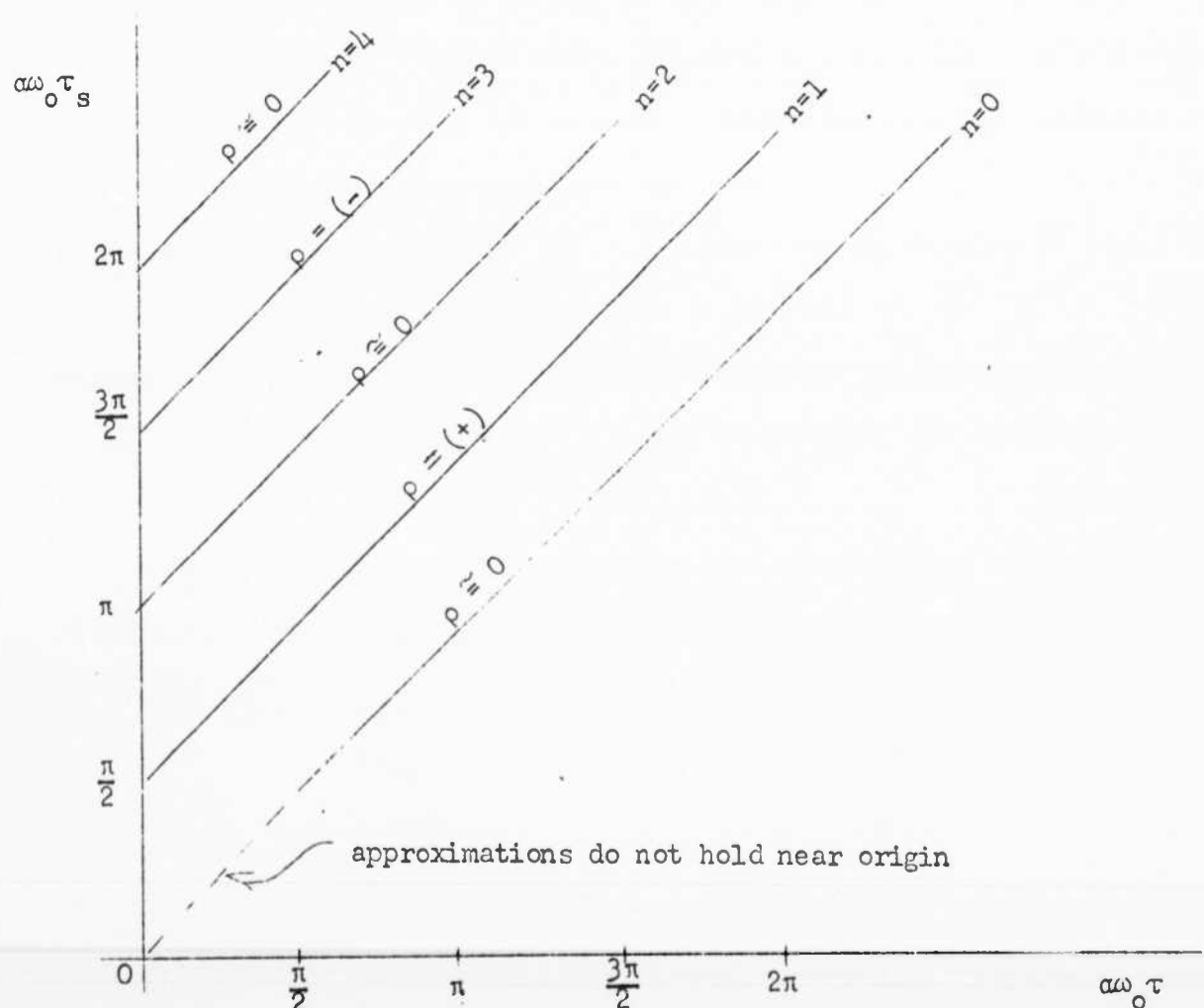

Fig. 5

The lines in Figure 5 for which n is even give approximate loci for which $\rho(\tau_s, \tau)$ is zero. The lines for which n = 1, 5, 9, etc. are the approximate loci for the ridges of the contour plot in regions where $\rho(\tau_s, \tau)$ is positive. Similarly, the lines for which n = 3, 7, 11, etc., describe the approximate loci for the ridges for negative values of $\rho(\tau_s, \tau)$. The relations are exact where $\alpha \omega_0 \tau = \frac{n\pi}{2}$.

Finally, from Equation (33) it can be seen that the upper bound on the magnitude of $\rho(\tau_s, \tau)$ for all values of τ_s and τ is

$$|\rho(\tau_s, \tau)| \leq \frac{\varepsilon^{-\zeta \omega_0 \tau_s}}{\sqrt{1 - \zeta^2}\, \omega_0 \tau_s} \; \cosh \zeta \omega_0 \tau < \frac{1}{\sqrt{1 - \zeta^2}\, \omega_0 \tau_s} \qquad \tau < \tau_s \tag{40}$$

For the two-dimensional noise field, substitution of Equation (28) into Equation (4) yields an integral which does not yield to the approximation techniques tried in Section III. Due to the oscillating nature of $\rho'(\tau')$, the integrand can have appreciable value over the entire interval of integration for small ζ. The Taylor series approximation in Equation (17) for the exponent is not useful since this approximation becomes inaccurate for values of $|\theta - \theta_0| > 1$. Such angular differences are well within the interval of integration, since $|\theta - \theta_0|$ can be as large as π.

Numerical integration seems to offer the most fruitful approach to the solution of $\rho(\tau_s, \tau)$ for narrow-band two-dimensional noise fields. This will not be attempted here.

V. Evaluation of Cross-Correlation Function – Case C

In order to gain insight into the question whether the results obtained thus far depend critically on the somewhat arbitrarily postulated

form of $\rho(\tau)$, a second narrowband model will be considered. For convenience in mathematical manipulation the normalized spectral density of each elementary noise source is represented by the equation

$$S(\omega) = \frac{|\omega|}{\omega_o \sqrt{2\pi}\, \sigma} \left[\varepsilon^{-\frac{(\omega-\omega_o)^2}{2\sigma^2}} + \varepsilon^{-\frac{(\omega+\omega_o)^2}{2\sigma^2}} \right], \quad \omega_o >> \sigma \qquad (41)$$

Equation (41) is not Wiener-Hopf factorable and therefore represents only a limiting form of a realistic spectral function. For the purposes of the present discussion this causes no difficulty.

The autocorrelation function corresponding to Equation (41) is

$$\rho(\tau) = \varepsilon^{-\frac{\tau^2 \sigma^2}{2}} \left[\cos \omega_o \tau - \tau \sigma \frac{\sigma}{\omega_o} \sin \omega_o \tau \right] \qquad (42)$$

With $\omega_o >> \sigma$ the second term is small compared to the first for the significant range of τ.

The desired cross-correlation for the three-dimensional field is most easily evaluated by use of the expression

$$\rho(\tau_s, \tau) = \frac{1}{2} \int_{-\infty}^{\infty} S(\omega)\, \frac{\sin \omega \tau_s}{\omega \tau_s}\, \varepsilon^{j\omega\tau}\, d\omega \qquad (43)[1]$$

Substitution of Equation (41) into Equation (43) leads to the result

$$\rho(\tau_s, \tau) = \frac{1}{2\omega_o \tau_s} \left[\varepsilon^{-\frac{\sigma^2}{2}(\tau_s - \tau)^2} \sin \omega_o (\tau_s - \tau) + \varepsilon^{-\frac{\sigma^2}{2}(\tau_s + \tau)^2} \sin \omega_o (\tau_s + \tau) \right] \qquad (44)$$

This relation is equivalent to Equation (32) in case B. The special cases $\tau = 0$ and $\tau = \tau_s$ yield

$$\rho(\tau_s, 0) = \varepsilon^{-\frac{1}{2}\left(\frac{\sigma}{\omega_0}\omega_0\tau_s\right)^2} \frac{\sin \omega_0\tau_s}{\omega_0\tau_s} \qquad (45)$$

$$\rho(\tau_s, \tau_s) = \varepsilon^{-2\left(\frac{\sigma}{\omega_0}\omega_0\tau_s\right)^2} \frac{\sin 2\omega_0\tau_s}{2\omega_0\tau_s} \qquad (46)$$

If one identifies $\frac{\sigma}{\omega_0}$ with ζ and considers $\zeta \ll 1$ Equations (45) and (46) are closely analogous to Equations (34) and (35) respectively.

An upper bound equivalent to Equation (40) can be obtained by replacing the sinusoidal functions by unity. Thus

$$\left|\rho(\tau_s, \tau)\right| \le \frac{1}{2\omega_0\tau_s}\left[\varepsilon^{-\frac{1}{2}\frac{\sigma^2}{\omega_0^2}\omega_0^2(\tau_s-\tau)^2} + \varepsilon^{-\frac{1}{2}\frac{\sigma^2}{\omega_0^2}\omega_0^2(\tau_s+\tau)^2}\right] \le \frac{1}{\omega_0\tau_s} \qquad (47)$$

On the other hand Equation (40) can be rewritten in the form

$$\frac{\varepsilon^{-\omega_0\tau_s}}{\sqrt{1-\zeta^2}\,\omega_0\tau_s}\cosh \zeta\omega_0\tau = \frac{1}{2\sqrt{1-\zeta^2}\,\omega_0\tau_s}\left[\varepsilon^{-\zeta\omega_0(\tau_s-\tau)} + \varepsilon^{-\zeta\omega_0(\tau_s+\tau)}\right]$$
$$\tau < \tau_s \qquad (48)$$

Again identifying ζ with $\frac{\sigma}{\omega_0}$ and letting $\zeta \ll 1$, one observes that Equation (48) is the direct analogue of Equation (47).

Finally it is clear that, except in a neighborhood of the origin sufficiently small so that $\sigma(\tau + \tau_s) \le 0(1)$, the function $\rho(\tau_s, \tau)$ of Equation (44) is characterized by ridges and valleys parallel to the line $\tau = \tau_s$ (for τ, $\tau_s > 0$), much as those shown in Figure 5. It therefore

appears that the general properties of $\rho(\tau_s, \tau)$ are relatively independent of the precise nature of the autocorrelation function assumed for the elementary noise sources.

VI. Conclusions

The results found in Equations (12) and (40) are valuable in that they allow a quick estimate of the maximum value of $\rho(\tau_s, \tau)$ for a given separation of transducers. The results for the wide-band case(A) and the narrow-band case (B) are approximately the same when ω_0 is interpreted to be the upper half power frequency in the first case, and the center frequency in the latter case. These answers in an approximate sense can be extended to other spectra, wide or narrow, if ω_0 is interpreted to be the upper half power frequency for the spectral density of each tiny noise generator in the field.

Also a general pattern of regularity has been established for $\rho(\tau_s, \tau)$ for the narrow-band, three-dimensional noise field. Coupled with Equation (40), Figure 5 can provide a more accurate estimate of $\rho(\tau_s, \tau)$. Figure 5 is also of value in determining transducer spacings that yield little or no cross-correlation.

A comparison of results for $\rho(\tau_s, \tau)$ for the three-dimensional noise field and for the two-dimensional noise field is also interesting. Under the assumption that the spectra of the individual noise generators are given by Equation (9) in both cases, $\rho(\tau_s, \tau)$ decreases for increasing τ and constant τ_s for the three-dimensional case, and increases for the same conditions in the two-dimensional case if $\omega_0 \tau_s$ is large enough.

A1-17

References

1. J. J. Faran and R. Hills, Tech. Memo 28, Harvard University Acoustics Research Laboratory (1952).

2. V. C. Anderson, J. Acoust. Soc. Am. 30, 470-477 (1958).

3. M. J. Jacobson, J. Acoust. Soc. Am. 34, 971-978 (1962).

4. Tables of the Error Function and Its Derivative, NBS Applied Mathematics Series, No. 41, October 1954.

5. E. Jahnke and F. Emde, Tables of Functions, p. 32. Dover Publications, 1945.

General Dynamics/Electric Boat Research
(53-00-10-0231)

Progress Report No. 2

by

Theron Usher, Jr.

Dunham Laboratory
Yale University
New Haven, Connecticut
March, 1963

Department of Engineering and Applied Science

Yale University

General Dynamics/Electric Boat Research
(53-00-10-0231)

SIGNAL DETECTION BY ARRAYS IN NOISE FIELDS

WITH LOCAL VARIATIONS

by

Theron Usher, Jr.

March, 1963

SIGNAL DETECTION BY ARRAYS IN NOISE FIELDS
WITH LOCAL VARIATIONS

I. Introduction

A considerable amount of work has been done in recent years[1,2,3,4,5] in analyzing systems composed of local arrays of transducers used to detect the presence of a plane wave signal in an isotropic noise background. Such systems have had direct application in undersea signal detection, and of particular interest in this field is the DIMUS system. The DIMUS system has been defined[2] to consist of the following steps in signal processing:

1. Sampling the output of each transducer at small, equal time intervals;

2. Providing infinite clipping for each sampled output;

3. Delaying the clipped signals electrically by integral multiples of the sampling interval;

4. Adding the delayed signals;

5. Squaring the sum;

6. Filtering the squared sum.

Analyses carried out by Faran and Hills,[3] and Rudnick[2] have assumed that the background noise power output of each transducer is the same. Furthermore, the average noise power output on a short-time basis was assumed to be constant for each transducer.

Although the system analyzed by Thomas and Williams[4] was not a DIMUS system, infinite clipping of signal plus noise was incorporated in the analysis. Thomas and Williams compared the performance of a system with

infinite clippers to a similar one without infinite clippers for the situation in which the short-term average noise power output of each transducer varies with time. However, this analysis is limited by the assumption that the short-term noise power outputs of every transducer are described by the same time function.

Experimental observations have shown that the average noise power outputs of transducers mounted in an underwater array are not the same from transducer to transducer. One possible explanation lies in the fact that different turbulent flow patterns are set up around each transducer when the array is in motion. Also, the self-noise due to the internal construction and possible malfunctions is different for each transducer.

The purpose of this report is to incorporate the variation in noise power output from transducer to transducer in the analysis of the performance of the array. A system which is essentially DIMUS in nature is analyzed and the performance is compared to a system which is identical in every respect except that the infinite clippers are absent. For each of the two systems, two quantities form the bases of comparison:

1. The maximum average signal output of the system, which occurs when the array "beam" is steered directly at the signal source.

2. The ratio of the square of the maximum average signal output to the variance of the output of the low-pass filter.

For purposes of comparison, two performance indices are calculated by forming the ratios of the quantities defined above for the system with clippers present and for the system with clippers absent. The assumptions involved in the analysis are listed in the following section.

II. Assumptions and Definitions

The system to be analyzed is shown in Figure 1.
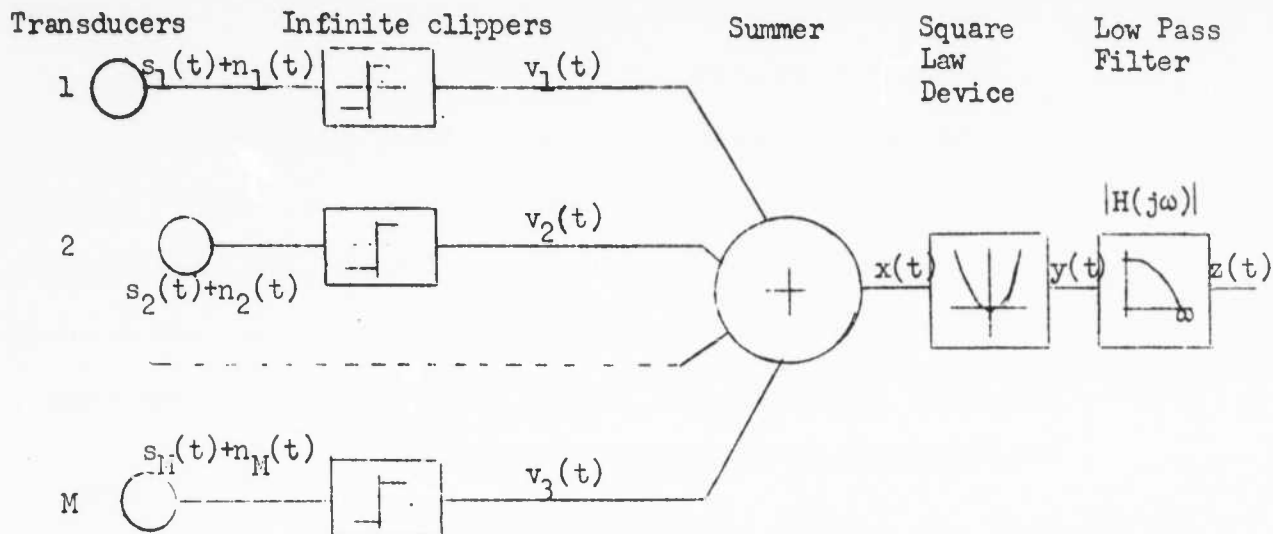
Fig. 1 Essential Configuration of a DIMUS System

1. The transducers in the array depicted in Figure 1 have omni-directional characteristics.

2. The normalized autocorrelation functions of both the signal and the noise inputs to the clippers in Figure 1 are identical.

3. The crosscorrelation between noise inputs for different channels is zero. In an actual system, the crosscorrelation may be made arbitrarily small. This assumption makes the following analysis mathematically tractable.

4. The signal and the noise inputs to the clippers are gaussian and stationary. Signal and noise are independent.

5. The signal power input to each clipper is the same, but the noise power input is allowed to vary from channel to channel.

6. It is assumed that the short-term averages for the input signal powers and input noise powers do not vary significantly for any particular channel.

7. The effect of sampling is neglected. Effectively, the sampling takes place at a high enough rate that the higher harmonic power spectra produced by sampling do not overlap the fundamental power spectral density.

8. The digital time delays have been omitted, since the analysis is primarily concerned with "on target" and "off target" quantities. It is assumed that such combinations of delays are available to electrically steer the array directly at the target, and to steer the array far enough away so that gain effects due to the array configuration are negligible.

III. General Form of System Directivity Patterns

The correlation matrix for the noise components is given by Eq. (1). It is assumed that $\overline{n_i(t)} = \overline{s_i(t)} = 0$.

$$\left\| \overline{n_i(t)\, n_j(t + \tau)} \right\| = \left\| N_{ij} \right\| \rho(\tau) = \begin{Vmatrix} N_1 & 0 & 0 & - & 0 \\ 0 & N_2 & 0 & - & 0 \\ 0 & 0 & N_3 & - & 0 \\ \hline 0 & 0 & 0 & - & N_M \end{Vmatrix} \rho(\tau) \quad (1)$$

The correlation matrix for the signal components of the array inputs is

$$\left\| \overline{s_i(t)\, s_j(t + \tau)} \right\| = S \left\| \rho(\tau_{ij} + \tau) \right\| = S \begin{Vmatrix} \rho(\tau) & \rho(\tau_{12} + \tau) & - & \rho(\tau_{1M} + \tau) \\ \rho(\tau_{21} + \tau) & \rho(\tau) & - & \rho(\tau_{2M} + \tau) \\ & & & \\ \rho(\tau_{M1} + \tau) & \rho(\tau_{M2} + \tau) & & \rho(\tau) \end{Vmatrix} \quad (2)$$

In Eqs. (1) and (2), the N_i are the noise power inputs to each channel, and S is the common signal power input to each channel. The function $\rho(\tau)$ is the normalized autocorrelation function for the signal and the noise. The delay factors τ_{ij} in Eq. (2) represent the combined effects of spatial time delays introduced by the plane wave signal relative to each pair of transducers, and also the electrical time delays which are usually introduced in all steered systems, but which are not included in Figure 1.

The average output of the squarer, $\overline{y}$, yields the so-called directivity pattern, which may be obtained by varying the electrical time delays and keeping the physical orientation of the array fixed, or by keeping the electrical time delays fixed and varying the physical orientation of the array relative to the plane wave signal. For the system in Figure 1, with the clippers removed, the average output has been shown[2,3] to be the sum of all the matrix elements in Eqs. (1) and (2) with $\tau = 0$.

The subscript A in Eq. (3) and following work is used to denote the fact that the clippers are removed.

$$
\begin{aligned}
\overline{y_A(\theta)} &= \sum_{i=1}^{M} \sum_{j=1}^{M} \left\{ N_{ij} + S\, \rho\,(\tau_{ij}) \right\} \\
&= \sum_{i=1}^{M} N_i + S\, M + 2S \sum_{i=1}^{M} \sum_{j=i+1}^{M} \rho\,(\tau_{ij})
\end{aligned}
\tag{3}
$$

The angle θ is defined as the steered beam angle and is a complicated function of the electrical time delays which make up part of the τ_{ij}.

Figure 2 shows a typical directivity pattern resulting from Eq. (3). The signal and noise are assumed to have low-pass spectra.
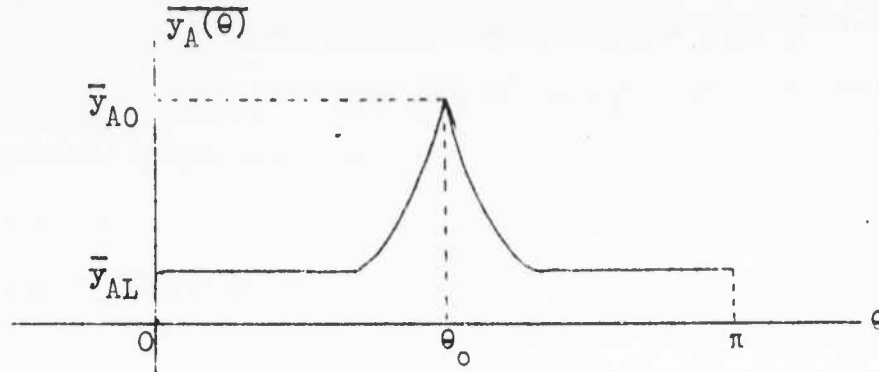
Fig. 2 Typical Directivity Pattern

At some angle, θ_o, the steered beam is "on target" and a maximum output, $\overline{y}_{AO}$, results. When the beam angle is greatly different from the target angle, θ_o, the directivity pattern approaches a lower asymptote, $\overline{y}_{AL}$, very closely, because the $\rho(\tau_{ij})$ approach zero. These quantities are

$$\overline{y}_{AO} = \sum_{i=1}^{M} N_i + SM^2 \tag{4}$$

$$\overline{y}_{AL} = \sum_{i=1}^{M} N_i + SM \tag{5}$$

With the infinite clippers present in the system, the directivity pattern has much the same shape as that in Fig. 2. However, in order to define $\overline{y(\theta)}$ mathematically, it is first necessary to define a normalized correlation function, $\mu_{ij}(\tau)$, for signal and noise:

$$\mu_{ij}(\tau) = \frac{\overline{\{s_i(t) + n_i(t)\}\{s_j(t+\tau) + n_j(t+\tau)\}}}{(S + N_i)^{1/2}(S + N_j)^{1/2}} \tag{6}$$

Furthermore,

$$\mu_{ij}(\tau) = \begin{cases} \dfrac{S}{(S + N_i)^{1/2}(S + N_j)^{1/2}} \, \rho(\tau + \tau_{ij}) & i \neq j \\[4mm] \rho(\tau) & i = j \end{cases} \tag{7}$$

The correlation functions for the clipper responses, with the assumption that the clipper output is either +1 or -1, have been shown[4] to be

$$\mu'_{ij}(\tau) = \overline{v_i(t)\, v_j(t + \tau)} = \frac{2}{\pi} \arcsin\left\{ \mu_{ij}(\tau) \right\} \tag{8}$$

Note that

$$\mu'_{ij}(0) = \begin{cases} \dfrac{2}{\pi} \arcsin\left\{ \dfrac{S}{(S + N_i)^{1/2}(S + N_j)^{1/2}} \, \rho(\tau_{ij}) \right\} & i \neq j \\[4mm] 1 & i = j \end{cases} \tag{9}$$

The directivity pattern is found by summing Eq. (9) over all i and j:

$$\overline{y(\theta)} = \sum_{i=1}^{M} \sum_{j=1}^{M} \frac{2}{\pi} \arcsin\left\{ \mu_{ij}(0) \right\}$$

$$= M + 2 \sum_{i=1}^{M} \sum_{j=i+1}^{M} \frac{2}{\pi} \arcsin\left\{ \frac{S}{(S + N_i)^{1/2}(S + N_j)^{1/2}} \, \rho(\tau_{ij}) \right\} \tag{10}$$

The "on target" and "off target" values, $\overline{y}_0$ and $\overline{y}_L$ respectively, are

$$\overline{y}_0 = M + 2 \sum_{i=1}^{M} \sum_{j=i+1}^{M} \frac{2}{\pi} \arcsin\left\{ \frac{S}{(S + N_i)^{1/2}(S + N_j)^{1/2}} \right\} \leq M^2 \tag{11}$$

$$\overline{y}_L = M \tag{12}$$

IV. Performance Comparison - Ratio of Average Signal Outputs

The average signal output is defined in Eq. (13) to be the difference between the "on target" value of the directivity pattern and the "off target" value for both systems. Note that the signal source is still present for both conditions.

$$\Delta \overline{y} = \overline{y}_0 - \overline{y}_L \tag{13}$$

For purposes of comparison, the directivity patterns for both systems are normalized with respect to the "off target" response in each case. The ratio of the normalized $\Delta \overline{y}$ in both cases then becomes meaningful as a performance index.

The indicated computation may be carried out for any particular system for which the N_i are known by measurement. However, in order to get some general results, it is convenient to assume a statistical distribution for the N_i which applies to all transducers. Of course, physical measurements should support any assumed distribution. Two simple statistical distributions are assumed and analyzed in detail, one of which is continuous, the other is discrete. The continuous distribution of $\hat{N}_i$ is described by the probability density function, $f(N_i)$.

$$f(N_i) = \begin{cases} (N_i \; \ell n \; N_H/N_L)^{-1} & N_L \leq N_i \leq N_H \\ \\ 0 & \text{elsewhere} \end{cases} \tag{14}$$

The discrete distribution is two-valued and is described in Eq. (15).

$$N_i = \begin{Bmatrix} N_H \\ \\ N_L \end{Bmatrix} \text{ with probability } \begin{Bmatrix} p \\ \\ (1 - p) \end{Bmatrix} \tag{15}$$

Statistical averages of $\Delta\bar{y}$ over the N_i are used in computing the ratio of the $\Delta\bar{y}$ for both systems.

For the system without clippers, from Eqs. (4), (5) and (13)

$$\langle \Delta\bar{y}_A \rangle = S(M^2 - M) \tag{16}$$

and

$$\langle \bar{y}_{AL} \rangle = M(\langle N_i \rangle + S) \tag{17}$$

The normalized signal output found in Eq. (18) is denoted by primes.

$$\langle \Delta\bar{y}_A \rangle' = \frac{\langle \Delta\bar{y}_A \rangle}{\langle \bar{y}_{AL} \rangle} = (M - 1)\frac{S}{S + \langle N_i \rangle} \tag{18}$$

For the system with clippers, the normalized signal output from Eqs. (11), (12) and (13) is found to be

$$\langle \Delta\bar{y} \rangle' = \frac{\langle \Delta\bar{y} \rangle}{\langle \bar{y}_L \rangle} = (M - 1)\frac{2}{\pi}\left\langle \arcsin\left\{ \frac{S}{(S + N_i)^{1/2}(S + N_j)^{1/2}} \right\}\right\rangle \tag{19}$$

The signal response ratio, which is an index of relative system performance with respect to average signal output, is defined to be the ratio of Eq. (19) to Eq. (18).

$$R_1 = \frac{\langle \Delta\bar{y} \rangle'}{\langle \Delta\bar{y}_A \rangle'} = \frac{2}{\pi}\left\langle \arcsin\left\{ \frac{S}{(S + N_i)^{1/2}(S + N_j)^{1/2}} \right\}\right\rangle\left(1 + \frac{\langle N_i \rangle}{S}\right) \tag{20}$$

Equation (20) remains to be evaluated for the two cases indicated in Eqs. (14) and (15).

For the continuous distribution in Eq. (14), which describes a uniform distribution of noise power on a logarithmic basis, we have

$$\langle N_i \rangle = \int_{N_L}^{N_H} N_i \left(N_i \; \ell n \; \frac{N_H}{N_L} \right)^{-1} dN_i = (N_H - N_L) \left(\ell n \; \frac{N_H}{N_L} \right)^{-1} \quad (21)$$

. If the definition $a_i = \dfrac{N_i}{S}$ is made,

$$\left(1 + \frac{\langle N_j \rangle}{S} \right) = 1 + (a_H - a_L) \left(\ell n \; \frac{a_H}{a_L} \right)^{-1} \quad (22)$$

Furthermore, the evaluation of the expectation of the arcsin function in Eq. (20) is simplified if the restriction is made that $a_H > a_L \geq 1$. Since the detection of strong signals presents no problem, the restriction is almost always satisfied, Thus,[7]

$$\left\langle \arcsin \frac{S}{(S + N_i)^{1/2}(S + N_j)^{1/2}} \right\rangle \cong \left\langle (1 + a_i)^{-1/2}(1 + a_j)^{-1/2} \right\rangle \quad (i \neq j)$$

$$= \left[\int_{a_L}^{a_H} (1 + a_i)^{-1/2} \left(a_i \; \ell n \; \frac{a_H}{a_L} \right)^{-1} da_i \right]^2$$

$$= \left[\ell n \left\{ \frac{\left[(1 + a_H)^{1/2} - 1 \right]}{\left[(1 + a_H)^{1/2} + 1 \right]} \cdot \frac{\left[(1 + a_L)^{1/2} + 1 \right]}{\left[(1 + a_L)^{1/2} - 1 \right]} \right\} \right]^2 \left(\ell n \; \frac{a_H}{a_L} \right)^{-2} \quad (23)$$

Substituting the results in Eqs. (22) and (23) into Eq. (20) yields R_1:

$$R_1 = \frac{2}{\pi} \left(\ell n \left\{ \frac{\left[(1 + a_H)^{1/2} - 1 \right] \left[(1 + a_L)^{1/2} + 1 \right]}{\left[(1 + a_H)^{1/2} + 1 \right] \left[(1 + a_L)^{1/2} - 1 \right]} \right\} \right)^2 \left(\ell n \; \frac{a_H}{a_L} + a_H - a_L \right) \left(\ell n \; \frac{a_H}{a_L} \right)^{-3} \quad (24)$$

If $a_H > a_L \gg 1$, and $a_H / a_L = b$, Eq. (24) further simplifies to

$$\boxed{R_1 \simeq \frac{8}{\pi} \frac{(b^{1/2} - 1)^2(b - 1)}{b(\ln b)^3} .}$$

(25)

The results given for R_1 in Eqs. (24) and (25) are evaluated for several values of a_L and plotted as functions of b in Figure 3. The results show that for sufficiently large b, the performance of the system with clippers is superior to that of the system with the clippers removed, although the results are certainly dependent to a great degree on the assumed distribution of noise power given in Eq. (14). Other assumed distributions show much less improvement.

For example, if

$$f(N_i) = \begin{cases} \dfrac{1}{N_H - N_L} & N_L < N_i < N_H \\ \\ 0 & \text{elsewhere} \end{cases}$$

(26)

the relation for R_1 becomes

$$R_1 = \frac{8}{\pi} \left[\frac{(1 + a_H)^{1/2} - (1 + a_L)^{1/2}}{a_H - a_L} \right]^2 \left[1 + \frac{a_H + a_L}{2} \right]$$

(27)

When a_L is large compared to unity, Eq. (27) becomes

$$R_1 \simeq \frac{4}{\pi} \frac{b + 1}{(b^{1/2} + 1)^2} = \begin{cases} \dfrac{2}{\pi} & \text{for } b = 1 \\ \\ \dfrac{4}{\pi} & \text{for } b \to \infty \end{cases}$$

(28)

Very little advantage of the system with clippers is shown, even for large b.

FIGURE 3

NORMALIZED AVERAGE SIGNAL RESPONSE RATIO AS A FUNCTION OF INPUT NOISE VARIATION

$$R_f = \frac{\langle \Delta \bar{y} \rangle'}{\langle \Delta \bar{y}_A \rangle'}$$

$$f(a) = \begin{cases} \dfrac{1}{a \, \ln \dfrac{a_{H}}{a_{L}}} & a_{L} < a < a_{N} \\ 0 & elsewhere \end{cases}$$

a_L
$\gg 1$
10
1
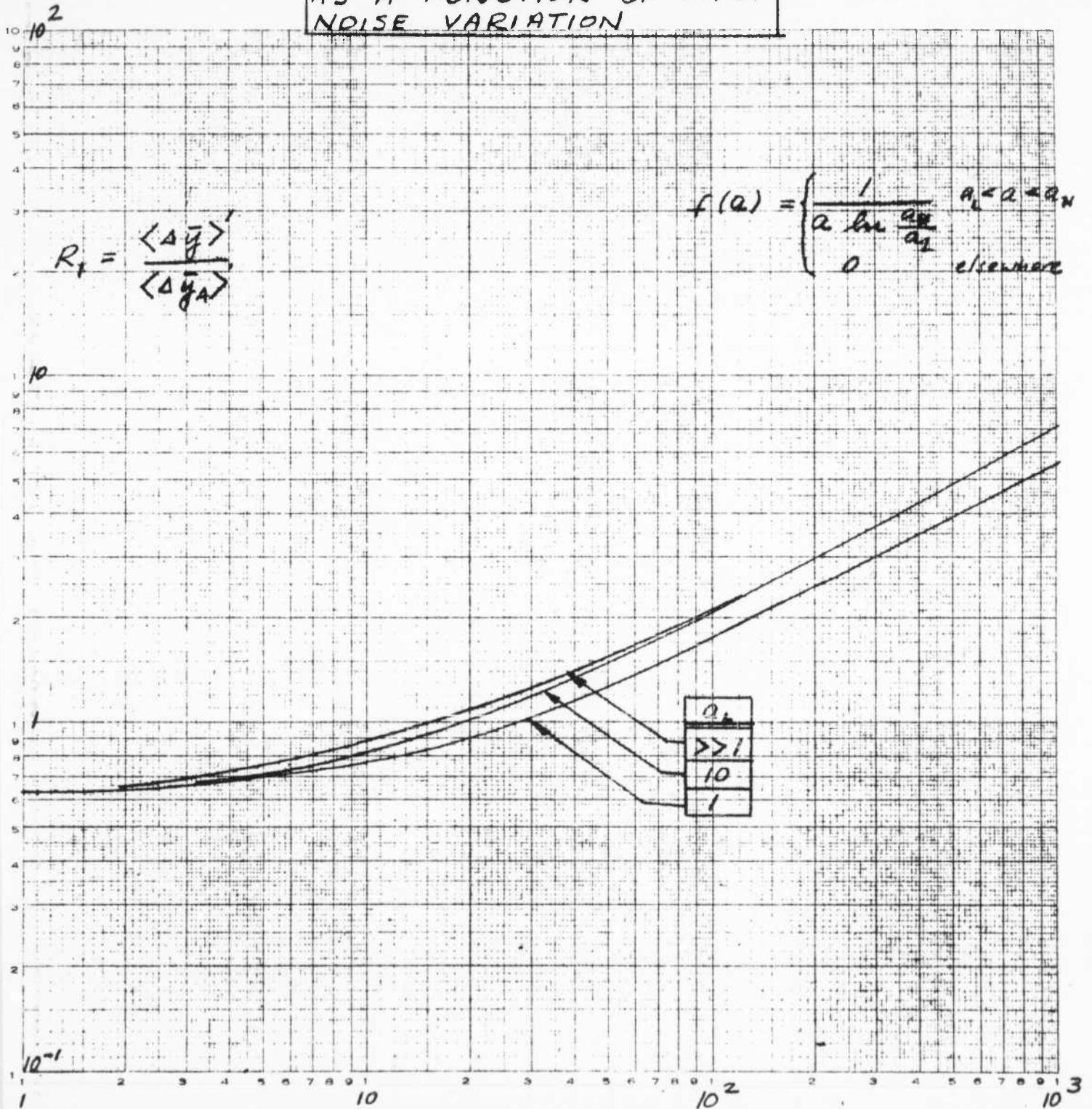
$$b = \frac{a_{H}}{a_{L}} = \frac{N_{H}}{N_{L}}$$

Similarly, if

$$f(N_1) = \begin{cases} \dfrac{N_H N_L}{N_H - N_L} \dfrac{1}{N_1^2} & N_L < N_1 < N_H \\ \\ 0 & \text{elsewhere} \end{cases} \qquad (29)$$

the relation giving R_1 is[7]

$$R_1 = \frac{2}{\pi}\left[\frac{(1 + a_L)^{1/2}}{a_L} - \frac{(1 + a_H)^{1/2}}{a_H} - \frac{1}{2}\, \ell n \left\{\frac{\left[(1 + a_H)^{1/2} - 1\right]\left[(1 + a_L)^{1/2} + 1\right]}{\left[(1 + a_H)^{1/2} + 1\right]\left[(1 + a_L)^{1/2} - 1\right]}\right\}\right]^2$$

$$\times \left[\frac{a_H a_L}{a_H - a_L}\right]^3 \left[\frac{a_H - a_L}{a_H a_L} + \ell n \frac{a_H}{a_L}\right] \qquad (30)$$

Equation (30) reduces to Eq. (31) with considerable manipulation if a_L is large compared to unity.

$$R_1 \cong \frac{8}{9\pi} \frac{(b^{3/2} - 1)^2}{(b - 1)^3} \ell n\, b \;=\; \begin{cases} \dfrac{2}{\pi} & \text{for } b = 0 \\ \\ \dfrac{8}{9\pi}\, \ell n\, b & \text{for large } b \end{cases} \qquad (31)$$

Evaluation of Eq. (31) for $b = 1000$ yields $R_1 = 1.95$. The system with clippers again shows very little advantage over the system without clippers.

Next, Eq. (20) is evaluated for the discrete distribution found in Eq. (15). The average noise power becomes

$$\left\langle N_i \right\rangle = p\, N_L + (1 - p)N_H \qquad (32)$$

A2-13

Also,

$$\langle (1 + a_i)^{-1/2}(1 + a_j)^{-1/2} \rangle = p^2(1 + a_L)^{-1} + 2p(1 - p)(1 + a_L)^{-1/2}(1 + a_H)^{-1/2}$$

$$+ (1 - p)^2(1 + a_H)^{-1}$$

$$= \frac{\left[p(1 + a_H)^{1/2} + (1 - p)(1 + a_L)^{1/2} \right]^2}{(1 + a_L)(1 + a_H)} \qquad (33)$$

Combination of Eqs. (20), (32) and (33) yields the relation for R_1:

$$R_1 = \frac{2}{\pi} \frac{\left[p(1 + a_H)^{1/2} + (1 - p)(1 + a_L)^{1/2} \right]^2 \left[p(1 + a_L) + (1 - p)(1 + a_H) \right]}{(1 + a_L)(1 + a_H)}$$

$$\boxed{R_1 = \frac{2}{\pi} \left[p(c^{1/2} - 1) + 1 \right]^2 \left[p(c^{-1} - 1) + 1 \right] .} \qquad (34)$$

where

$$c = \frac{1 + a_H}{1 + a_L} \qquad (35)$$

Note that $c \cong b$ for $a_L >> 1$.

The maximum value of R_1 occurs for

$$p = \frac{2c^{1/2} + 1}{3(c^{1/2} + 1)} = \begin{cases} 1/2 \text{ for } c = 1 \\ \\ 2/3 \text{ for } c \to \infty \end{cases} \qquad (36)$$

The maximum value of R_1 is plotted as a function of c in Figure 4.

Also of interest are the limiting forms of Eq. (34) for which either the percentage of noisy transducers is small, or the percentage of quiet transducers is small. For a small percentage of noisy transducers, $(1 - p)$ is small, and Eq. (34) becomes

FIGURE 4
NORMALIZED AVERAGE SIGNAL RESPONSE RATIO AS A FUNCTION OF INPUT NOISE VARIATION

$$p = \frac{2C^{3/2} - 3C + 1}{3(C^{1/2} - 1)(C - 1)}$$

$$a_i = \begin{cases} a_L \text{ with prob } p \\ a_H \text{ with prob } (1-p) \end{cases}$$

ASYMPTOTE = .095 C

$$C = \frac{1 + a_H}{1 + a_L} = \frac{S + N_H}{S + N_L}$$

A2-15
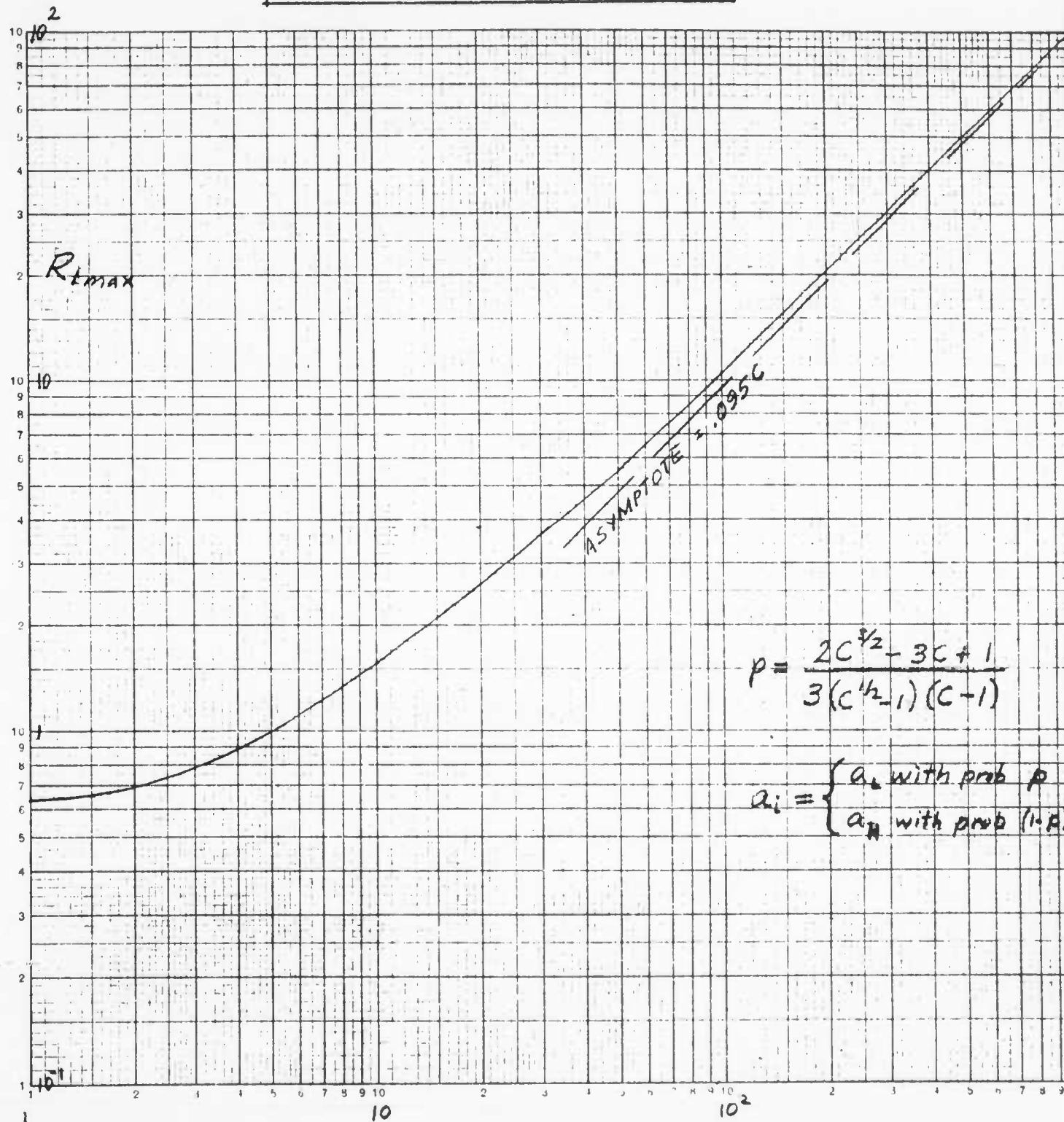
$$R_1 \cong \frac{2}{\pi} \left[1 + (c - 3 + 2c^{-1/2})(1 - p) \right] \qquad (37)$$

For a small percentage of quiet transducers, p is small, and Eq. (34) becomes

$$R_1 \cong \frac{2}{\pi} \left[1 + (2c^{1/2} - 3 + c^{-1})p \right] \qquad (38)$$

V. Performance Comparison – Ratio of Output Signal-to-Noise Ratios

The output signal-to-noise ratio for both systems is defined in Eq. (39), where $\langle \Delta \bar{y} \rangle$ is the average signal output, and $\langle \sigma_z^2 \rangle$ is the variance of the output of the low pass filter, shown in Fig. 1, averaged over the N_i.

$$r = \frac{\langle \Delta \bar{y} \rangle^2}{\langle \sigma_z^2 \rangle} \qquad \text{and} \qquad r_A = \frac{\langle \Delta y_A \rangle^2}{\langle \sigma_{zA}^2 \rangle} \qquad (39)$$

The performance index, R_2, considered in the following analysis is the square root of the ratio of r, for the system with clippers, to r_A for the system without clippers. It can be seen in Eq. (40) that R_2 is closely related to R_1, which is calculated in detail in Section IV.

$$R_2 = \left(\frac{r}{r_A} \right)^{1/2}$$

$$= \frac{\langle \Delta \bar{y} \rangle}{\langle \Delta \bar{y}_A \rangle} \left(\frac{\langle \sigma_{zA}^2 \rangle}{\langle \sigma_z^2 \rangle} \right)^{1/2} = R_1 \left(\frac{\langle \sigma_{zA}^2 \rangle}{\langle \sigma_z \rangle} \right)^{1/2} \frac{1}{S + \langle N_i \rangle} \qquad (40)$$

From Eq. (40), it can be seen that the major part of the analysis in determining R_2 involves the calculation of the average variance of the output of the low-pass filter for both systems. Both distributions of input noise power given in Eqs. (14) and (15) must also be considered.

A2-16

Since all the input signal and noise time functions are assumed to be gaussian, the sum, $x(t)$, shown in Figure 1 is also gaussian for the system without clippers. Under these conditions,[6]

$$R_{yA}(\tau) = R_x^2(0) + 2 R_x^2(\tau) \tag{41}$$

where $R_{yA}(\tau)$ is the autocorrelation function for $y(t)$, and $R_x(\tau)$ is the autocorrelation function for $x(t)$. In Eq. (41), $R_x^2(0)$ simply represents the average output of the squarer, which has been given the symbol $\overline{y}_A$. Thus the variational component of $y(t)$ has the autocorrelation function $2 R_x^2(\tau)$.

The spectral density of the function $y(t)$ is

$$S_{yA}(\omega) = \frac{1}{\pi} \int_{-\infty}^{\infty} 2 R_x^2(\tau) \varepsilon^{-j\omega\tau} d\tau \tag{42}$$

The variance of the output, $z(t)$, of the low-pass filter is found in Eq. (43), where $H_z(j\omega)$ is the frequency response function of the filter.

$$\sigma_{zA}^2 = \int_0^{\infty} S_y(\omega) \left| H_z(j\omega) \right|^2 d\omega \tag{43}$$

In order to make the value of r_A large, the bandwidth of the low-pass filter must be much smaller than the bandwidth of $S_y(\omega)$, the input spectral density. Under this assumption, we have

$$\sigma_{zA}^2 \cong S_y(0) \int_0^{\infty} \left| H_z(j\omega) \right|^2 d\omega \tag{44}$$

A2-17

Furthermore, if $H_z(j\omega)$ has the form

$$H_z(j\omega) = \frac{1}{1 + j\frac{\omega}{\omega_F}} \qquad (45)$$

then Eqs. (42), (44) and (45) combine to yield

$$\sigma_{zA}^2 = 2 \omega_F \int_0^\infty R_x^2(\tau) \, d\tau \qquad (46)$$

For the "on target" situation, the function $R_x(\tau)$ is simply the sum of all the matrix elements in Eqs. (1) and (2), with $\tau_{ij} = 0$.

$$R_x(\tau) = \left(\sum_{i=1}^M N_i + M^2 S \right) \rho(\tau) \qquad (47)$$

and

$$R_x^2(\tau) = \left(\sum_{i=1}^M N_i + M^2 S \right)\left(\sum_{j=1}^M N_j + M^2 S \right) \rho^2(\tau)$$

$$= \left(\sum_{i=1}^M \sum_{j=1}^M N_i N_j + 2 M^2 S \sum_{i=1}^M N_i + M^4 S^2 \right) \rho^2(\tau) \qquad (48)$$

Combining Eqs. (46) and (48) and averaging over the N_i we have

$$\left\langle \sigma_{zA}^2 \right\rangle = 2\omega_F \left\{ M\left\langle N_i^2 \right\rangle + (M^2 - M) \left\langle N_i \right\rangle^2 + 2 M^3 S \left\langle N_i \right\rangle + M^4 S^2 \right\} \int_0^\infty \rho^2(\tau) \, d\tau \qquad (49)$$

The ratio of the square of Eq. (16) to Eq. (49) gives the signal-to-noise ratio for the unclipped system.

$$r_A = \frac{(M - 1)^2 \left|\frac{S}{\langle N_i \rangle}\right|^2}{\left[\frac{1}{M}\frac{\langle N_i^2 \rangle}{\langle N_i \rangle^2} + \left(1 - \frac{1}{M}\right) + 2M\frac{S}{\langle N_i \rangle} + M^2\left(\frac{S}{\langle N_i \rangle}\right)^2\right]\left[2\omega_F \int_0^\infty \rho^2(\tau)\ d\tau\right]} \quad (50)$$

The first denominator factor is nearly a perfect square if M is large so that

$$r_A\left(2\omega_F \int_0^\infty \rho^2(\tau)\ d\tau\right) \cong \left[\frac{\left(\frac{S}{\langle N_i \rangle}\right)(M - 1)}{\left(\frac{S}{\langle N_i \rangle}\right)M + 1}\right]^2 \quad (51)$$

The result in Eq. (51) is plotted in Fig. 5 on logarithmic coordinates. For values of $S/\langle N_i \rangle$ significantly less than $1/M$, the value of r_A varies
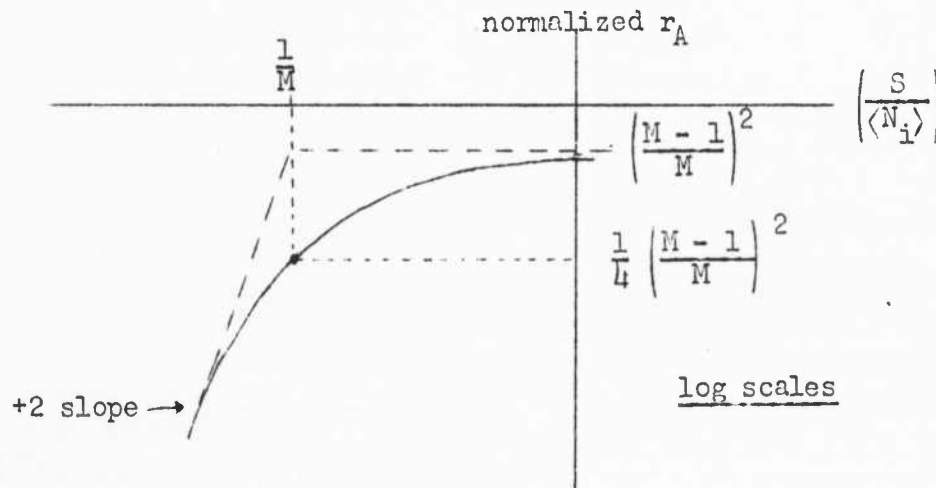

Fig. 5 Normalized Output Signal-to-Noise Ratio as a
Function of Input Signal-to-Average Noise Ratio

as the square of $S/\langle N_i \rangle$, and the first two terms (noise x noise) can be used to accurately determine $\langle \sigma_{zA}^2 \rangle$.

This result is of quantitative value in the analysis of the system with clippers in estimating the region of validity of the result for

$\left\langle \sigma_z^{\,2} \right\rangle$. In this case only the noise x noise terms are easily evaluated. The assumption of low input signal-to-noise ratio is not unduly restrictive, since only low input signal-to-noise ratios cause any detection problems.

In the analysis of the system in Fig. 1 with clippers present, it is assumed that the signal components, $s_i(t)$, of the inputs to the clippers are negligible. This assumption makes the mathematical analysis for the evaluation of $\left\langle \sigma_z^{\,2} \right\rangle$ tractable.

The output of the square law device is given by

$$y(t) = \sum_{i=1}^{M} \sum_{j=1}^{M} v_i(t)\, v_j(t) \tag{52}$$

The autocorrelation function for $y(t)$ is

$$R_y(\tau) = E\left[\sum_{i=1}^{M} \sum_{j=1}^{M} v_i(t)\, v_j(t) \sum_{k=1}^{M} \sum_{m=1}^{M} v_k(t+\tau)\, v_m(t+\tau) \right] \tag{53}$$

The evaluation of Eq. (53) is helped by breaking down the terms into different categories as shown in Table 1.

Subscript relations	No. of terms	Evaluation and comments
$i = j$ and $k = m$	M^2	Each term is unity since $v_i^2 = 1$
$i = j$ and $k \neq m$	$M^3 - M^2$	These terms are all zero because each is of the form
$i \neq j$ and $k = m$	$M^3 - M^2$	$E\left[v_i^2 v_k v_m\right] = E\left[v_k v_m\right] = 0$ $k \neq m$
$i \neq j$ and $k \neq m$	$M^4 - 2M^3 + M^2$	Only terms of the type where $i = k$, $j = m$; and $i = m$, $j = k$ are non-zero. $2(M^2 - M)$ in number.

Table 1 Classification of Terms in Eq. (53)

In view of the information in Table 1, Eq. (53) reduces to

$$R_y(\tau) = M^2 + 4 \sum_{i=1}^{M} \sum_{j=i+1}^{M} E\left[v_i(t)\, v_i(t+\tau)\right] E\left[v_j(t)\, v_j(t+\tau)\right] \qquad (54)$$

From Eqs. (7) and (8), Eq. (54) becomes

$$R_y(\tau) = M^2 + 2(M^2 - M)\frac{4}{\pi^2}\left[\arcsin \rho(\tau)\right]^2 \qquad (55)$$

In Eq. (55), M^2 represents the squared average output of the squarer, and the second term is the one which represents the time-varying component of $y(t)$. By a development similar to that in Eqs. (41) through (46), it may be shown that

$$\sigma_z^2 = \omega_F \int_0^\infty R_y{}'(\tau)\, d\tau \qquad (56)$$

where $R_y{}'(\tau)$ is the second term in Eq. (55). Then

$$\sigma_z^2 = \frac{8}{\pi^2}\,\omega_F\,(M^2 - M)\int_0^\infty \left[\arcsin \rho(\tau)\right]^2 d\tau \qquad S << \langle N_i \rangle \qquad (57)$$

Since the clippers effectively normalize their inputs, σ_z^2 is not a function of the N_i and

$$\left\langle \sigma_z^2 \right\rangle = \sigma_z^2 \qquad (58)$$

The substitution of Eqs. (49), (57), and (58) into Eq. (40) yields the expression for R_2.

A2-21

$$R_2 = R_1 \frac{\pi}{2} \left[\frac{\langle N_i^2 \rangle + (M-1)\langle N_i \rangle^2}{(M-1)} \right]^{1/2} \left[\frac{\int_0^\infty \rho^2(\tau)\, d\tau}{\int_0^\infty \left[\arcsin \rho(\tau) \right]^2 d\tau} \right]^{1/2} \frac{1}{\langle N_i \rangle} \tag{59}$$

It should be remembered that only the first two terms in Eq. (49) are used in Eq. (59) and also the S in Eq. (40) is neglected. Furthermore, if M is reasonably large, the $\langle N_i^2 \rangle$ may be neglected in Eq. (59). Then

$$R_2 \cong K \frac{\pi}{2} R_1 \tag{60}$$

and K is the square root of the ratio of integrals in Eq. (59).

The integral terms in Eq. (59) remain to be evaluated. Three representative normalized autocorrelation functions are chosen in Eqs. (61), (62) and (63).

$$\rho_1(\tau) = \varepsilon^{-\omega_1 |\tau|} \tag{61}$$

$$\rho_2(\tau) = \varepsilon^{-\omega_2 |\tau|}(1 - \omega_2 |\tau|) \tag{62}$$

$$\rho_3(\tau) = \frac{1}{\sqrt{1-\zeta^2}} \varepsilon^{-\zeta \omega_3 |\tau|} \cos\left[\sqrt{1-\zeta^2}\, \omega_3 |\tau| + \cos^{-1}\sqrt{1-\zeta^2} \right] \tag{63}$$

$$\zeta < 1$$

The function $\rho_1(\tau)$ represents a process with a low-pass spectral density having a half-power frequency at ω_1; $\rho_2(\tau)$, a process with center frequency ω_2 and bandwidth $2\omega_2$; $\rho_3(\tau)$, a process with center frequency ω_3, and bandwidth $2\zeta\omega_3$.

Table 2 gives the exact value of the integral $\int_0^\infty \rho^2(\tau)\, d\tau$ for the three autocorrelation functions.

$\rho_1(\tau)$	$\rho_2(\tau)$	$\rho_3(\tau)$
$\dfrac{1}{2\omega_1}$	$\dfrac{1}{4\omega_2}$	$\dfrac{1}{4\xi\,\omega_3}$

$$\text{Table 2 \quad Values for } \int_0^\infty \rho^2(\tau)\ d\tau$$

It should be noticed that the integral yields the following general result in each case:

$$\int_0^\infty \rho^2(\tau)\ d\tau = \frac{1}{2\ (\text{process bandwidth})} \tag{64}$$

The evaluation of the integral involving the arcsin function is most easily accomplished by means of a series approximation.

$$\arcsin \rho(\tau) = \rho + \frac{1}{6}\rho^3 + \frac{3}{40}\rho^5 + \frac{5}{112}\rho^7 + \ldots \tag{65}$$

Squaring,

$$\left[\arcsin \rho(\tau)\right]^2 = \rho^2 + .333\,\rho^4 + .178\,\rho^6 + .114\,\rho^8 + \ldots \tag{66}$$

Evaluation of the integral $\int_0^\infty \left[\sin^{-1}\rho(\tau)\right]^2 d\tau$ using the first four terms of the series approximation of $\left[\sin^{-1}\rho(\tau)\right]^2$ yields the values listed in Table 3. The integration for $\rho_3(\tau)$ is accomplished by

A2-23

$\rho_1(\tau)$	$\rho_2(\tau)$	$(\mathcal{G} << 1)$ $\rho_3(\tau)$
$\dfrac{.63}{\omega_1}$	$\dfrac{.62}{2\omega_2}$	$\dfrac{.60}{2\mathcal{G}\,\omega_3}$

Table 3   Values for $\displaystyle\int_0^\infty \left[\sin^{-1}\rho(\tau)\right]^2 d\tau$

replacing the even powers of the cosine function in Eq. (63) by the average value of the function.[4]

$$\left\langle \cos^{2n}\left(\sqrt{1-\mathcal{G}^2}\;\omega_3\tau + \cos^{-1}\sqrt{1-\mathcal{G}^2}\right)\right\rangle = \frac{(2n)!}{2^{2n}(n!)^2} \tag{67}$$

This is an additional approximation, but the result should be accurate for low $\mathcal{G}$. It can be seen that the values for the arcsin integral are remarkably close, regardless of the nature of the autocorrelation function.

From Tables 2 and 3, the factor K is evaluated:

$$K = \left(\frac{.50}{.62}\right)^{1/2} = .90 \tag{68}$$

Combining Eq. (68) with Eq. (60), we have

$$\boxed{R_2 \cong 1.41\,R_1} \qquad\qquad \begin{array}{l} M >> 1 \\ \langle N_i \rangle >> S \end{array} \tag{69}$$

An obvious consequence of Eq. (69) is that the results for the normalized signal response ratio, R_1, in Figs. 3 and 4 may be applied directly to the determination of the ratio of signal-to-noise factors, R_2.

VI. Conclusions

The results in Section IV for the average signal response ratio, R_1, have shown that the system with clippers is superior to the system without clippers if the variation in transducer noisiness is fairly large. However, in the case of the continuous distribution for the noise powers, the value of R_1 is dependent to a great degree on the form of the probability density function that the N_i exhibit. Very little advantage is shown for most monotonic density functions, except the one which varies inversely with the noise power. This particular density function describes the situation in which the number of transducers having noise powers above the geometric mean of the extreme values is equal to the number having noise powers below the geometric mean.

Qualitatively, this result agrees with the result obtained for the two-valued discrete distribution of noise powers. Maximum benefit offered by the system with clippers is obtained when approximately half the transducers produce the lower noise power, and half produce the upper noise power.

The significant result of Section V is the effective equivalence of the two performance indices. From Eqs. (60) and (69), R_2 is just a multiple of R_1. The numerical factors entering into the multiplier are consequences of the types of elements used in processing the signals. The factor $\pi/2$ in Eq. (60) clearly arises from the presence of the infinite clippers, and the factor K arises from both the clipping and squaring operations.

A2-25

Finally, the result for R_2 is seen not to depend greatly on the autocorrelation function for the signal and noise. For the three different functions chosen, the results are essentially the same. The exact properties of the low-pass filter are not important, either, since the filtering effect is exactly the same for both systems.

References

1. Anderson, V. C., "Digital Array Phasing," J.A.S.A., 32, 867 (1960).

2. Rudnick, P., "Small Signal Detection in the Dimus Array," J.A.S.A., 32, 871 (1960).

3. Faran, J. J. and R. Hills, The Application of Correlation Techniques to Acoustic Receiving Systems, Acoustics Research Lab., Tech. Memo. No. 28, Harvard University, Nov. 1, 1952.

4. Thomas, J. B. and T. R. Williams, "On the Detection of Signals in Non-Stationary Noise by Product Arrays," J.A.S.A., 31, 453 (1959).

5. Middleton, D., "A Theoretical Evaluation of Directivity Patterns, Signal-to-Noise Ratios, and Expected Signal Accuracy in a DIMUS System," Appendix A, Raytheon Report, FR 176.

6. Davenport, W. B. and W. L. Root, An Introduction to the Theory of Random Signals and Noise, Ch.12, McGraw Hill, 1958.

7. Burington, R. S., Handbook of Mathematical Tables and Formulas, pp. 61,62 (Integrals 72 and 74), Handbook Publ., Inc.

General Dynamics/Electric Boat Research

(53-00-10-0231)

Progress Report No. 3

by

Peter M. Schultheiss

Dunham Laboratory
Yale University
New Haven, Connecticut
May, 1963

Department of Engineering and Applied Science

Yale University

General Dynamics/Electric Boat Research

(53-00-10-0231)

OPTIMAL DETECTION OF DIRECTIONAL GAUSSIAN SIGNALS

IN AN ISOTROPIC GAUSSIAN NOISE FIELD

by

Peter M. Schultheiss

May, 1963

SUMMARY

The performance of an optimal detector is compared with that of a standard detector; each uses the same array of hydrophones in an effort to detect the presence of a directional Gaussian signal in an isotropic Gaussian noise field. Output signal to noise ratio is used as a figure of merit. The following results are obtained:

1) If signal and noise both have flat power spectra of sufficient bandwidth so that the waveshapes received by different hydrophones are uncorrelated, then the optimum detector and standard detector are identical in performance.

2) If the noise spectrum is flat as in 1) but the signal spectrum is not, the optimal detector is better than the standard detector by an amount depending on the differences of the spectral properties of signal and noise.

3) If the signal and noise spectra are identical in shape the optimum detector is theoretically capable of detecting a signal with any desired degree of certainty in an arbitrarily small length of time. In practice the noise always contains more high frequency components than the signal. This phenomenon limits the improvement attainable through optimum detection to a moderate amount in most practical cases.

4) Knowledge of small differences in the shapes of signal and noise spectra is of limited value in detection.

5) Correlation between noise disturbances received by different hydrophones appears to degrade the performance of the standard

detector. One case of this type has been worked out in detail. It assumes a linear array of five hydrophones spaced at two-foot intervals and signal and noise spectra falling off with the second power of frequency above 1500 cps.

6) An attempt is made to estimate the probable high frequency behavior of the signal spectrum in order to set realistic bounds on detectability by means of the optimum system. Using a model for signal transmission due to Eckart, a range-dependent expression is obtained for the ratio of performance figures of optimal and standard detectors. At ranges of practical interest the ratio assumes values not larger than 8.

In general, if signal and noise are characterized only by total power and spectral properties, one is led to the conclusion that the optimal detector exhibits only a limited advantage over the standard detector unless the spectral properties of signal and noise differ drastically.

I. Introduction

This report deals with the problem of optimal detection of a weak directional signal in a very much stronger isotropic noise field by means of a given array of hydrophones. Both signal and noise are assumed to be Gaussian random processes with known power spectra. The investigation has two primary purposes:

1) To set bounds on the detectability of signals characterized only by their total power and spectral properties in a noise background similarly described. If a signal is not detectable with the instrumentation considered here, then it is not detectable at all with the given array unless additional properties of signal or noise are known.

2) To determine how far conventional data processing procedures fall below the optimum. As in many optimization problems, the best instrumentation may well be too complex for practical realization and serves primarily as a standard of comparison for more realistic procedures.

It is well known that the optimization problem described above is formally solved by a likelihood ratio detector. The physical realization of such a detector has been discussed by F. Bryn.[1] Bryn goes on to compare the performance of the optimal detector with that of standard detectors, primarily on the basis of a figure of merit which he designates as the "array gain," $G_n \equiv G(\omega_n)$. It may be defined as follows

$$G(\omega_n) = \left(\frac{\text{Contribution to average detector output of signal at frequency } \omega_n}{\text{Contribution to average detector output of noise at frequency } \omega_n} \right) \div \left(\begin{array}{l} \text{Input signal to} \\ \text{noise ratio at each} \\ \text{hydrophone at} \\ \text{frequency } \omega_n \end{array} \right)$$

---

[1]Finn Bryn, Optimal Signal Processing of Three Dimensional Arrays Operating on Gaussian Signals and Noise. J. of the Acoustical Society of America, Vol. 34 No. 3, March 1962, pp. 289-297.

The array gain is therefore a steady state (DC) performance criterion depending only on array geometry. For the purpose of the present discussion a more useful performance criterion is the signal to noise ratio at the output of the detector. Its computation will therefore be the first task.

II. Nomenclature

The first part of this report will draw heavily on Bryn's work and his nomenclature will therefore be used as far as practicable. Thus the signal $e_i(t)$ received by the ith hydrophone will be represented over the observation interval $0 \leq t \leq T$ by the Fourier series

$$e_i(t) = \sum_n \left[A_i(n) \cos \omega_n t + B_i(n) \sin \omega_n t \right]$$

where $\omega_n = \frac{2\pi n}{T}$ and the summation extends over all frequencies in the signal band. Signal and noise are assumed to be independent Gaussian processes with power spectra $S(\omega)$ and $N(\omega)$ respectively. Then if T is large compared to the correlation time of the signal and noise processes one can make the following statements:

a) $A_i(n)$ and $B_i(n)$ are Gaussian random variables with zero mean and variance $\left[S(\omega_n) + N(\omega_n) \right] \Delta\omega$, where $\Delta\omega = \frac{2\pi}{T}$

b) $A_i(n)$ is statistically independent of $A_j(m)$ for all j (including $j = i$) if $n \neq m$

c) $A_i(n)$ is statistically independent of $B_i(n)$

However, $A_i(n)$ is not in general independent of $A_j(n)$. For ease in later manipulation Bryn introduces the symbolism

$$x_i(n) = \begin{cases} A_i(n) & 1 \leq i \leq M \\ B_i(n) & M+1 \leq i \leq 2M \end{cases} \tag{1}$$

A3-4

M is the number of hydrophones in the array. The symbol $\langle\ \rangle_S$ is used to indicate the statistical average of the bracketed quantity when only signal is present. $\langle\ \rangle_N$ designates a similar average when only noise is present. Still following Bryn we define

$$\langle x_i(n)\ x_h(n)\rangle_S = S(\omega_n)\ \Delta\omega\ p_{ih}(n) \tag{2}$$

and

$$\langle x_i(n)\ x_h(n)\rangle_N = N(\omega_n)\ \Delta\omega\ q_{ih}(n) \tag{3}$$

Thus $p_{ih}(n)$ and $q_{ih}(n)$ are the elements of the normalized correlation matrices of signal and noise respectively:

$$P(n) = \begin{bmatrix} p_{11}(n) & \cdots & p_{1,M}(n) & p_{1,M+1}(n) & \cdots & p_{1,2M}(n) \\ \vdots & & \vdots & \vdots & & \vdots \\ p_{M,1}(n) & \cdots & p_{M,M}(n) & p_{M,M+1}(n) & \cdots & p_{M,2M}(n) \\ p_{M+1,1}(n) & \cdots & p_{M+1,M}(n) & p_{M+1,M+1}(n) & \cdots & p_{M+1,2M}(n) \\ \vdots & & \vdots & \vdots & & \vdots \\ p_{2M,1}(n) & \cdots & p_{2M,M}(n) & p_{2M,M+1}(n) & \cdots & p_{2M,2M}(n) \end{bmatrix}$$

$$\tag{4}$$

and

$$Q(n) = \begin{bmatrix} q_{11}(n) & \cdots & q_{1,M}(n) & q_{1,M+1}(n) & \cdots & q_{1,2M}(n) \\ \vdots & & \vdots & \vdots & & \vdots \\ q_{M,1}(n) & \cdots & q_{M,M}(n) & q_{M,M+1}(n) & \cdots & q_{M,2M}(n) \\ q_{M+1,1}(n) & \cdots & q_{M+1,M}(n) & q_{M+1,M+1}(n) & \cdots & q_{M+1,2M}(n) \\ \vdots & & \vdots & \vdots & & \vdots \\ q_{2M,1}(n) & \cdots & q_{2M,M}(n) & q_{2M,M+1}(n) & \cdots & q_{2M,2M}(n) \end{bmatrix}$$

$$\tag{5}$$

Finally it will be convenient to have symbols for the square matrices consisting of the first M rows and columns of Eqs. (4) and (5):

$$
P_1(n) = \begin{bmatrix} p_{11}(n) & \cdots & p_{1M}(n) \\ \vdots & & \vdots \\ p_{M1}(n) & \cdots & p_{MM}(n) \end{bmatrix} \tag{6}
$$

and

$$
Q_1(n) = \begin{bmatrix} q_{11}(n) & \cdots & q_{1M}(n) \\ \vdots & & \vdots \\ q_{M1}(n) & \cdots & q_{MM}(n) \end{bmatrix} \tag{7}
$$

The inverse of $Q(n)$, and hence of $Q_1(n)$, will be assumed to exist. Since $Q(n)$ is a correlation matrix this represents no significant restriction.

III. Optimum Detection

Bryn gives the likelihood ratio LR, the output of the optimum detector, as

$$
LR = 1 + \sum_n \left\{ W(\omega_n) - \langle W(\omega_n) \rangle_N \right\} \tag{8}
$$

where

$$
W(\omega_n) \equiv \frac{1}{2} \sum_{i=1}^{2M} \sum_{h=1}^{2M} \frac{S(\omega_n)\Delta\omega}{\left[N(\omega_n)\Delta\omega \right]^2} p_{ih}(n) \sum_{j=1}^{2M} \sum_{k=1}^{2M} \frac{Q_{ij}(n)}{|Q(n)|} \frac{Q_{kh}(n)}{|Q(n)|} x_j(n) x_k(n) \tag{9}
$$

$\dfrac{Q_{ij}(n)}{|Q(n)|}$ is the ji element of the matrix Q^{-1}.

The only term in Eq. (8) dependent on the signal and noise actually received by the various hydrophones is $\sum_n W(\omega_n)$. Hence the change in DC output due to the presence of a signal is simply

$$\Delta(\text{DC output}) = \frac{1}{2} \sum_n \left\langle W(\omega_n) \right\rangle_S$$

$$= \frac{1}{2} \sum_n \left[\frac{S(\omega_n)}{N(\omega_n)} \right]^2 \sum_{i=1}^{2M} \sum_{h=1}^{2M} \sum_{j=1}^{2M} \sum_{k=1}^{2M} p_{ih}(n) \frac{Q_{ij}(n)}{|Q(n)|} \frac{Q_{kh}(n)}{|Q(n)|} p_{jk}(n) \quad (10)$$

Using the fact that the matrices P and Q are symmetrical this expression can be written in the matrix form

$$\Delta(\text{DC output}) = \frac{1}{2} \sum_n \left[\frac{S(\omega_n)}{N(\omega_n)} \right]^2 \text{Tr}\left(P(n)\ Q^{-1}(n)\ P(n)\ Q^{-1}(n) \right)$$

$$= \frac{1}{2} \sum_n \left[\frac{S(\omega_n)}{N(\omega_n)} \right]^2 \text{Tr}\left\{ \left[P(n)\ Q^{-1}(n) \right]^2 \right\} \quad (11)$$

where $\text{Tr}\{\ \}$ is the trace of the indicated matrix.
Bryn has shown that

$$\sum_{i=1}^{2M} \sum_{h=1}^{2M} \sum_{j=1}^{2M} \sum_{k=1}^{2M} p_{ih}(n) \frac{Q_{ij}(n)}{|Q(n)|} \frac{Q_{kh}(n)}{|Q(n)|} p_{jk}(n) = 2 \left[\sum_{i=1}^{M} \sum_{j=1}^{M} \frac{Q_{ij}(n)}{|Q(n)|} p_{ij}(n) \right]^2$$

$$(12)$$

or in matrix form

$$\text{Tr}\left\{ \left[P(n)\ Q^{-1}(n) \right]^2 \right\} = 2\left\{ \text{Tr}\left[P_1(n)\ Q_1^{-1}(n) \right] \right\}^2 \quad (13)$$

A3-7

Hence Eq. (11) becomes

$$\Delta(\text{DC output}) = \sum_n \left\{ \frac{S(\omega_n)}{N(\omega_n)} \; \text{Tr} \left[P_1(n) \; Q_1^{-1}(n) \right] \right\}^2 \tag{14}$$

Next it is necessary to compute the rms fluctuation of the detector output. This quantity will be designated by the symbol D(output). If the input signal to noise ratio is very low, a condition already assumed in the derivation of Eq. (8), essentially all of the output fluctuation can be attributed to noise and the signal component can be ignored. Then

$$D^2(\text{output}) = \left\langle \left[\sum_n W(\omega_n) \right]^2 \right\rangle_N - \left[\sum_n \left\langle W(\omega_n) \right\rangle_N \right]^2 \tag{15}$$

From Eq. (9)

$$\left\langle \left[\sum_n W(\omega_n) \right]^2 \right\rangle_N = \frac{1}{4} \sum_n \sum_m \frac{S(\omega_n) \, \Delta\omega \, S(\omega_m) \, \Delta\omega}{N^2(\omega_n)(\Delta\omega)^2 \, N^2(\omega_m) \, \Delta\omega} \; \times$$

$$\sum_{\substack{i,j,h,k, \\ i',j',h',k' = 1}}^{2M} p_{ih}(n) \, p_{i'h'}(m) \, \frac{Q_{ij}(n)}{|Q(n)|} \, \frac{Q_{i'j'}(m)}{|Q(m)|} \, \frac{Q_{kh}(n)}{|Q(n)|} \, \frac{Q_{k'h'}(m)}{|Q(m)|} \, \left\langle x_j(n) \, x_k(n) \, x_{j'}(m) \, x_{k'}(m) \right\rangle_N$$

$$\tag{16}$$

Now since $\left[x_j(n), \; x_k(n), \; x_j(m), \; x_k(m) \right]$ is Gaussian in four dimensions

$$\left\langle x_j(n) \, x_k(n) \, x_j(m) \, x_k(m) \right\rangle_N =$$

$$\underbrace{\left\langle x_j(n) \, x_k(n) \right\rangle_N \left\langle x_j(m) \, x_k(m) \right\rangle_N}_{\text{term (1)}} + \underbrace{\left\langle x_j(n) \, x_j(m) \right\rangle_N \left\langle x_k(n) \, x_k(m) \right\rangle_N}_{\text{term (2)}} + \underbrace{\left\langle x_j(n) \, x_k(m) \right\rangle_N \left\langle x_k(n) \, x_j(m) \right\rangle_N}_{\text{term (3)}}$$

$$(17)[1]$$

---

[1] J. H. Laning and R. H. Battin, Random Processes in Automatic Control, pp. 82-84. McGraw-Hill Book Co., 1956.

The substitution of Eq. (17) into Eq. (16) leads to three terms that will be treated separately.

$$\left\langle x_j(n)\, x_k(n) \right\rangle_N \left\langle x_j(m)\, x_k(m) \right\rangle_N = q_{jk}(n)\, q_{jk}(m)\ N(\omega_n)\, \Delta\omega\, N(\omega_m)\, \Delta\omega \qquad (18)$$

Hence term (1) is

$$\frac{1}{4} \sum_n \sum_m \frac{S(\omega_n)\, \Delta\omega\, S(\omega_m)\, \Delta\omega}{N(\omega_n)\, \Delta\omega\, N(\omega_m)\, \Delta\omega} \quad \times$$

$$\sum_{\substack{i,j,h,k,\\ i',j',h',k' = 1}}^{2M} p_{ih}(n)\, p_{i'h'}(m)\, \frac{Q_{ij}(n)}{|Q(n)|}\, \frac{Q_{i'j'}(m)}{|Q(m)|}\, \frac{Q_{kh}(n)}{|Q(n)|}\, \frac{Q_{kh'}(m)}{|Q(m)|}\, q_{jk}(n)\, q_{j'k'}(m)$$

$$= \left\{ \frac{1}{2} \sum_n \frac{S(\omega_n)\, \Delta\omega}{N^2(\omega_n)(\Delta\omega)^2} \sum_{i,j,k,h = 1}^{2M} p_{ih}(n)\, \frac{Q_{ih}(n)}{|Q(n)|}\, \frac{Q_{kh}(n)}{|Q(n)|}\, q_{jk}(n) \right\}^2$$

$$= \left[\sum_n \left\langle W(\omega_n) \right\rangle_N \right]^2 \qquad (19)$$

The last step of this computation follows from inspection of Eq. (9). Returning to Eq. (17) and using conditions b) and c) on page 2

$$\left\langle x_j(n)\, x_{j'}(m) \right\rangle_N \left\langle x_k(n)\, x_{k'}(m) \right\rangle_N = \begin{cases} q_{jj'}(n)\, q_{kk'}(n)\, N^2(\omega_n)(\Delta\omega)^2 & m = n \\[2mm] 0 & m \neq n \end{cases}$$

$$(20)$$

Thus term (2) assumes the form

$$\frac{1}{4} \sum_n \left[\frac{S(\omega_n)}{N(\omega_n)}\right]^2 \sum_{\substack{i,j,h,k, \\ i',j',h',k'= 1}}^{2M} p_{ih}(n) \ p_{i'h'}(n) \ \frac{Q_{ij}(n)}{|Q(n)|} \ \frac{Q_{i'j'}(n)}{|Q(n)|} \ \frac{Q_{kh}(n)}{|Q(n)|} \ \frac{Q_{k'h'}(n)}{|Q(n)|} \ q_{jj'}(n) \ q_{kk'}(n)$$

$$= \frac{1}{4} \sum_n \left[\frac{S(\omega_n)}{N(\omega_n)}\right]^2 \ \text{Tr}\left[P(n) \ Q^{-1}(n) \ Q(n) \ Q^{-1}(n) \ P(n) \ Q^{-1}(n) \ Q(n) \ Q^{-1}(n)\right]$$

$$= \frac{1}{4} \sum_n \left[\frac{S(\omega_n)}{N(\omega_n)}\right]^2 \ \text{Tr}\left\{\left[P(n) \ Q^{-1}(n)\right]^2\right\}$$

$$= \frac{1}{2} \sum_n \left\{\frac{S(\omega_n)}{N(\omega_n)} \ \text{Tr}\left[P_1(n) \ Q_1^{-1}(n)\right]\right\}^2 \tag{21}$$

The last step results from Eq. (13).

Finally, returning once more to Eq. (17)

$$\left\langle x_j(n) \ x_k(m)\right\rangle_N \ \left\langle x_k(n) \ x_j(m)\right\rangle_N \ = \begin{cases} q_{jk'}(n) \ q_{kj'}(n) \ N^2(\omega_n)(\Delta\omega)^2 & m = n \\ \\ 0 & m \neq n \end{cases}$$

$$\tag{22}$$

Thus term (3) reduces to

$$\frac{1}{4} \sum_n \left[\frac{S(\omega_n)}{N(\omega_n)}\right]^2 \sum_{\substack{i,j,k,h, \\ i',j',k',h'=1}}^{2M} p_{ih}(n)\, p_{i'h'}(n)\, \frac{Q_{ij}(n)}{|Q(n)|}\, \frac{Q_{i'j'}(n)}{|Q(n)|}\, \frac{Q_{kh}(n)}{|Q(n)|}\, \frac{Q_{k'h'}(n)}{|Q(n)|}\, q_{jk}(n)\, q_{k'j'}(n)$$

$$= \frac{1}{4} \sum_n \left[\frac{S(\omega_n)}{N(\omega_n)}\right]^2 \mathrm{Tr}\left[P(n)\, Q^{-1}(n)\, Q(n)\, Q^{-1}(n)\, P(n)\, Q^{-1}(n)\, Q(n)\, Q^{-1}(n)\right]$$

$$= \frac{1}{2} \sum_n \left\{\frac{S(\omega_n)}{N(\omega_n)}\, \mathrm{Tr}\left[P_1(n)\, Q_1^{-1}(n)\right]\right\}^2 \tag{23}$$

Substituting Eqs. (19), (21) and (23) into Eq. (15) we obtain

$$D^2(\text{output}) = \sum_n \left\{\frac{S(\omega_n)}{N(\omega_n)}\, \mathrm{Tr}\left[P_1(n)\, Q_1^{-1}(n)\right]\right\}^2 \tag{24}$$

Equations (14) and (24) together determine the rms signal to noise ratio at the output of the detector

$$\frac{\Delta(\text{DC output})}{D(\text{output})} = \sqrt{\sum_n \left\{\frac{S(\omega_n)}{N(\omega_n)}\, \mathrm{Tr}\left[P_1(n)\, Q_1^{-1}(n)\right]\right\}^2} \tag{25}[1]$$

Equation (25) may be rewritten conveniently in terms of Bryn's "array gain"

$$G(\omega_n) = \sum_{i=1}^{M} \sum_{j=1}^{M} p_{ih}(n)\, \frac{Q_{ih}(n)}{|Q(n)|} \tag{26}$$

---

[1]This expression is similar to, but not identical with, an expression described by Bryn as the output signal to noise ratio (S_o). Since Bryn gives no derivation or physical definition for S_o it is not clear whether he is in fact referring to a closely related measure of performance.

A3-11

or in matrix form

$$G(\omega_n) = Tr\left[P_1(n)\, Q_1^{-1}(n) \right] \tag{27}$$

Hence Eq. (25) becomes

$$\frac{\Delta(DC\ output)}{D(output)} = \sqrt{\sum_n \left[\frac{S(\omega_n)}{N(\omega_n)}\ G(\omega_n) \right]^2} \tag{28}$$

The frequency index n ranges over the entire band to which the hydrophones are sensitive.

If T is sufficiently large so that the signal and noise spectra are essentially constant over a frequency interval of $\Delta\omega = \frac{2\pi}{T}$ rad/sec., Eq. (28) can be expressed in integral form

$$\frac{\Delta(DC\ output)}{D(output)} = \sqrt{\frac{T}{2\pi}}\sqrt{\sum_n \left[\frac{S(\omega_n)}{N(\omega_n)}\ G(\omega_n) \right]^2 \Delta\omega} \cong \sqrt{\frac{T}{2\pi}}\sqrt{\int_{\omega_1}^{\omega_2}\left[\frac{S(\omega)}{N(\omega)}\ G(\omega) \right]^2 d\omega} \tag{29}$$

ω_1 and ω_2 are respectively the lower and upper bounds of the frequency range being processed by the hydrophones.

Two special cases are of particular interest.

a) If signal and noise spectra are identical in shape, a situation closely resembling conditions encountered in practice if one ignores periodic components of signal and noise

$$\frac{\Delta(DC\ output)}{D(output)} \cong \sqrt{\frac{T}{2\pi}}\ \frac{S}{N}\sqrt{\int_{\omega_1}^{\omega_2}\left[G(\omega) \right]^2 d\omega} \tag{30}$$

A3-12

where $\bar{S} = \int_0^\infty S(\omega)\, d\omega$ and $N = \int_0^\infty N(\omega)\, d\omega$ represent the total signal

power and noise power respectively. At sufficiently high frequencies the correlation between noise disturbances received by different hydrophones tends to zero, that is

$$q_{ih}(n) \rightarrow \begin{cases} 1 & \text{for } i = h \\ 0 & \text{for } i \neq h \end{cases} \tag{31}$$

Then $Q_1(n)$ reduces to the identity matrix and $G(\omega_n) \rightarrow \text{Tr}\left[P_1(n)\right]$. Thus $G(\omega)$ approaches a positive constant so that Eq. (30) tends to infinity if one permits $\dot{\omega}_2$ to grow without bound. In other words, perfect detection is theoretically possible in a finite time under the stated conditions. This is not unreasonable, for the ratio of signal power to noise power is the same in any frequency band of a given width. Thus the optimum detector can be thought of as operating simultaneously on an infinite number of bands, extracting equally significant information concerning the presence of a signal from each. In practice, of course, the noise has components that do not fall off with frequency as rapidly as the signal so that the input signal to noise ratio $\dfrac{S(\omega)}{N(\omega)}$ tends to zero for sufficiently large ω. Noise electrically generated in the hydrophones or associated circuitry will certainly have this property even if the acoustical noise does not. Determination of the frequency at which the effective input signal to noise ratio begins to decline sharply is therefore an important practical problem.

b) If the hydrophones are sufficiently far apart so that $q_{ih}(n) \cong 0$ for all $i \neq h$ throughout the frequency range processed by the hydrophones, the array gain is simply $\text{Tr}\left[P_1(n)\right]$. If one further assumes that the array

A3-13

is linear and mechanically steered on target or that, for a general array, appropriate delays are introduced at each hydrophone to compensate for relative differences in distance to the target, then the elements of the P_1 matrix are all unity. It follows that the array gain is simply equal to M, the number of hydrophones in the array. In that case the output signal to noise ratio is

$$\frac{\Delta(\text{DC output})}{D(\text{output})} \cong \sqrt{\frac{T}{2\pi}} \ M \sqrt{\int_{\omega_1}^{\omega_2} \left[\frac{S(\omega)}{N(\omega)}\right]^2 d\omega} \tag{32}$$

The general expression for output signal to noise ratio $\left[\text{Eq. (29)}\right]$ also deserves some further comment. The linear dependence of detectability on $\sqrt{T}$ was, of course, to be expected on general statistical grounds. It is interesting, however, that knowledge of small differences in the shapes of signal and noise spectra contributes almost nothing to the detection process. Differences in spectral shape become important only if they result in a value of $\frac{S(\omega)}{N(\omega)}$ very much larger than $\frac{S}{N}$ over some frequency range. A case of this type would be one in which a finite amount of signal power is concentrated in a very narrow band (i.e., the signal contains a quasi-sinusoidal component). Because the integrand is squared Eq. (29) then leads to a large value of output signal to noise ratio even if the total power of the quasi-sinusoidal component is quite small. One must keep in mind, however, that the optimum detector now depends heavily on knowledge of the precise frequency range in which the quasi-sinusoidal signal component is located. In most practical situations it would probably be unrealistic to assume such knowledge. An interesting problem that has not been solved to date would be the determination of signal

A3-14

detectability in the sense of Eq. (29) when the signal contains one or more quasisinusoidal components whose frequencies are unknown, or at least not known accurately.

IV. Standard Detection

The performance of the optimum detector will now be compared with that of a standard detector using the same array of hydrophones. The standard detector simply adds the outputs of the various hydrophones, squares the sum and averages the resultant signal over a time interval T (see Fig. 1).
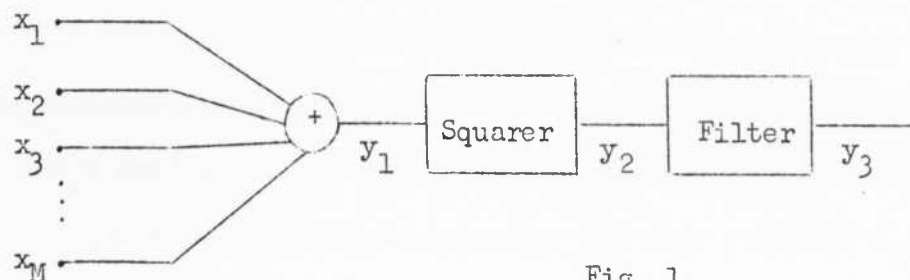

Fig. 1

Practical instrumentations frequently include · clippers and digital time delays. These are omitted here for two reasons:

1) It is desired to compare the likelihood ratio detector with the best version of the standard detector. Under the conditions assumed in this computation clipping and digital delay are known to degrade performance.

2) The degradation in performance due to clipping and digital delays has been discussed elsewhere[1] and it is therefore not necessary to introduce this added computational complexity here.

It will be assumed that the array has been steered "on target," so that the signal component $s(t)$ of each hydrophone output is the same. The

[1]P. Rudnick, Small Signal Detection in the Dimus Array. J. of the Acoustical Society of America, Vol. 32 No. 7, July 1960, pp. 871-877.

noise output of the ith hydrophone will be designated as $n_i(t)$. It is assumed to have zero mean and to be independent of $s(t)$. Then from Fig. 1 the DC component of y_3 is

$$E\left[y_3\right] = E\left\{\left[\sum_{i=1}^{M}\left(s(t) + n_i(t)\right)\right]^2\right\} = M^2 E\left\{\left[s(t)\right]^2\right\} + \sum_{i=1}^{M}\sum_{j=1}^{M}E\left[n_i(t)\, n_j(t)\right]$$

(33)

Thus the increase in DC output due to the signal is

$$\Delta(\text{DC output}) = M^2 E\left\{\left[s(t)\right]^2\right\} = M^2 \mathcal{S}$$

(34)

where $\mathcal{S}$ is again the average signal power at each hydrophone.

Calculation of the rms output fluctuation is perhaps accomplished most readily by integrating the continuous portion of the power spectrum $W_3(\omega)$ of y_3. For direct comparison with the optimal detector the smoothing filter will be defined simply as a device which averages $y_2(t)$ over T seconds. Its weighting function is therefore

$$h(t) = \begin{cases} \dfrac{1}{T} & 0 \leq t \leq T \\ 0 & \text{elsewhere} \end{cases}$$

(35)

By Fourier transforming one obtains the transfer function

$$H(\omega) = \frac{1}{T}\int_0^T e^{-j\omega t}\, dt = \frac{1 - \cos \omega t + j\, \sin \omega t}{j\omega T}$$

(36)

Hence

$$\left|H(\omega)\right|^2 = \frac{2 - 2\cos \omega T}{(\omega T)^2} = \left(\frac{\sin \dfrac{\omega T}{2}}{\dfrac{\omega T}{2}}\right)^2$$

(37)

A3-16

Therefore the variance of y_3 is

$$D^2(y_3) = \int_0^\infty W_2(\omega) \left(\frac{\sin \frac{\omega T}{2}}{\frac{\omega T}{2}} \right)^2 d\varphi \qquad (38)$$

where $W_2(\omega)$ is the power spectrum of y_2.

For low signal to noise ratios the smoothing time must be long compared to the inverse bandwidth of $W_2(\omega)$. Under these assumptions $W_2(\omega)$ in Eq. (38) can be considered constant at $W_2(0) = \lim_{\omega \to 0+} W_2(\omega)$. Thus

$$D^2(y_3) = W_2(0) \int_0^\infty \left(\frac{\sin \frac{\omega T}{2}}{\frac{\omega T}{2}} \right)^2 d\omega = \frac{\pi}{T} W_2(0) \qquad (39)$$

$W_2(0)$ is calculated most readily from the corresponding autocorrelation function $\psi_2(\tau)$

$$W_2(\omega) = \frac{1}{\pi} \int_{-\infty}^\infty \psi_2(\tau) \, e^{-j\omega t} \, d\tau \qquad (40)$$

Now $\psi_2(\tau) = E\left[y_2(t) \, y_2(t + \tau) \right]$

$$= \sum_{i=1}^M \sum_{j=1}^M \sum_{h=1}^M \sum_{k=1}^M E\left\{ \left[s(t) + n_i(t) \right] \left[s(t) + n_j(t) \right] \left[s(t + \tau) + n_h(t + \tau) \right] \right. \qquad \times$$

$$\left[s(t + \tau) + n_k(t + \tau) \right] \right\}$$

$$= \sum_{i=1}^M \sum_{j=1}^M \sum_{h=1}^M \sum_{k=1}^M E\left\{ s^2(t) \, s^2(t + \tau) \right.$$

$$+ s(t) \, s(t + \tau)\left[n_j(t) \, n_k(t + \tau) + n_i(t) \, n_h(t + \tau) \right] + s^2(t) \, n_h(t + \tau) \, n_k(t + \tau)$$

$$\left. + s^2(t + \tau) \, n_i(t) \, n_j(t) + n_i(t) \, n_j(t) \, n_h(t + \tau) \, n_k(t + \tau) \right\}$$

$$(41)$$

A3-17

The symbol $E\left\{\right\}$ is used to designate the mathematical expectation of the bracketed quantity.

The first term of Eq. (41) results from the intermodulation of signal with signal, the next three from intermodulation of signal with noise, and the last term from intermodulation of noise with noise. When the signal to noise ratio is low (the situation of primary interest) the last term dominates. One can therefore approximate

$$\psi_2(\tau) = \sum_{i=1}^{M} \sum_{j=1}^{M} \sum_{h=1}^{M} \sum_{k=1}^{M} E\left\{n_i(t)\ n_j(t)\ n_h(t+\tau)\ n_k(t+\tau)\right\} \quad (42)$$

An equivalent approximation was made by Bryn in the derivation of the likelihood ratio detector. When the noise is Gaussian, one can use Eq. (17) to express Eq. (42) in the form

$$E\left\{n_i(t)n_j(t)n_h(t+\tau)n_k(t+\tau)\right\}$$
$$= E\left\{n_i(t)n_j(t)\right\} E\left\{n_h(t+\tau)n_k(t+\tau)\right\} + E\left\{n_i(t)n_h(t+\tau)\right\} E\left\{n_j(t)n_k(t+\tau)\right\}$$
$$+ E\left\{n_i(t)n_k(t+\tau)\right\} E\left\{n_j(t)n_h(t+\tau)\right\} \quad (43)$$

Introducing the nomenclature

$$E\left\{n_i(t)\ n_j(t+\tau)\right\} = N\ q_{ij}(\tau) \quad (44)$$

Eq. (43) becomes

$$E\left\{n_i(t)\ n_j(t)\ n_h(t+\tau)\ n_k(t+\tau)\right\} = N^2\left[q_{ij}(0)\ q_{hk}(0) + q_{ih}(\tau)\ q_{jk}(\tau)\right.$$
$$\left. + q_{ik}(\tau)\ q_{jh}(\tau)\right] \quad (45)$$

A3-18

N is the average noise power at each hydrophone (as in part III) and $q_{ij}(\tau)$ is the normalized crosscorrelation between the noise components at hydrophones i and j. Using Eqs. (39), (40), (42) and (45) and recognizing that the term $q_{ij}(0)\, q_{hk}(0)$ contributes only DC power, one obtains

$$D^2(y_3) = \frac{2N^2}{T} \sum_{i=1}^{M} \sum_{j=1}^{M} \sum_{h=1}^{M} \sum_{k=1}^{M} \int_{-\infty}^{\infty} q_{ih}(\tau)\, q_{jk}(\tau)\, d\tau \qquad (46)$$

Hence the figure of merit corresponding to Eq. (29) is

$$\frac{\Delta(\text{DC output})}{D(y_3)} = \frac{M^2 S}{\left[\dfrac{2N^2}{T} \displaystyle\sum_{i=1}^{M} \sum_{j=1}^{M} \sum_{h=1}^{M} \sum_{k=1}^{M} \int_{-\infty}^{\infty} q_{ih}(\tau)\, q_{jk}(\tau)\, d\tau\right]^{1/2}}$$

$$= \frac{S}{N} \sqrt{\frac{T}{2}} \; \frac{M^2}{\left[\displaystyle\sum_{i=1}^{M} \sum_{j=1}^{M} \sum_{h=1}^{M} \sum_{k=1}^{M} \int_{-\infty}^{\infty} q_{ih}(\tau)\, q_{jk}(\tau)\, d\tau\right]^{1/2}} \qquad (47)$$

Thus the figure of merit depends rather critically on $\displaystyle\int_{-\infty}^{\infty} q_{ih}(\tau)\, q_{jk}(\tau)\, d\tau$.

Two cases will be considered.

1) Uncorrelated Noise

If the hydrophones are separated sufficiently so that $q_{ih}(\tau) = 0$ for $i \neq h$, then

$$\int_{-\infty}^{\infty} q_{ih}(\tau)\, q_{jk}(\tau)\, d\tau = \begin{cases} \displaystyle\int_{-\infty}^{\infty} \rho^2(\tau)\, d\tau & i = h,\; j = k \\[2mm] 0 & \text{elsewhere} \end{cases} \qquad (48)[1]$$

---

[1] This corresponds to the assumptions made in Progress Report No. 2.

$\rho(\tau) \equiv q_{ii}(\tau)$ is the normalized autocorrelation function of the noise at each hydrophone. When Eq. (48) is satisfied

$$\frac{\Delta(\text{DC output})}{D(y_3)} = \frac{S}{N} \sqrt{\frac{T}{2}} \frac{M}{\left[\int_{-\infty}^{\infty} \rho^2(\tau) \, d\tau \right]^{1/2}} \tag{49}$$

The equivalent result for the likelihood ratio detector is Eq. (32).

A typical situation in which Eq. (48) is at least approximately satisfied would be the following: The noise has a power spectrum flat over a wide band $0 \leq \omega \leq \omega_a$ and vanishing for $\omega > \omega_a$. Then

$$\rho(\tau) = \frac{\sin \omega_a \tau}{\omega_a \tau} , \quad \omega_a \text{ large} \tag{50}$$

Thus

$$\int_{-\infty}^{\infty} \rho^2(\tau) \, d\tau = \int_{-\infty}^{\infty} \frac{\sin^2 \omega_a \tau}{(\omega_a \tau)^2} \, d\tau = \frac{\pi}{\omega_a} \tag{51}$$

Hence Eq. (49) assumes the form

$$\frac{\Delta(\text{DC output})}{D(y_3)} = \frac{S}{N} \sqrt{\frac{T\omega_a}{2\pi}} \, M \tag{52}$$

Introducing the symbol $N_o = \dfrac{N}{\omega_a}$, the value of the noise spectral density for $0 \leq \omega \leq \omega_a$

$$\frac{\Delta(\text{DC output})}{D(y_3)} = \frac{S}{N_o} \sqrt{\frac{T}{2\pi}} \frac{1}{\sqrt{\omega_a}} \, M \tag{53}$$

If the frequency range being processed by the optimum detector coincides with $0 \leq \omega \leq \omega_a$, Eq. (32) can be written in the following form $\left[\text{for} \right.$ $\left. N(\omega) = N_o, \quad 0 \leq \omega \leq \omega_a \right]$

A3-20

$$\frac{\Delta(\text{DC output})}{D(\text{output})} = \frac{S}{N_o} \sqrt{\frac{T}{2\pi}} \; M \sqrt{\int_0^{\omega_a} \left[\frac{S(\omega)}{S}\right]^2 d\omega} \tag{54}$$

The ratio of the two figures of merit is

$$\frac{\text{performance index of optimum detector}}{\text{performance index of standard detector}} = \sqrt{\frac{\omega_a}{S^2} \int_0^{\omega_a} \left[S(\omega)\right]^2 d\omega} \tag{55}$$

The reason for terminating the processing range of the optimum detector at ω_a is almost certainly that virtually all of the signal power is concentrated in the range $0 \leq \omega \leq \omega_a$. Thus it is reasonable to assume that

$$\int_0^{\omega_a} S(\omega) \; d\omega = S \tag{56}$$

If one expresses the spectral function by

$$S(\omega) = \frac{S}{\omega_a} + F(\omega)$$

then Eq. (56) demands

$$\int_0^{\omega_a} F(\omega) \; d\omega = 0$$

It follows that

$$\int_0^{\omega_a} \left[S(\omega)\right]^2 d\omega = \int_0^{\omega_a} \left[\frac{S^2}{\omega_a^2} + 2\frac{S}{\omega_a} F(\omega) + F^2(\omega)\right] d\omega$$

$$= \frac{S^2}{\omega_a} + \int_0^{\omega_a} F^2(\omega) \; d\omega \geq \frac{S^2}{\omega_a} \tag{57}$$

A3-21

with equality if and only if $S(\omega) = \dfrac{S}{\omega_a}$.

When $S(\omega) = \dfrac{S}{\omega_a}$ the ratio of the performance indices $\left[$ Eq. (55)$\right]$ is

unity. In general, therefore,

$$\frac{\text{performance index of optimum detector}}{\text{performance index of standard detector}} \geq 1 \qquad (58)$$

Thus if the signal as well as the noise has properties of white noise bandlimited to $0 \leq \omega \leq \omega_a$ the optimum detector is identical in performance with the standard detector. If the signal has different spectral properties the optimum detector makes use of these properties to improve performance while the standard detector is only sensitive to total signal power.

2) Markov Noise

If the crosscorrelation between hydrophones does not vanish, additional terms in the quadruple sum of Eq. (47) must be considered. Assuming that the noise at each hydrophone consists primarily of far field noise, a reasonable approximation to the noise autocorrelation function might be

$$\rho(\tau) = e^{-\omega_o |\tau|} \qquad (59)$$

ω_o is the frequency (in radians per second) at which the noise spectrum has fallen to half of its low frequency value. Where numerical computations are called for the numerical value $\omega_o = 2\pi \times 1500 = 9420$ radians/second will be used.

The problem of computing $q_{ih}(\tau)$ from $\rho(\tau)$ has been discussed in Progress Report No. 1. With a spherically isotropic noise field the required relation is

$$q_{ih}(\tau) = \frac{1}{2\tau_{ih}} \int_{\tau-\tau_{ih}}^{\tau+\tau_{ih}} \rho(\tau) \; d\tau \qquad (60)$$

where $\tau_{ih} = \dfrac{d_{ih}}{c}$. d_{ih} is the distance between the ith and h^{th} hydrophones (a non-negative quantity) and c is the velocity of sound in water.

Substituting Eq. (59) into Eq. (60) one obtains by straightforward computation

$$q_{ih}(\tau) = \begin{cases} \dfrac{1}{\omega_o \, \tau_{ih}} \left[1 - e^{-\omega_o \tau_{ih}} \cosh \omega_o \tau \right] & |\tau| \le \tau_{ih} \\[4mm] \dfrac{1}{\omega_o \tau_{ih}} \, e^{-\omega_o |\tau|} \sinh \omega_o \, \tau_{ih} & |\tau| \ge \tau_{ih} \end{cases}$$

(61)

$q_{ih}(\tau)$ is evidently non-negative for all values of τ and τ_{ih}. Thus all terms in the fourfold sum of Eq. (47) are non-negative. It follows that noise coherence from hydrophone to hydrophone (at least of the type assumed here) can only reduce the figure of merit relative to the value given by Eq. (49).

The computation of $\displaystyle\int_{-\infty}^{\infty} q_{ih}(\tau) \, q_{jk}(\tau) \, d\tau$ is tedious but straightforward.

Assuming $\tau_{jk} \ge \tau_{ih}$ and taking advantage of the fact that $q_{ih}(\tau)$ is an even function of τ one obtains

$$\int_{-\infty}^{\infty} q_{ih}(\tau) \, q_{jk}(\tau) \, d\tau =$$

$$\frac{2}{\omega_o^2 \, \tau_{ih} \, \tau_{jk}} \int_0^{\tau_{ih}} \left[1 - e^{-\omega_o \tau_{ih}} \cosh \omega_o \tau \right] \left[1 - e^{-\omega_o \tau_{jk}} \cosh \omega_o \tau \right] d\tau$$

$$+ \frac{2}{\omega_o^2 \, \tau_{ih} \, \tau_{jk}} \int_{\tau_{ih}}^{\tau_{jk}} e^{-\omega_o \tau} \sinh \omega_o \, \tau_{ih} \left[1 - e^{-\omega_o \tau_{jk}} \cosh \omega_o \tau \right] d\tau$$

$$+ \frac{2}{\omega_o^2 \, \tau_{ih} \, \tau_{jk}} \int_{\tau_{jk}}^{\infty} e^{-2\omega_o \tau} \sinh \omega_o \, \tau_{ih} \sinh \omega_o \, \tau_{jk} \, d\tau \qquad (62)$$

A3-23

After integration and some algebraic manipulation this becomes

$$\int_{-\infty}^{\infty} q_{ih}(\tau)\, q_{jk}(\tau)\, d\tau =$$

$$\frac{2}{\omega_o^2\, \tau_{ih}\, \tau_{jk}} \left\{ \tau_{ih} - \frac{1}{\omega_o} \left(e^{-\omega_o \tau_{ih}} + e^{-\omega_o \tau_{jk}} \right) \sinh \omega_o \tau_{ih} \right.$$

$$+ \frac{1}{2} e^{-\omega_o(\tau_{ih}+\tau_{jk})} \left(\frac{1}{\omega_o} \sinh \omega_o \tau_{ih} \cosh \omega_o \tau_{ih} + \tau_{ih} \right)$$

$$+ \frac{1}{\omega_o} \sinh \omega_o \tau_{ih} \left(e^{-\omega_o \tau_{ih}} - e^{-\omega_o \tau_{jk}} \right)$$

$$- \frac{1}{2} e^{-\omega_o \tau_{jk}} \sinh \omega_o \tau_{ih} \left[\tau_{jk} - \tau_{ih} + \frac{1}{2\omega_o} \left(e^{-2\omega_o \tau_{ih}} - e^{-2\omega_o \tau_{jk}} \right) \right]$$

$$\left. + \frac{1}{2\omega_o} \sinh \omega_o \tau_{ih} \sin \omega_o \tau_{jk}\, e^{-2\omega_o \tau_{jk}} \right\} \qquad (63)$$

For numerical values likely to occur in practice this equation can be simplified considerably. If the minimum distance between hydrophones is 2 feet and one uses $c = 4750$ ft/sec, $\tau_{ih} \geq \frac{2}{4750} = 4.21 \times 10^{-4}$ sec. for $i \neq h$. With $\omega_o = 9420$ rad/sec, $\omega_o \tau_{ih} \geq 3.97$ for $i \neq h$. Hence the approximation

$$\sinh \omega_o \tau_{ih} \cong \cosh \omega_o \tau_{ih} \cong \frac{1}{2} e^{\omega_o \tau_{ih}} \quad , \quad i \neq h \qquad (64)$$

introduces negligible error. Using Eq. (64) and discarding terms of order $e^{-2\omega_o \tau_{ih}}$ and smaller, one obtains

A3-24

$$\int_{-\infty}^{\infty} q_{ih}(\tau) \, q_{jk}(\tau) \, d\tau \cong$$

$$\frac{2}{\omega_o^2 \, \tau_{ih} \, \tau_{jk}} \left\{ \tau_{ih} - \frac{1}{2\omega_o} \left[1 + e^{-\omega_o(\tau_{jk}-\tau_{ih})} \right] + \frac{1}{8\omega_o} e^{-\omega_o(\tau_{jk}-\tau_{ih})} \right.$$

$$\left. + \frac{1}{2\omega_o} \left[1 - e^{-\omega_o(\tau_{jk}-\tau_{ih})} \right] - \frac{1}{4} e^{-\omega_o(\tau_{jk}-\tau_{ih})} (\tau_{jk} - \tau_{ih}) + \frac{1}{8\omega_o} e^{-\omega_o(\tau_{jk}-\tau_{ih})} \right\}$$

$$= \frac{2}{\omega_o^2 \, \tau_{jk}} \left\{ 1 - \frac{1}{4\omega_o \, \tau_{ih}} e^{-\omega_o(\tau_{jk}-\tau_{ih})} \left[3 + \omega_o(\tau_{jk} - \tau_{ih}) \right] \right\}, \quad i \neq h \, , \, j \neq k$$

$$\tag{65}$$

when $\tau_{jk} = \tau_{ih}$ this reduces to

$$\int_{-\infty}^{\infty} q_{ih}(\tau) \, q_{jk}(\tau) \, d\tau \cong \frac{2}{\omega_o^2 \, \tau_{jk}} \left\{ 1 - \frac{3}{4\omega_o \, \tau_{ih}} \right\} , \quad i \neq h, \, j \neq k, \, \tau_{jk} = \tau_{ih} \tag{66}$$

Similar expressions must now be obtained for the cases $i = h$, $j = k$ and $i = h$, $j \neq k$.

$$\int_{-\infty}^{\infty} q_{ii}(\tau) \, q_{jj}(\tau) \, d\tau = \int_{-\infty}^{\infty} e^{-2\omega_o|\tau|} d\tau = \frac{1}{\omega_o} \tag{67}$$

A3-25

$$\int_{-\infty}^{\infty} q_{ii}(\tau) \, q_{jk}(\tau) \, d\tau = 2 \int_{0}^{\infty} q_{ii}(\tau) \, q_{jk}(\tau) \, d\tau$$

$$= \frac{2}{\omega_o \, \tau_{jk}} \int_{0}^{\tau_{jk}} \left(1 - e^{-\omega_o \tau_{jk}} \cosh \omega_o \tau \right) e^{-\omega_o \tau} \, d\tau + \frac{2}{\omega_o \, \tau_{jk}} \int_{\tau_{jk}}^{\infty} e^{-2\omega_o \tau} \sinh \omega_o \, \tau_{jk} \, d\tau$$

$$= \frac{2}{\omega_o^2 \, \tau_{jk}} \left[1 - e^{-\omega_o \tau_{jk}} \left(1 + \frac{1}{2} \omega_o \, \tau_{jk} \right) \right] \tag{68}$$

Results for Linear Array with Equally Spaced Elements

All of the terms of the fourfold sum in Eq. (47) are now available and the evaluation of the output signal to noise ratio becomes in principle a straightforward computational problem. Unfortunately the number of terms grows very rapidly with M and manual computation quickly becomes impractical unless some simplifications are made. A configuration leading to particularly simple results is a linear array with equally spaced elements. Here

$$\tau_{ih} = |i - h| \, \tau_o \tag{69}$$

where τ_o is the time required by a sound wave to traverse the distance between adjacent hydrophones.

If one uses the notation

$$\int_{-\infty}^{\infty} q_{ih}(\tau) \, q_{jk}(\tau) \, d\tau = C_{i,h,j,k} \tag{70}$$

then for the array satisfying Eq. (69)

$$C_{i,h,j,k} = C_{|i-h|,|j-k|} \tag{71}$$

i.e., the coefficients of the fourfold sum can be characterized effectively by two rather than four subscripts. With the change of variable

$$i - h = \ell \tag{72}$$

the sum becomes

$$\sum_{i,j,h,k = 1}^{M} C_{i,h,j,k} = \sum_{i,j,h,k = 1}^{M} C_{|i-h|, |j-k|}$$

$$= \sum_{j,k = 1}^{M} M \, C_{o,|j-k|} + 2 \sum_{j,k = 1}^{M} \sum_{\ell = 1}^{M-1} (M - \ell) C_{\ell, |j-k|} \tag{73}$$

A scheme for counting the number of identical terms for each value of ℓ is indicated in Fig. 2.

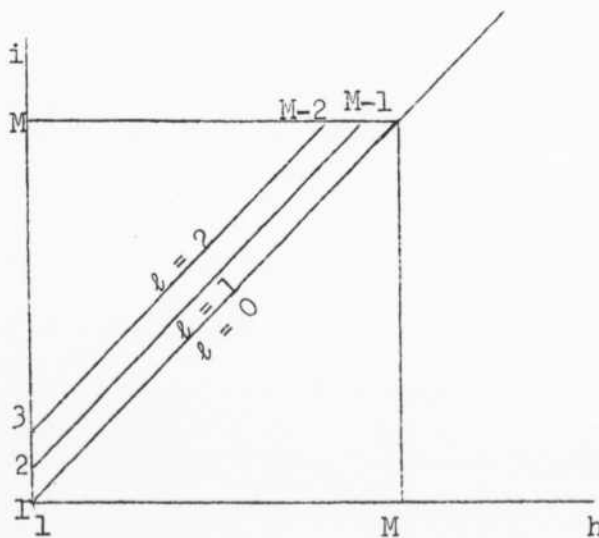
Fig. 2

The further change of variable

$$|j - k| = s \qquad (74)$$

leads to the form

$$\sum_{i,j,h,k = 1}^{M} C_{i,h,j,k} = M^2 C_{0,0} + 2M \sum_{s=1}^{M-1} (M - s)\, C_{0,s} + 2M \sum_{\ell=1}^{M-1} (M - \ell)\, C_{\ell,0}$$

$$+ 4 \sum_{\ell=1}^{M-1} \sum_{s=1}^{M-1} (M - \ell)(M - s)\, C_{\ell,s}$$

$$= M^2 C_{0,0} + 4M \sum_{s=1}^{M-1} (M - s)\, C_{0,s} + 4 \cdot \sum_{\ell=1}^{M-1} \sum_{s=1}^{M-1} (M - \ell)(M - s) C_{\ell,s}$$

$$(75)$$

The coefficients $C_{0,0}$, $C_{0,s}$ and $C_{\ell,s}$ are given by Eqs. (67), (68), and (65) respectively (with $\tau_{jk} = s\tau_0$, $\tau_{ih} = \ell\tau_0$).

A further considerable simplification can be made if we recognize that for the numerical values introduced on page 22 ($\omega_0 = 9420$ rad./sec., hydrophone spacing $\tau_0 = 2$ ft.), $\omega_0 \tau_0 = 3.97$. Hence $e^{-\omega_0 \tau_0} = 0.0189$, so that the exponential terms in the definitions of the coefficients $C_{\ell,s}$ can be omitted with only very minor error. Then

$$C_{0,0} = \frac{1}{\omega_0} \qquad (76)$$

$$C_{0,s} \cong \frac{1}{\omega_0} \frac{2}{s\omega_0 \tau_0} \qquad s \neq 0 \qquad (77)$$

$$
C_{\ell,s} \cong \begin{cases}
\dfrac{1}{\omega_o}\,\dfrac{2}{s\omega_o\tau_o}\,, & s > \ell \\[2ex]
\dfrac{1}{\omega_o}\,\dfrac{2}{\ell\omega_o\tau_o}\,, & \ell > s \\[2ex]
\dfrac{1}{\omega_o}\,\dfrac{2}{s\omega_o\tau_o}\left(1 - \dfrac{3}{4\omega_o\tau_o s}\right), & s = \ell
\end{cases} \quad \left. \right\} \; s,\ell \neq 0 \qquad (78)
$$

Now

$$
\sum_{i,h,j,k\,=\,1}^{M} C_{|i-h|,\,|j-k|} \cong
$$

$$
\frac{1}{\omega_o}\left\{ M^2 + 8M\sum_{s=1}^{M-1}\frac{M-s}{s\omega_o\tau_o} + 4\sum_{s=1}^{M-1}(M-s)^2\frac{2}{s\omega_o\tau_o}\left(1-\frac{3}{4\omega_o\tau_o s}\right) \right.
$$

$$
\left. + 4\sum_{s=2}^{M-1}\sum_{\ell=1}^{s-1}(M-\ell)(M-s)\frac{2}{s\omega_o\tau_o} + 4\sum_{\ell=2}^{M-1}\sum_{s=1}^{\ell-1}(M-\ell)(M-s)\frac{2}{\ell\omega_o\tau_o} \right\}
$$

$$
= \frac{1}{\omega_o}\left\{ M^2 + \frac{8}{\omega_o\tau_o}\left[M\sum_{s=1}^{M-1}\frac{M-s}{s} + \sum_{s=1}^{M-1}\frac{(M-s)^2}{s}\left(1-\frac{3}{4\omega_o\tau_o s}\right) \right. \right.
$$

$$
\left. \left. + 2\sum_{s=2}^{M-1}\sum_{\ell=1}^{s-1}\frac{(M-\ell)(M-s)}{s} \right] \right\} \qquad (79)
$$

Hence the figure of merit of Eq. (47) is

$$
\frac{\Delta(\text{DC output})}{D(y_3)} \cong
$$

$$
\frac{S}{N}\sqrt{\frac{T\omega_o}{2}}\,\frac{M}{\left\{ 1 + \dfrac{8}{\omega_o\tau_o}\left[\dfrac{1}{M}\displaystyle\sum_{s=1}^{M-1}\dfrac{M-s}{s} + \dfrac{1}{M^2}\displaystyle\sum_{s=1}^{M-1}\dfrac{(M-s)^2}{s}\left(1-\dfrac{3}{4\omega_o\tau_o s}\right) + \dfrac{2}{M^2}\displaystyle\sum_{s=2}^{M-1}\displaystyle\sum_{\ell=1}^{s-1}\dfrac{(M-\ell)(M-s)}{s}\right]\right\}^{\frac{1}{2}}}
$$

$$(80)$$

Discussion

a) If $\omega_o \tau_o \ggg 1$, $C_{\ell,s} \cong 0$ unless $s = \ell = 0$. In this case (noise components at different hydrophones uncorrelated) Eq. (80) reduces to the simple form

$$\frac{\Delta(\text{DC output})}{D(y_3)} = \frac{S}{N} \sqrt{\frac{T\omega_o}{2}} \quad M \tag{81}$$

This expression is similar in form to Eq. (52), but differs by a numerical constant because the noise spectrum has a different shape than that assumed in the earlier computation.

b) If $\omega_o \tau_o = 3.97$, $\omega_o = 9420$ rad./sec., as assumed earlier, and $M = 5$, the figure of merit becomes

$$\frac{\Delta(\text{DC output})}{D(y_3)} = 129 \frac{S}{N} \sqrt{T} \tag{82}$$

If signal and noise spectra have the same shape, the output signal to noise ratio for the optimum detector using the same 5-element linear array with 2-foot hydrophone spacing is from Eq. (30):

$$\frac{\Delta(\text{DC output})}{D(\text{output})} = \sqrt{\frac{T}{2\pi}} \frac{S}{N} \sqrt{\int_0^{\omega_2} [G(\omega)]^2 \, d\omega} \tag{83}$$

Bryn has plotted the array gain for a five-element equally spaced linear array. Adapting his plot to the parameters used in this computation one finds that $G(\omega)$ has essentially reached its maximum value of 5 at $\omega = 7500$ rad./sec. Making a rough approximation to the curve below that frequency, one obtains the following numerical expression for output signal to noise ratio in terms of the frequency ω_2

$$\frac{\Delta(\text{DC output})}{D(\text{output})} \cong \sqrt{\frac{T}{2\pi}} \ \frac{S}{N} \ \sqrt{25 \ \omega_2 - 5.55 \times 10^3} \qquad (84)$$

If $\omega_2 = 2\pi \times 5000 = 31,000$ rad./sec., this reduces to

$$\frac{\Delta(\text{DC output})}{D(\text{output})} \cong 340 \ \frac{S}{N} \ \sqrt{T} \qquad (85)$$

If $\omega_2 = 2\pi \times 10,000 = 62,800$ rad./sec., the corresponding value is

$$\frac{\Delta(\text{DC output})}{D(\text{output})} \cong 490 \ \frac{S}{N} \ \sqrt{T} \qquad (86)$$

Thus the rms output signal to noise ratio of the optimal detector is better than that of the standard detector by a factor of about 2.6 if the range of frequencies processed by the optimum detector extends to 5000 cps and by a factor of about 3.8 if the processed range extends to 10,000 cps.[1] Which, if either, of these figures is realistic depends on the frequency range over which the assumed equality in shape of signal and noise spectra corresponds reasonably well to the actual facts.

c) In order to remove the somewhat arbitrary upper bound ω_2 of the frequency range processed by the optimum detector, an attempt will be made to gain more insight into the probably high frequency behavior of the signal spectrum. One factor that should undoubtedly be considered is the frequency dependence of the transmission characteristics of water. Using a model discussed by Eckart[2] one can write the following expression for the signal spectrum received at each hydrophone

---

[1]No band limitation was assumed in the standard detector.

[2]C. Eckart, Optimal Rectifier Systems for the Detection of Steady Signals. University of Califomia, Marine Physics Laboratory of the Scripps Institution of Oceanography, SIO Reference 52-11, 4 March 1952, p. 13, Eq. (18).

A3-31

$$\text{Received spectrum} = \frac{10^6}{r^2} e^{-6 \times 10^{-14} r \omega^2} S(\omega) \qquad (87)$$

$S(\omega)$ is the signal spectrum at a point close to the target and r is the target range in yards. Assuming $S(\omega)$ and $N(\omega)$ identical in shape, one obtains from Eq. (29)

$$\frac{\Delta(\text{DC output})}{D(\text{output})} = \sqrt{\frac{T}{2\pi}} \; \frac{S}{N} \; \frac{10^6}{r^2} \sqrt{\int_0^\infty e^{-12 \times 10^{-14} r \omega^2} \left[G(\omega)\right]^2 d\omega} \qquad (88)$$

$S = \int_0^\infty S(\omega) \, d\omega$ is the signal power at the reference point. Evaluation of the integral is cumbersome because of frequency dependence of $G(\omega)$. However, since $G(\omega)$ only varies from a minimum of 3.55 near $\omega = 0$ to a maximum of 5 above $\omega = 7500$ rad./sec., a reasonable approximation can be obtained by treating it as a constant. Then

$$\frac{\Delta(\text{DC output})}{D(\text{output})} \cong \frac{S}{N} \sqrt{T} \; G \; \frac{6.41 \times 10^8}{r^{9/4}} \qquad (89)$$

For $G = 4$ this is

$$\frac{\Delta(\text{DC output})}{D(\text{output})} \cong \frac{2.56 \times 10^9}{r^{9/4}} \; \frac{S}{N} \sqrt{T} \qquad (90)$$

For $G = 5$ the value is

$$\frac{\Delta(\text{DC output})}{D(\text{output})} \cong \frac{3.20 \times 10^9}{r^{9/4}} \; \frac{S}{N} \sqrt{T} \qquad (91)$$

Except at extreme ranges (above 10^5 yards) Eq. (91) should be the better approximation and will be used in further comparisons.

A3-32

For the standard detector the shape of the signal spectrum is unimportant; only the total signal power matters. Hence the factor $e^{-6\times10^{-14}r\omega^2}$ can be ignored if it is essentially equal to unity over the effective bandwidth of the signal spectrum. This is true if

$$6 \times 10^{-14} \times 1500 \times 2\pi r \ll 1$$

or

$$r \ll 1.89 \times 10^5 \tag{92}$$

Then the figure of merit for the standard detector becomes $\left[\text{from Eq. (82)}\right]$

$$\frac{\Delta(\text{DC output})}{D(y_3)} = \frac{1.29 \times 10^8}{r^2} \ \frac{S}{N} \ \sqrt{T} \tag{93}$$

The ratio of Eqs. (91) and (93) assumes the form

$$\frac{\text{rms signal to noise ratio of optimal detector}}{\text{rms signal to noise ratio of standard detector}} = \frac{24.8}{r^{1/4}} \ , \ r \ll 1.89 \times 10^5 \tag{94}$$

Thus even at a range of 100 yards the possible improvement due to the use of optimal detection procedures is limited to a factor of somewhat less than 8. (If the assumption of low signal to noise ratio remains valid.)

V. Concluding Remarks

The report has compared the performance of a likelihood ratio detector with that of a standard detector on the basis of output signal to noise ratio. Under the conditions investigated, the improvement attainable through use of optimal (likelihood ratio) techniques was in most cases only moderate. It may therefore be important to review once more the basic assumptions underlying the analysis.

1) Signal and noise were assumed to be independent Gaussian random processes.

2) The signal to noise ratio at each hydrophone was assumed to be small compared to unity.

3) Signal and noise processes were assumed to be stationary and the signal to noise ratio at each hydrophone was assumed to be the same.

4) Numerical calculations were concerned primarily with cases of relatively broadband signals and noises, mostly with similar or identical power spectra.

5) The array of hydrophones was considered fixed. Numerical calculations dealt particularly with a linear array of equally spaced elements.

Assumption 1) is particularly important. It implies that signal and noise can be characterized only by their total power and spectral properties. Of these two features the standard detector uses only total power, hence it is in general inferior to the optimum detector. However, the report indicates that (unless the spectra of signal and noise are drastically different) the benefit to be derived from use of spectral properties is quite limited. Further work is planned to investigate the improvements possible with optimal detection schemes when there are pronounced differences in signal and noise spectra. Signals containing narrowband components at known or unknown frequencies would be a case of particular interest.

The analytical treatment of non-Gaussian random processes tends to be very difficult, and an attempt to solve the problem under such assumptions does not appear promising. However, if information concerning waveshapes of expected signals were attainable, great improvements in detector performance might be possible. The analytical tools for handling this case

A3-34

are also available. An effort to search out features of the expected signals related to waveshape rather than spectral properties therefore appears indicated.

Assumptions 3) and 5) suggest additional possibilities for further investigations. It has been shown, for instance, that clipping can improve the performance of a power detector when the noise power varies from hydrophone to hydrophone,[1] or as a function of time.[2] It would be interesting to investigate whether the optimum detector also performs an operation analogous to clipping under these conditions. If hydrophone locations are regarded as an additional set of adjustable parameters the optimization procedure can, in principle at least, be carried one step further. One could then perhaps inquire into the best location for a fixed number of hydrophones in a given volume and the performance index of the associated optimal detector. It appears unlikely that a very general solution to this problem would be computationally feasible, but it would be of interest to gain even limited insight into the dependence of system performance on hydrophone location.

Finally the theory of optimal detection may provide a means for assessing realistic costs of such signal processing techniques as clipping. One could, for instance, compare the performance of an optimal detector operating on clipped hydrophone data with the performance of an optimal detector operating on unclipped data. Whether such a comparison is computationally manageable for cases of practical interest has not yet been investigated.

---

[1]T. Usher, Signal Detection by Arrays in Noise Fields with Local Variations. Progress Report No. 2. Electric Boat Co. Research. Yale University, March 1963.

[2]J. B. Thomas, T. R. Williams, On the Detection of Signals in Non-Stationary Noise by Product Arrays. J. Acoust. Soc. of America. Vol. 34, No.4, pp. 453-462, April 1959.

A3-35

General Dynamics/Electric Boat Research

(53-00-10-0231)

Progress Report No. 4

by

Theron Usher, Jr.

Dunham Laboratory

Yale University

New Haven, Connecticut

June 1963

Department of Engineering and Applied Science

Yale University

General Dynamics/Electric Boat Research

(53-00-10-0231)

SIGNAL DETECTION BY ARRAYS WITH

ARBITRARY PROCESSORS AND DETECTORS

by

Theron Usher, Jr.

June 1963

SIGNAL DETECTION BY ARRAYS WITH
ARBITRARY PROCESSORS AND DETECTORS

I.   Introduction

The signal detection characteristics of local arrays of transducers have been extensively analyzed[1,2,3] for the situation in which:

1. The output of each transducer is subject to infinite clipping or purely linear processing;

2. The processed output signal from each transducer is summed;

3. The summed result is applied to a square-law detector;

4. The squared sum is filtered.

However, the effect of a general nonlinear processor following each transducer relative to signal detection efficiency has not been determined. Neither has the effect of a general non-square law detector been examined. It is the purpose of this report to investigate both effects.

The two performance indices defined in Reference 3 are used to provide a numerical indication of the signal detection efficiency.

The signal response ratio, R_1, is defined to be the ratio of the normalized average signal output of the system with either the nonlinear processor or the non-square law detector to the normalized average signal output for the system with the linear processor and square-law detector.

Similarly, the index, R_2, is defined to be the ratio of the square root of the signal-to-noise ratio of the directivity pattern for the system with either the nonlinear processor or the non-square law detector to that for the system with the linear processor and square-law detector.

The major purpose of the analysis is to determine optimum processor functions and optimum detector functions for maximizing both response indices. Another consequence of the analysis is a derivation of a general expression giving the autocorrelation function for the output of a nonlinear device in terms of the input autocorrelation function. The major assumptions of the analysis are listed in the following section.

II. Assumptions and Definitions

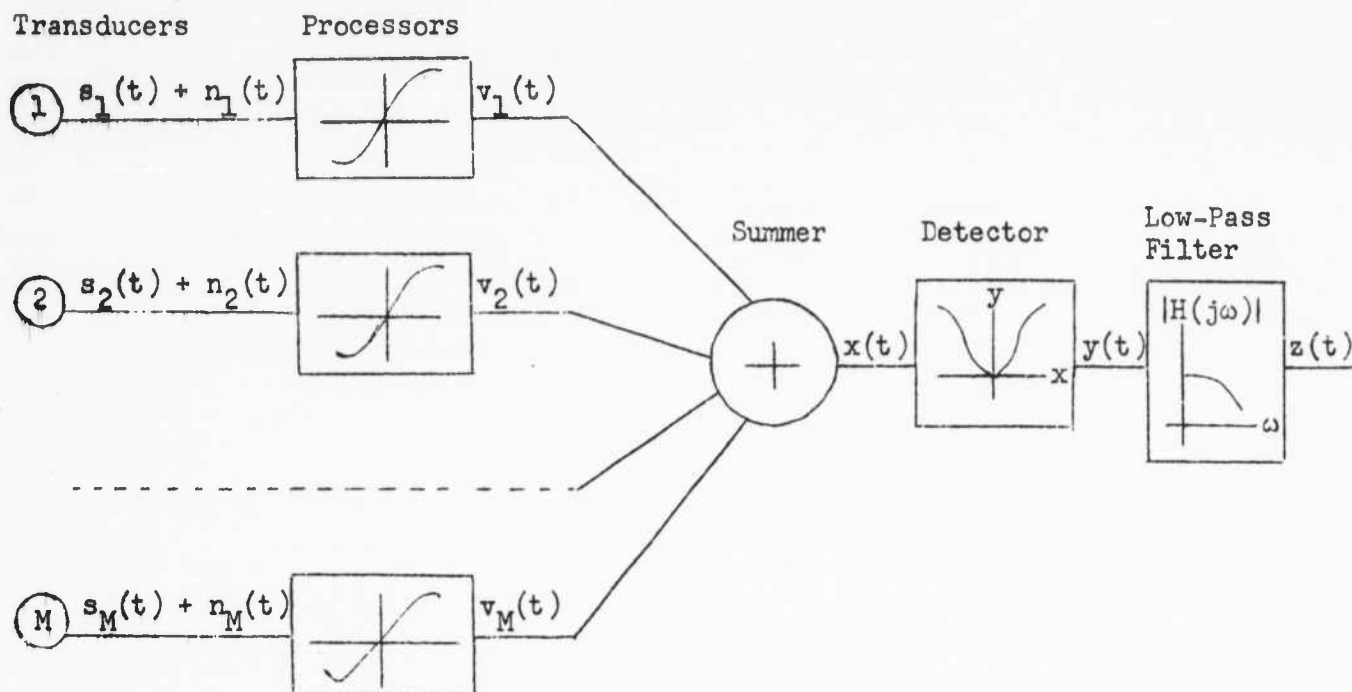The system analyzed in the following sections is shown in Fig. 1.

Fig. 1 Array with Nonlinear Processors and Non-Square Law Detector

Following are the major assumptions inherent in the analysis:

1. The transducers in the array have omnidirectional characteristics.

2. The autocorrelation functions of both the signal and the noise inputs to the processors are identical. The signal power input and the noise power input to each processor do not vary from channel to channel.

3. The cross-correlation between noise inputs for different channels is zero.

4. The signal and the noise inputs to the processors are Gaussian and stationary. Signal and noise are independent.

5. The processor is an odd-function, zero-memory device.

6. The detector is an even-function device.

III. Correlation Between the Output Signals of Identical Nonlinear Devices

Since the analysis of array performance in following sections requires an evaluation of the cross-correlation of the output signals from two identical nonlinear devices, or the evaluation of the autocorrelation for the output signal of a nonlinear device, a general derivation applicable to both situations is made in this section.

It is assumed that the input variables are Gaussian, with zero mean, and equal variances. Furthermore, the two-dimensional probability density function is given by

$$f(e_1, e_2) = \frac{1}{2\pi\sigma^2 \sqrt{1 - a^2}} \exp\left[-e_1^2 + e_2^2 - 2ae_1e_2\right] \tag{1}$$

The characteristic function of $f(e_1, e_2)$ in terms of the complex variables w_1 and w_2 is

$$\oint(w_1, w_2) = \int_{-\infty}^{\infty} \int_{-\infty}^{\infty} \exp\left[e_1w_1 + e_2w_2\right] f(e_1, e_2) \, de_1 de_2$$

$$= \exp\left[\frac{\sigma^2}{2}\left(w_1^2 + w_2^2 + 2aw_1w_2\right)\right] \tag{2}$$

It is desired to find the statistical average of $g(e_1)g(e_2)$ where $g(e)$ is a general nonlinear function with zero memory. The development follows the transform method used in Chapter 13 of Reference 4. The correlation function $\overline{g(e_1)g(e_2)}$ in its final form is expressed in terms of a power series in $\underline{a}$, the normalized correlation between e_1 and e_2.

It is convenient to define the function $g(e)$ in two parts:

$$g_+(e) = \begin{cases} g(e) & e \geq 0 \\ \\ 0 & e < 0 \end{cases} \tag{3}$$

A4-5

and

$$g_-(e) = \begin{cases} 0 & e > 0 \\ \\ g(e) & e \leq 0 \end{cases} \tag{4}$$

Then

$$g(e) = g_+(e) + g_-(e) \tag{5}$$

The Laplace transforms for the two parts of $g(e)$ are

$$G_+(w) = \int_0^\infty g_+(e)\, \varepsilon^{-we}\, de \tag{6}$$

$$G_-(w) = \int_{-\infty}^0 g_-(e)\, \varepsilon^{-we}\, de \tag{7}$$

The inverse relations are found in Eqs. (8) and (9).

$$g_+(e) = \frac{1}{2\pi j} \int_C G_+(w)\, \varepsilon^{ew}\, dw \tag{8}$$

$$g_-(e) = \frac{1}{2\pi j} \int_D G_-(w)\, \varepsilon^{ew}\, dw \tag{9}$$

The required contours of integration are shown in Fig. 2. The infinitesimal displacement Δ in each case is required for convergence of the transforms. It is assumed that $g(e)$ does not increase exponentially.

For contour C $w = \Delta + jv$
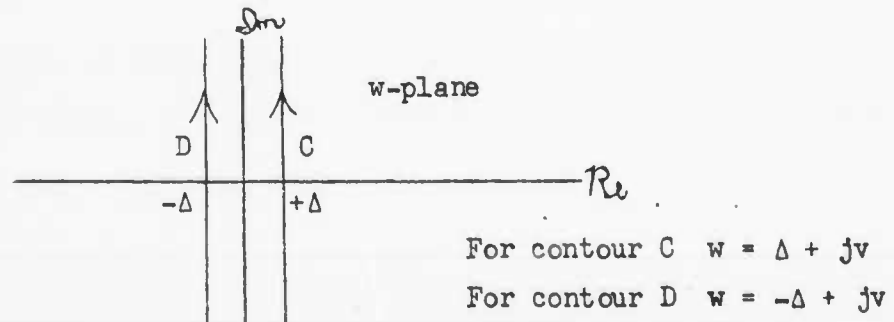For contour D $w = -\Delta + jv$

Fig. 2   Contours of Integration in the Complex w-Plane

The correlation between $g(e_1)$ and $g(e_2)$ is

$$\overline{g(e_1)\,g(e_2)} = \int_{-\infty}^{\infty} \int_{-\infty}^{\infty} g(e_1)\,g(e_2)\,f(e_1,e_2)\,de_1 de_2 \qquad (10)$$

Substitution of the results of Eqs. (5), (8) and (9) into Eq. (10) gives

$$\overline{g(e_1)\,g(e_2)} = \frac{1}{(2\pi j)^2} \int_{-\infty}^{\infty} \int_{-\infty}^{\infty} \left[\int_C G_+(w_1)\, \varepsilon^{e_1 w_1}\, dw_1 + \int_D G_-(w_1)\, \varepsilon^{e_1 w_1}\, dw_1 \right]$$

$$\times \left[\int_C G_+(w_2)\, \varepsilon^{e_2 w_2}\, dw_2 + \int_D G_-(w_2)\, \varepsilon^{e_2 w_2}\, dw_2 \right] f(e_1,e_2)\,de_1 de_2$$

$$(11)$$

With the application of the definition in Eq. (2), Eq. (11) becomes

$$\overline{g(e_1)\,g(e_2)} = \frac{1}{(2\pi j)^2} \left[\int_C \int_C G_+(w_1)\,G_+(w_2)\,\bar{\Phi}(w_1,w_2)\,dw_1 dw_2 \right.$$

$$+ \int_C \int_D G_+(w_1)\,G_-(w_2)\,\Phi(w_1,w_2)\,dw_1 dw_2$$

$$+ \int_D \int_C G_-(w_1)\,G_+(w_2)\,\Phi(w_1,w_2)\,dw_1 dw_2$$

$$\left. + \int_D \int_D G_-(w_1)\,G_-(w_2)\,\Phi(w_1,w_2)\,dw_1 dw_2 \right] \qquad (12)$$

If the infinite series for $\exp\left[\sigma^2 a\, w_1 w_2\right]$ is utilized for the corresponding term in $\Phi(w_1,w_2)$, the double integrals in Eq. (12) become separable as products of integrals.

A4-7

Since

$$\exp\left[\sigma^2 a \, w_1 w_2\right] = \sum_{n=0}^{\infty} \frac{\sigma^{2n} a^n w_1{}^n w_2{}^n}{n!} \qquad (13)$$

then,

$$\overline{g(e_1)\,g(e_2)} = \sum_{n=0}^{\infty} \frac{\sigma^{2n} a^n}{n!} \frac{1}{(2\pi j)^2} \left[\int_C w_1{}^n \, G_+(w_1) \, \varepsilon^{\frac{\sigma^2 w_1{}^2}{2}} dw_1 \int_C w_2{}^n \, G_+(w_2) \, \varepsilon^{\frac{\sigma^2 w_2{}^2}{2}} dw_2 \right.$$

$$+ \int_C w_1{}^n \, G_+(w_1) \, \varepsilon^{\frac{\sigma^2 w_1{}^2}{2}} \, w_1 \int_D w_2{}^n \, G_-(w_2) \, \varepsilon^{\frac{\sigma^2 w_2{}^2}{2}} dw_2$$

$$+ \int_D w_1{}^n G_-(w_1) \, \varepsilon^{\frac{\sigma^2 w_1{}^2}{2}} dw_1 \int_C w_2{}^n \, G_+(w_2) \, \varepsilon^{\frac{\sigma^2 w_2{}^2}{2}} dw_2$$

$$\left. + \int_D w_1{}^n \, G_-(w_1) \, \varepsilon^{\frac{\sigma^2 w_1{}^2}{2}} dw_1 \int_D w_2{}^n \, G_-(w_2) \, \varepsilon^{\frac{\sigma^2 w_2{}^2}{2}} dw_2 \right] \qquad (14)$$

Due to the product form of Eq. (14), it may be rewritten as

$$\overline{g(e_1)\,g(e_2)} = \sum_{n=0}^{\infty} \frac{\sigma^{2n} a^n}{n!} \frac{1}{(2\pi j)^2} \left[\int_C w^n \, G_+(w) \, \varepsilon^{\frac{\sigma^2 w^2}{2}} dw + \int_D w^n \, G_-(w) \, \varepsilon^{\frac{\sigma^2 w^2}{2}} dw \right]^2 \qquad (15)$$

It may be shown that

$$\int_0^{\infty} g_+'(e) \, \varepsilon^{-we} \, de = w \, G_+(w) - g(0) \qquad (16)$$

and

$$\int_{-\infty}^{0} g_-'(e) \, \varepsilon^{-we} \, de = w \, G_-(w) + g(0) \qquad (17)$$

where

$$g'(e) = \frac{dg}{de} \tag{18}$$

Furthermore, the relations in Eqs. (16) and (17) may be extended for the nth derivative to yield

$$\int_0^\infty g_+^{[n]}(e) \, \varepsilon^{-we} \, de = w^n \, G_+(w) - \sum_{m=1}^n w^{(n-m)} g^{[m-1]}(0) \tag{19}$$

and

$$\int_{-\infty}^0 g_-^{[n]}(e) \, \varepsilon^{-we} \, de = w^n \, G_-(w) + \sum_{m=1}^n w^{(n-m)} g^{[m-1]}(0) \tag{20}$$

where

$$g^{[n]}(e) = \frac{d^n g}{de^n} \tag{21}$$

When the results of Eqs. (19) and (20) are substituted into Eq. (15), Eq. (22) is obtained.

$$\overline{g(e_1) \, g(e_2)} = \sum_{n=0}^\infty \frac{\sigma^{2n} a^n}{n!} \frac{1}{(2\pi j)^2} \left[\int_C dw \, \varepsilon^{\frac{\sigma^2 w^2}{2}} \int_0^\infty g_+^{[n]}(e) \, \varepsilon^{-we} \, de \right.$$

$$+ \sum_{m=1}^n \int_C w^{(n-m)} g^{[m-1]}(0) \, \varepsilon^{\frac{\sigma^2 w^2}{2}} dw + \int_D dw \, \varepsilon^{\frac{\sigma^2 w^2}{2}} \int_{-\infty}^0 g_-^{[n]}(e) \, \varepsilon^{-we} \, de$$

$$\left. - \sum_{m=1}^n \int_D w^{(n-m)} g^{[m-1]}(0) \, \varepsilon^{\frac{\sigma^2 w^2}{2}} dw \right]^2 \tag{22}$$

A4-9

It can be shown that the terms involving $g^{[m-1]}(0)$ cancel (See Appendix A) because the difference of the integrals over contours C and D may be made as small as desired by making Δ in Fig. 2 arbitrarily small.

The inverse transform of the single-dimensional characteristic function, yields the Gaussian probability density function:

$$\frac{1}{2\pi j} \int_{C'} \varepsilon^{\frac{\sigma^2 w^2}{2}} \varepsilon^{-we} \, dw = \frac{1}{\sqrt{2\pi} \, \sigma} \varepsilon^{-\frac{e^2}{2\sigma^2}} = f(e) \tag{23}$$

The contour C' is the imaginary axis of the w-plane. Since C and D may be made arbitrarily close to the imaginary axis of the w-plane, Eq. (22) becomes

$$\overline{g(e_1) \, g(e_2)} = \sum_{n=0}^{\infty} \frac{\sigma^{2n} a^n}{n!} \left[\int_0^\infty g_+^{[n]}(e) \, f(e) \, de + \int_{-\infty}^0 g_-^{[n]}(e) \, f(e) \, de \right]^2 \tag{24}$$

Finally,

$$\overline{g(e_1) \, g(e_2)} = \sum_{n=0}^{\infty} \frac{\sigma^{2n}}{n!} \overline{g^{[n]}(e)}^2 a^n \tag{25}$$

In Eq. (25) the bar indicates an average with Gaussian statistics for e. An alternate form of Eq. (25) is possible since it can be shown (See Appendix B) that

$$\overline{g^{[n]}(e)} = \sigma^{-n} \overline{H_n\left(\frac{e}{\sigma}\right) g(e)} \tag{26}$$

In Eq. (26) $H_n\left(\frac{e}{\sigma}\right)$ is the Hermite polynomial of order n with $\frac{e}{\sigma}$ as the argument.

Then

$$\overline{g(e_1) \, g(e_2)} = \sum_{n=0}^{\infty} \frac{1}{n!} \overline{H_n\left(\frac{e}{\sigma}\right) g(e)}^2 a^n \tag{27}$$

A4-10

The results in Eq. (25) and (27) can be used in determining the cross-correlation between the output variables of identical nonlinear processors. In this case, $\underline{a}$ is the normalized cross-correlation between the input variables of the processors. The result can also be used to determine the autocorrelation function of the output of a nonlinear processor. In the latter case, e_1 and e_2 represent the input variable at two different times and $\underline{a}$ is the normalized autocorrelation function of the input variable.

A4-11

IV.   Average Signal Output--Nonlinear Processors and Square Law Detector

The symbols and definitions in Reference 3 will be followed as closely as possible. For the system with the nonlinear processors, the directivity pattern is

$$\bar{y}(\Theta) = \sum_{i=1}^{M} \sum_{j=1}^{M} \overline{g\left\{s_i(t) + n_i(t)\right\} g\left\{s_j(t) + n_j(t)\right\}} \qquad (28)$$

For the input signals to the processors,

$$\sigma^2 = S + N \qquad (29)$$

The normalized cross-correlation a is

$$a = \frac{\overline{\left[s_i(t) + n_i(t)\right]\left[s_j(t) + n_j(t)\right]}}{S + N} = \begin{cases} \dfrac{S}{S + N}\,\rho(\tau_{ij}) & i \neq j \\[4mm] 1 & i = j \end{cases} \qquad (30)$$

In Eqs. (29) and (30), ρ is the normalized autocorrelation function for the signal, S is the total signal power, and N is the total noise power. The τ_{ij} depend on the spatial time delays and electrical time delays associated with the typical steered array.

The results in Eqs. (25) and (27) may be used to simplify Eq. (28). It should be noted, however, that when a = 1, Eq. (25) reduces to one term, the mean square value of g(e). Furthermore, the processor function in the array has been assumed to have odd symmetry, so that only odd order terms in Eqs. (25) and (27) are present.

Using Eq. (25), we have

$$\overline{y(\Theta)} = M\,\overline{g(e)^2} + 2 \sum_{i=1}^{M} \sum_{j=i+1}^{M} \sum_{n=0}^{\infty} \frac{S^{(2n+1)}}{(2n+1)!} \overline{g^{[2n+1]}(e)}^2\, \rho^{2n+1}(\tau_{ij}) \qquad (31)$$

A4-12

The "on target" response occurs when all $\tau_{ij} = 0$, and the "off target" response occurs when the τ_{ij} are all large enough so that the $\rho(\tau_{ij})$ approach zero. These responses are found in Eqs. (32) and (33) respectively.

$$\bar{y}_0 = M \overline{g'(e)^2} + (M^2 - M) \sum_{n=0}^{\infty} \frac{S^{(2n+1)}}{(2n + 1)!} \overline{g^{[2n+1]}(e)}^2 \tag{32}$$

$$\bar{y}_L = M \overline{g(e)^2} \tag{33}$$

The normalized signal output $\Delta\bar{y}$ is

$$\Delta\bar{y}^{\,!} = \frac{\bar{y}_0 - \bar{y}_L}{\bar{y}_L} = (M - 1) \frac{\displaystyle\sum_{n=0}^{\infty} \frac{S^{(2n+1)}}{(2n + 1)!} \overline{g^{[2n+1]}(e)}^2}{\overline{g(e)^2}} \tag{34}$$

For the system with linear processors, $g(e) = Ke$ and

$$\bar{y}_{AO} = K^2(MN + SM^2) \tag{35}$$

$$\bar{y}_{AL} = K^2 M(N + S) \tag{36}$$

$$\Delta\bar{y}_A^{\,!} = (M - 1) \frac{S}{S + N} \tag{37}$$

The signal response ratio, R_1, has previously been defined to be the ratio of $\Delta\bar{y}$ to $\Delta\bar{y}_A$.

$$\boxed{R_1 = \frac{\Delta\bar{y}}{\Delta\bar{y}_A} = \left(\frac{S + N}{S}\right) \frac{\displaystyle\sum_{n=0}^{\infty} \frac{S^{2n+1}}{(2n + 1)!} \overline{g^{[2n+1]}(e)}^2}{\overline{g(e)^2}}} \tag{38}$$

A4-13

An alternate form of R_1 is obtained by using Eq. (26):

$$R_1 = \frac{\sum_{n=0}^{\infty} \frac{1}{(2n+1)!}\left(\frac{S}{S+N}\right)^{2n} \overline{H_{2n+1}\left(\frac{e}{\sqrt{S+N}}\right) g(e)}^{\,2}}{\overline{g(e)^2}} \qquad (39)$$

From Eq. (39) it is evident that only the first term of the series is important for small values of input signal to noise ratio. Then

$$R_1 \simeq \frac{\sigma^2\; \overline{g^{(1)}(e)}^{\,2}}{\overline{g(e)^2}} = \frac{\overline{eg(e)}^{\,2}}{\sigma^2\; \overline{g(e)^2}} \qquad \text{for } \frac{S}{N} << 1 \qquad (40)$$

It is interesting to note from Eq. (38) that for large values of signal to noise ratio

$$\frac{S}{S+N} = a \rightarrow 1$$

and the sum in the numerator of Eq. (38) approaches $\overline{g(e)^2}$. Thus the signal response ratio approaches unity. Under strong signal conditions, then, the average signal performance of the system with nonlinear processors approaches that of the system with linear processors.

Also if one considers the non-negative function

$$\overline{(\lambda\, g(e) + e)^2} \geq 0 \qquad (41)$$

where λ is an arbitrary parameter, we have by expansion,

$$\lambda^2 \overline{g(e)^2} + 2\lambda\, \overline{eg(e)} + \sigma^2 \geq 0 \qquad (42)$$

Since there can be no real, unequal roots for λ,

$$\overline{eg(e)}^2 - \sigma^2\, \overline{g(e)^2} \leq 0 \qquad (43)$$

Applying the result in Eq. (43) to the small signal approximation for R_1, we have

$$R_1 \leq 1 \qquad \text{for} \qquad \frac{S}{N} < < 1 \qquad\qquad (44)$$

Since all terms in the series expression for R_1 are positive, unity is an upper bound for R_1 for all ratios of signal to noise. Furthermore, the equality in Eqs. (41) through (43) holds only if $g(e)$ is a linear function of e (i.e., $g(e) = ke$), so that the signal response ratio is less than unity for all finite input signal-to-noise ratios for all nonlinear processors. Thus the linear processor is optimum in the sense of producing maximum average output signal for the array.

V. Signal-to-Noise Ratio at Output of Array--Nonlinear Processors and Square Law Detector

The goal of this section is the development of an expression for the performance index, R_2, which is the ratio of the square root of the signal-to-noise ratio for the system with nonlinear processors to that for the system with linear processors. Since the expressions for average signal output were developed in the previous section, most of the analytical development in this section will be concerned with the evaluation of the variance of the output of the low-pass filter in Fig. 1.

In general

$$R_y(\tau) = E\left[y(t)\ y(t + \tau)\right] = \bar{y}^2 + R_y{}'(\tau). \tag{45}$$

where $\bar{y}$ represents the average array output, and $R'(\tau)$ is the autocorrelation function for the variational component of $y(t)$. If

$$H_Z(j\omega) = \frac{1}{1 + j\,\dfrac{\omega}{\omega_F}} \tag{46}$$

from Eq. (56), Reference 3, we have

$$\sigma_Z^2 \cong \omega_F \int_0^\infty R_y{}'(\tau)\ d\tau \qquad (\omega_F \text{ small}) \tag{47}$$

For the analysis of array performance with nonlinear processors, it will be assumed that the input signal-to-noise ratio is sufficiently small so that only the input noise contributes to noise (σ_Z^2) at the output. This assumption is necessary for making the analysis tractable, and also is not unduly restrictive, since only small signal-to-noise ratios produce any detection problems.

. Thus the autocorrelation function for $y(t)$ becomes

$$R_y(\tau) = E\left[x^2(t)\, x^2(t + \tau)\right]$$

$$= E\left[\sum_{i=1}^{M}\sum_{j=1}^{M} g\{n_i(t)\}\, g\{n_j(t)\} \sum_{k=1}^{M}\sum_{\ell=1}^{M} g\{n_k(t + \tau)\}\, g\{n_\ell(t + \tau)\}\right] \quad (48)$$

The evaluation of Eq. (48) is helped by separating the terms into the different categories as shown in Table 1.

Subscript relations	Number of terms	Evaluation and comments
$i = j$ and $k = \ell$	M^2	$i \neq k$ yields $M^2 - M$ terms. $E\left[g^2(n_i)\right] E\left[g^2(n_k)\right] = \overline{g}^2$ $i = k$ yields M terms. $E\left[g^2\{n_i(t)\}\, g^2\{n_i(t + \tau)\}\right]$
$i = j$ and $k \neq \ell$ $i \neq j$ and $k = \ell$	$2(M^3 - M^2)$	Yields $E\left[g^2(n_i)\, g(n_k)\, g(n_\ell)\right] = 0$ because n_k and n_ℓ are uncorrelated and $g(n)$ is odd.
$i \neq j$ and $k \neq \ell$	$M^4 - 2M^3 + M^2$	Only terms of the type where $i = k$, $j = \ell$; and $i = \ell$, $j = k$ are non-zero. $2(M^2 - M)$ in number)

Table 1 Classification of Terms in Eq. (48)

A4-17

From Table 1, Eq. (48) becomes

$$R_y(\tau) = (M^2 - M)\,\overline{g^2(e)}^2 + M\,\overline{g^2\{e(t)\}\,g^2\{e(t + \tau)\}} + 2(M^2 - M)\,\overline{g\{e(t)\}\,g\{e(t + \tau)\}}^2$$

<div align="right">(49)</div>

Both the second and third terms of Eq. (49) may be evaluated using the
result in Eq. (26). For the second term, since $g^2(e)$ is an even function,
we have

$$\overline{g^2(e_1)\,g^2(e_2)} = \sum_{n=0}^{\infty} \frac{1}{(2n)!}\,\overline{H_{2n}\!\left(\frac{e}{\sigma}\right)g^2(e)}^2 \rho^{2n}(\tau)$$

$$= \overline{g^2}^2 + \frac{1}{2!}\,\overline{H_2\!\left(\frac{e}{\sigma}\right)g^2}^2 \rho^2(\tau) + \frac{1}{4!}\,\overline{H_4\!\left(\frac{e}{\sigma}\right)g^2}^2 \rho^4(\tau)$$

$$+ \frac{1}{6!}\,\overline{H_6\!\left(\frac{e}{\sigma}\right)g^2}^2 \rho^6(\tau) + \ldots$$

<div align="right">(50)</div>

For the third term,

$$\overline{g(e_1)\,g(e_2)}^2 = \left[\sum_{n=0}^{\infty} \frac{1}{(2n+1)!}\,\overline{H_{2n+1}\!\left(\frac{e}{\sigma}\right)g(e)}^2 \rho^{2n+1}(\tau)\right]^2$$

$$= \overline{H_1\!\left(\frac{e}{\sigma}\right)g}^4 \rho^2(\tau) + \frac{2}{3!}\,\overline{H_1\!\left(\frac{e}{\sigma}\right)g}^2\,\overline{H_3\!\left(\frac{e}{\sigma}\right)g}^2 \rho^4(\tau)$$

$$+ \left[\frac{1}{3!3!}\,\overline{H_3\!\left(\frac{e}{\sigma}\right)g}^4 + \frac{2}{5!}\,\overline{H_1\!\left(\frac{e}{\sigma}\right)g}^2\,\overline{H_5\!\left(\frac{e}{\sigma}\right)g}^2\right] \rho^6(\tau)$$

$$+ \left[\frac{2}{3!5!}\,\overline{H_3\!\left(\frac{e}{\sigma}\right)g}^2\,\overline{H_5\!\left(\frac{e}{\sigma}\right)g}^2 + \frac{2}{7!}\,\overline{H_1\!\left(\frac{e}{\sigma}\right)g}^2\,\overline{H_7\!\left(\frac{e}{\sigma}\right)g}^2\right] \rho^8(\tau) + \ldots$$

<div align="right">(51)</div>

Substituting the results from Eqs. (50) and (51) into Eq. (49) and collecting terms, we have

$$R_y(\tau) = \left(M \overline{g^2} \right)^2 + M\left(\frac{1}{2!} \overline{H_2 g^2} \rho^2 + \frac{1}{4!} \overline{H_4 g^2} \rho^4 + \ldots \right)$$
$$+ 2(M^2 - M)\left(\overline{H_1 g}^4 \rho^2 + \frac{2}{3!} \overline{H_1 g}^2 \overline{H_3 g}^2 \rho^4 + \ldots \right) \tag{52}$$

For large M, the terms multiplying M in Eq. (52) may be neglected in comparison with those multiplying $2(M^2 - M)$, since in general the order of magnitude of internal terms multiplying ρ^{2n} is generally the same. Also the term $\left(\overline{Mg^2} \right)^2$ in Eq. (52) is simply the $\overline{y}^2$ term in Eq. (45). From Eq. (47),

$$\sigma_Z^2 \cong 2\omega_F(M^2 - M)\left[\overline{H_1 g}^4 \int_0^\infty \rho^2 d\tau + \frac{2}{3!} \overline{H_1 g}^2 \overline{H_3 g}^2 \int_0^\infty \rho^4 d\tau + \ldots \right] \tag{53}$$

$$\frac{S}{N} << \frac{1}{M}$$

For the linear system for small signals, from Eq. (49), Reference 3, we have

$$\sigma_{ZA}^2 \cong 2\omega_F M^2 K^4 N^2 \int_0^\infty \rho^2 d\tau \qquad \frac{S}{N} << \frac{1}{M} \tag{54}$$

The definition of R_2 yields

$$R_2 = \frac{\overline{y}_0 - \overline{y}_L}{\overline{y}_{A0} - \overline{y}_{AL}} \cdot \frac{\sigma_{ZA}}{\sigma_Z} \tag{55}$$

Substitution of the results in Eqs. (32), (33), (35), (36), (53) and (54) for small $\frac{S}{N}$ results in the following expression.

A4-19

$$R_2 = \left[1 + \frac{2}{3!} \frac{\overline{H_3 g}^2}{\overline{H_1 g}^2} \cdot \frac{A_4}{A_2} + \left(\frac{1}{3!3!} \frac{\overline{H_3 g}^4}{\overline{H_1 g}^4} + \frac{2}{5!} \frac{\overline{H_5 g}^2}{\overline{H_1 g}^2} \right) \frac{A_6}{A_2} + \ldots \right]^{-1/2}$$

$$\frac{S}{N} << \frac{1}{M} << 1 \qquad\qquad (56)$$

In Eq. (56) A_{2n} is defined to be

$$A_{2n} = \int_0^\infty \rho^{2n}(\tau)\, d\tau \qquad\qquad (57)$$

The alternative form of Eq. (56) utilizing derivatives of $g(e)$ is

$$R_2 = \left[1 + \sigma^4 \frac{2}{3!} \frac{\overline{g^{[3]}}^2}{\overline{g^{[1]}}^2} \frac{A_4}{A_2} + \sigma^8 \left(\frac{1}{3!3!} \frac{\overline{g^{[3]}}^4}{\overline{g^{[1]}}^4} + \frac{2}{5!} \frac{\overline{g^{[5]}}^2}{\overline{g^{[1]}}^2} \right) \frac{A_6}{A_2} + \ldots \right]^{-1/2} \quad (58)$$

An inspection of Eq. (58) reveals that R_2 is less than unity for all $g(e)$ for which

$$\overline{H_{2n+1}\left(\frac{e}{\sigma}\right) g(e)} = \sigma^{2n+1} \overline{g^{[2n+1]}(e)} \neq 0 \qquad \text{for } n \geq 1 \quad (59)$$

The only function excluded from the inequality in Eq. (59) is the linear function $g(e) = ke$, for which

$$\overline{H_1\left(\frac{e}{\sigma}\right) g(e)} = \sigma \overline{g^{[1]}(e)} = \sigma k \qquad\qquad (60)$$

and

$$\overline{H_{2n+1}\left(\frac{e}{\sigma}\right) g(e)} = \sigma^{(2n+1)} \overline{g^{[2n+1]}(e)} = 0 \qquad \text{for } n \geq 1 \quad (61)$$

Thus the linear processor is optimum because it produces a signal-to-noise ratio at the array output which is greater than the signal-to-noise ratio for any nonlinear processor.

In the following section, the general results in Sections IV and V are evaluated for several types of nonlinear processors.

VI. Evaluation of R_1 and R_2 for Specific Nonlinear Processors

A wide class of nonlinear processors is described by the general power law relation found in Eq. (62). Note that $g(e)$ is an odd function of e.

$$g(e) = \begin{cases} K\,e^m & \text{for } e > 0 \\ 0 & \text{for } e = 0 \\ -K|e|^m & \text{for } e < 0 \end{cases} \tag{62}$$

From Reference 6, page 20, it is given that

$$\int_0^\infty \frac{1}{\sqrt{2\pi}}\, \varepsilon^{-\frac{x^2}{2}}\, x^k\, dx = \frac{1}{\sqrt{2\pi}}\, 2^{\frac{k-1}{2}} \left(\frac{k-1}{2}\right)! \tag{63}$$

where $(k)!$ is the general factorial function (k is not necessarily an integer).

The averages of the functions found in Eq. (40) are calculated below.

$$\overline{e\,g(e)} = 2\int_0^\infty e\, K\, e^m\, \frac{1}{\sqrt{2\pi}\,\sigma}\, \varepsilon^{-\frac{e^2}{2\sigma^2}} de = \frac{K}{\sqrt{2\pi}}\, \sigma^{m+1}\, 2^{\frac{m}{2}+1} \left(\frac{m}{2}\right)! \tag{64}$$

Also,

$$\overline{g(e)^2} = 2\int_0^\infty K^2\, e^{2m}\, \frac{1}{\sqrt{2\pi}\,\sigma}\, \varepsilon^{-\frac{e^2}{2\sigma^2}} de = \frac{K^2}{\sqrt{2\pi}}\, \sigma^{2m}\, 2^{m+\frac{1}{2}} \left(m-\frac{1}{2}\right)! \tag{65}$$

The performance index R_1 becomes

$$R_1(m) = \frac{2}{\sqrt{\pi}}\, \frac{\left(\frac{m}{2}\right)!\left(\frac{m}{2}\right)!}{\left(m-\frac{1}{2}\right)!} = \frac{1}{2^{m-1}}\, \frac{\left(\frac{m}{2}\right)!\ m!}{\left(\frac{m}{2}-\frac{1}{2}\right)!\left(m-\frac{1}{2}\right)!} \tag{66}$$

The last term in Eq. (66) is evident because of the identity (see Reference 6, p. 18)

$$\left(\frac{m}{2}\right)!\ \left(\frac{m}{2}-\frac{1}{2}\right)! = \sqrt{\pi}\, \frac{m!}{2^m} \tag{67}$$

The result in Eq. (66) is plotted in Fig. 3. It can be seen that the maximum value of R_1 occurs for m = 1. However, the peak is sufficiently broad so that the value of m may vary between zero and three so that the value of $R_1 \geq .6$. -Note that the value m = 0 yields the function which describes the infinite clipper.

Next, the performance index R_2 found in Eq. (58) will be evaluated for the odd-function power-law processor. The averaged derivatives in Eq. (58) are

$$\overline{g^{[1]}(e)} = \overline{\frac{e\ g(e)}{\sigma^2}} = \frac{2K}{\sqrt{2\pi}} \sigma^{m-1} 2^{\frac{m}{2}} \left|\frac{m}{2}\right|! \tag{68}$$

$$\overline{g^{[3]}(e)} = 2\int_0^\infty K\ m(m-1)(m-2)\ e^{m-3} \frac{1}{\sqrt{2\pi}\ \sigma} \varepsilon^{-\frac{e^2}{2\sigma^2}} de$$

$$= \frac{2K}{\sqrt{2\pi}} \sigma^{m-3} 2^{\frac{m}{2}} (m-1)\left|\frac{m}{2}\right|! \tag{69}$$

$$\overline{g^{[5]}(e)} = 2\int_0^\infty K\ \frac{m!}{(m-5)!}\ e^{m-5} \frac{1}{\sqrt{2\pi}\ \sigma} \varepsilon^{-\frac{e^2}{2\sigma^2}} de$$

$$= \frac{2K}{\sqrt{2\pi}} \sigma^{m-5} 2^{\frac{m}{2}} (m-1)(m-3)\left|\frac{m}{2}\right|! \tag{70}$$

Using

$$\rho(\tau) = \varepsilon^{-\omega_0|\tau|} \tag{71}$$

one obtains from Eq. (57)

$$\frac{A_{2n}}{A_2} = \frac{1}{n} \tag{72}$$

Thus R_2 becomes

$$R_2(m) = \left[1 + \frac{1}{6}(m-1)^2 + \left\{ \frac{1}{108}(m-1)^4 + \frac{1}{180}(m-1)^2(m-3)^2 \right\} + \ldots \right]^{1/2} \tag{73}$$
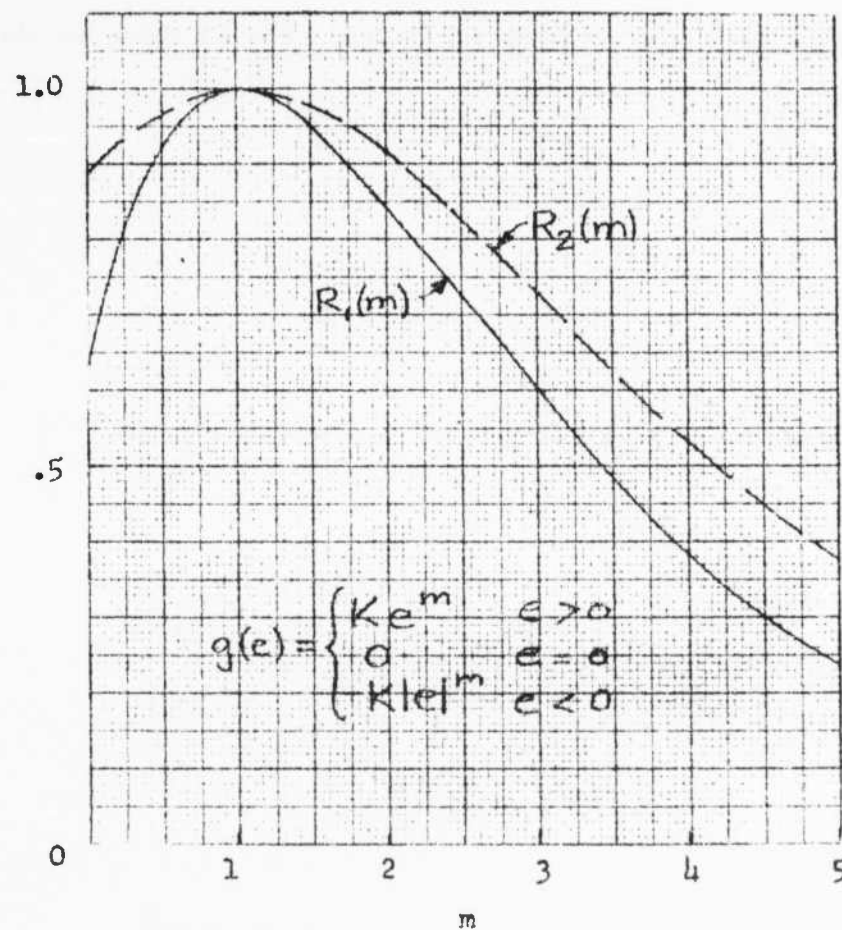
A4-22

Fig. 3 Performance Indices for Odd-Function Power-Law Processors

Equation (73) is evaluated and plotted as a function of m in Fig. 3. It may be noted that the series terminates when m is an odd integer, and converges rapidly when m is reasonably small.

The maximum value of R_2 is seen to occur for m = 1, as expected. The peak of the function, however, is again very broad.

Another processor function which has evoked some interest is the infinite clipper with a dead zone at high amplitude. The function is shown in Fig. 4.
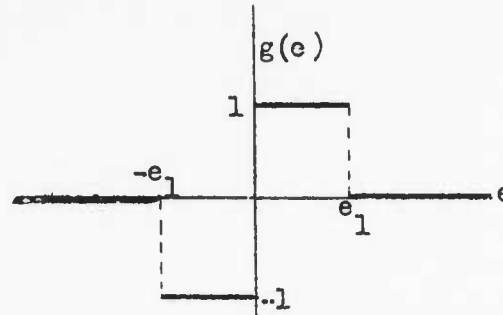

Fig. 4 Infinite Clipper with High Amplitude Dead Zone

In order to evaluate R_1 in Eq. (40) we have

$$\overline{e\,g(e)} = 2 \int_0^{e_1} e\,\frac{1}{\sqrt{2\pi}\,\sigma}\,\varepsilon^{-\frac{e^2}{2\sigma^2}}\,de = \sqrt{\frac{2}{\pi}}\,\sigma\left[1 - \varepsilon^{-\frac{e_1^2}{2\sigma^2}}\right] \tag{74}$$

$$\overline{g(e)^2} = 2 \int_0^{e_1} \frac{1}{\sqrt{2\pi}\,\sigma}\,\varepsilon^{-\frac{e^2}{2\sigma^2}}\,de = P\left(\frac{e_1}{\sigma}\right) \tag{75}$$

In Eq. (75), the normal probability function P(X) is defined by[7]

$$P(X) = \int_{-X}^{X} \frac{1}{\sqrt{2\pi}}\,\varepsilon^{-\frac{x^2}{2}}\,dx \tag{76}$$

A4-24

Thus the index R_1 is

$$R_1(\alpha) = \frac{\frac{2}{\pi}\left[1 - \varepsilon^{-\frac{\alpha^2}{2}}\right]^2}{P(\alpha)} \qquad \alpha = \frac{e_1}{\sigma} \qquad (77)$$

For small α, Eq. (77) reduces to

$$R_1(\alpha) = \frac{1}{2\sqrt{2\pi}}(\alpha)^3 \qquad \alpha << 1 \qquad (78)$$

Equation (77) is evaluated and plotted in Fig. 5.

It is evident from an examination of Fig. 5 and Eq. (78) that the infinite clipper with high-amplitude dead-band is an extremely poor processor to use if the variance of input noise is large relative to the level at which the dead zone appears. For all values of α the device is inferior to a simple infinite clipper.

An expression for the signal-to-noise performance index may be written following the calculation of the required averaged functions found in Eq. (56).

$$\overline{H_1\left(\frac{e}{\sigma}\right)g(e)} = 2\int_0^{e_1} \frac{e}{\sigma}\frac{1}{\sqrt{2\pi}\,\sigma}\varepsilon^{-\frac{e^2}{2\sigma^2}}\,de = \sqrt{\frac{2}{\pi}}\left[1 - \varepsilon^{-\frac{\alpha^2}{2}}\right] \qquad (79)$$

Also

$$\overline{H_{2n+1}\left(\frac{e}{\sigma}\right)g(e)} = 2\int_0^{e_1} H_{2n+1}\left(\frac{e}{\sigma}\right)f\left(\frac{e}{\sigma}\right)d\left(\frac{e}{\sigma}\right) = 2\left[H_{2n}(0)\,f(0) - H_{2n}(\alpha)\,f(\alpha)\right]$$
$$n = 0,1,2,\ldots \qquad (80)$$

In Eq. (80) $f(\alpha)$ is the Gaussian density function of the normalized variable α. Since

$$H_n(\alpha)\,f(\alpha) = (-1)^n\,f^{[n]}(\alpha) \qquad (81)$$

A4-25

Eq. (80) becomes

$$\overline{H_{2n+1}\left(\frac{e}{\sigma}\right) g(e)} = 2\left[f^{[2n]}(0) - f^{[2n]}(\alpha)\right] \doteq 2\,B_{2n}(\alpha) \qquad (82)$$

The functions in Eq. (82) are tabulated in Reference 8. The performance index R_2 in Eq. (83) is obtained by using Eq. (56). Note that higher order terms have been added to Eq. (83).

$$R_2(\alpha) = \left[1 + \frac{1}{6}\left(\frac{B_2}{B_0}\right)^2 + \left\{ \frac{1}{108}\left(\frac{B_2}{B_0}\right)^4 + \frac{1}{180}\left(\frac{B_4}{B_0}\right)^2 \right\} \right.$$

$$+ \left\{ \frac{1}{1440}\left(\frac{B_2}{B_0}\right)^2\left(\frac{B_4}{B_0}\right)^2 + \frac{1}{10080}\left(\frac{B_6}{B_0}\right)^2 \right\}$$

$$+ \left\{ \frac{1}{72000}\left(\frac{B_4}{B_0}\right)^4 + \frac{1}{75600}\left(\frac{B_2}{B_0}\right)^2\left(\frac{B_6}{B_0}\right)^2 + \frac{1}{907,200}\left(\frac{B_8}{B_0}\right)^2 \right\}$$

$$+ \left\{ \frac{1}{1,815,000}\left(\frac{B_4}{B_0}\right)^2\left(\frac{B_6}{B_0}\right)^2 + \frac{1}{6,530,000}\left(\frac{B_2}{B_0}\right)^2\left(\frac{B_8}{B_0}\right)^2 \right.$$

$$\left. + \frac{1}{1.2 \times 10^8}\left(\frac{B_{10}}{B_0}\right)^2 + \cdots \right]^{-1/2} \qquad (83)$$

The series in Eq. (83) does not converge well for values of $\alpha < 1$. For $\alpha = 0$, the series is definitely divergent so that $R_2(0) = 0$. Results from Eq. (83) are plotted in Fig. 5.

From Fig. 5, it can be seen that the performance of the infinite clipper with high-amplitude dead-band approaches that of the simple infinite clipper for large $\alpha = e_1/\sigma$, as expected. Below $\alpha = 3$, however, the performance indices decrease rather sharply, which indicates that the device has little utility as a processor.
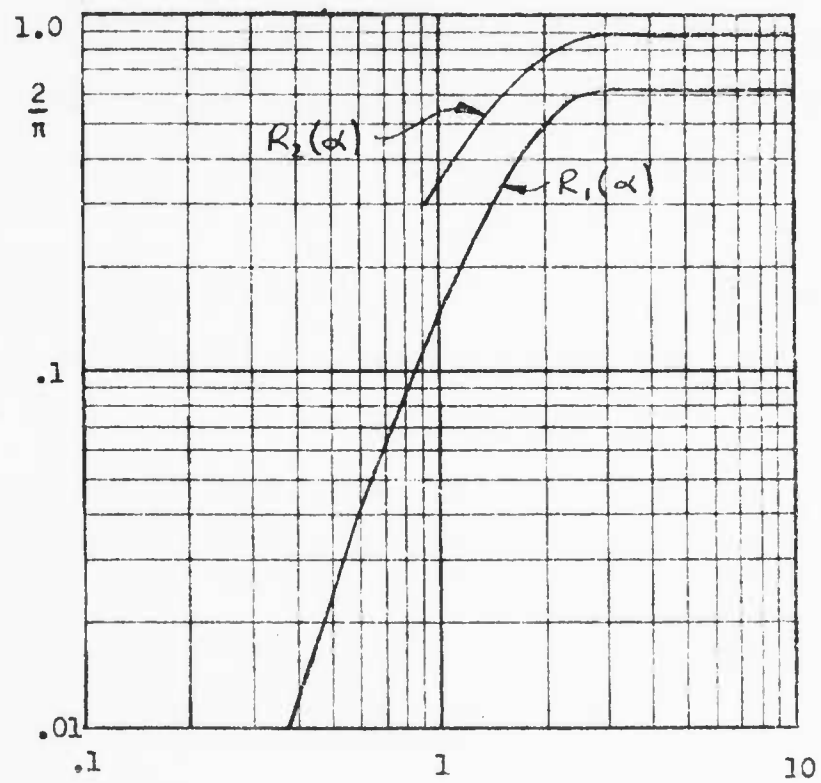
Fig. 5 Performance Indices for Infinite Clipper
with High Amplitude Dead Band

A4-27

VII. Average Signal Output--Linear Processors and Non-Square Law Detector

In preceding sections it has been determined that the use of linear processors with a square-law detector maximizes both performance indices. In this section the performance of a non-square law detector with linear processors will be examined. It would be desirable to obtain expressions for the performance indices of arrays utilizing nonlinear processors and a non-square law detector, but the mathematical expressions become extremely cumbersome. For this reason, the following analysis is limited as indicated. Since the use of linear processors with square-law detectors was optimum, perhaps the use of linear processors with non-square law detectors is not unduly restrictive.

With reference to Fig. 1, the detector function $y(x)$ is assumed to be an even function of x. The input x is Gaussian because the transducer outputs are all Gaussian, and the processors are linear. For the "on target" case, the signal components from each channel are completely correlated and the noise components are assumed to be uncorrelated. For the "on target" case $x(t)$ becomes

$$x(t) = x_0(t) = M\, s(t) + M^{1/2} n(t) \tag{84}$$

where $s(t)$ and $n(t)$ are representative signal and noise time functions at any transducer output. For the "off target" case, the signal components are uncorrelated, and so are the noise components. We have

$$x(t) = x_L(t) = M^{1/2} s(t) + M^{1/2} n(t) \tag{85}$$

A4-28

The "on target" and "off target" array outputs are defined by Eqs. (86) and (87).

$$\bar{y}_0 = \overline{y(x_0)} = \overline{y(Ms + M^{1/2}n)} \tag{86}$$

$$\bar{y}_L = \overline{y(x_L)} = \overline{y(M^{1/2}s + M^{1/2}n)} \tag{87}$$

Both $y(x_0)$ and $y(x_L)$ can be expanded in a Taylor series around the argument $M^{1/2}n$ and the averages taken as indicated in Eqs. (86) and (87). These operations yield

$$\bar{y}_0 = \overline{y(M^{1/2}n)} + \frac{\overline{(Ms)^2}}{2!}\,\overline{y^{[2]}(M^{1/2}n)} + \frac{\overline{(Ms)^4}}{4!}\,\overline{y^{[4]}(M^{1/2}n)} + \ldots$$

$$\ldots + \frac{\overline{(Ms)^{2n}}}{(2n)!}\,\overline{y^{[2n]}(M^{1/2}n)} + \ldots \tag{88}$$

and

$$\bar{y}_L = \overline{y(M^{1/2}n)} + \frac{\overline{Ms^2}}{2!}\,\overline{y^{[2]}(M^{1/2}n)} + \frac{\overline{M^2s^4}}{4!}\,\overline{y^{[4]}(M^{1/2}n)} + \ldots$$

$$\ldots + \frac{\overline{M^n s^{2n}}}{(2n)!}\,\overline{y^{[2n]}(M^{1/2}n)} + \ldots \tag{89}$$

Only even order terms appear in Eqs. (88) and (89) since the average of odd order derivatives of even functions yield zero.

The normalized signal output is

$$(\Delta\bar{y})' = \frac{\bar{y}_0 - \bar{y}_L}{\bar{y}_L} = \frac{\displaystyle\sum_{k=1}^{\infty} \frac{M^{2k} - M^k}{(2k)!}\, s^k\, \overline{y^{[2k]}(M^{1/2}n)}}{\displaystyle\sum_{k=0}^{\infty} \frac{M^k}{(2k)!}\, s^k\, \overline{y^{[2k]}(M^{1/2}n)}} \tag{90}$$

A4-29

For the square law detector,

$$(\Delta y)'_A = \frac{(M^2 - M)S}{M(S + N)} = (M - 1)\frac{S}{S + N} \tag{91}$$

Thus the signal performance index is

$$R_1 = \frac{(\Delta y)'_T}{(\Delta y)'_A} = \frac{N + S}{S} \frac{\displaystyle\sum_{k=1}^{\infty} \frac{M^{2k-1} + M^{2k-2} + \ldots + M^k}{(2k)!} S^k \overline{y^{[2k]}(M^{1/2}n)}}{\displaystyle\sum_{k=0}^{\infty} \frac{M^k}{(2k)!} S^k \overline{y^{[2k]}(M^{1/2}n)}} \tag{92}$$

From Eq. (26)

$$\overline{y^{[2k]}(M^{1/2}n)} = \left(\frac{1}{MN}\right)^k \overline{H_{2k}\left(\frac{n}{N^{1/2}}\right) y(M^{1/2}n)} \tag{93}$$

With the relation in Eq. (93), Eq. (92) may be put in an alternate form:

$$R_1 = \frac{N + S}{S} \frac{\displaystyle\sum_{k=1}^{\infty} \frac{M^{k-1} + M^{k-2} + \ldots + 1}{(2k)!} \left(\frac{S}{N}\right)^k \overline{H_{2k}\left(\frac{n}{N^{1/2}}\right) y(M^{1/2}n)}}{\displaystyle\sum_{k=0}^{\infty} \frac{1}{(2k)!} \left(\frac{S}{N}\right)^k \overline{H_{2k}\left(\frac{n}{N^{1/2}}\right) y(M^{1/2}n)}} \tag{94}$$

It is evident from an examination of Eq. (94) that only the first term of each series expression is not negligible for small values of $\frac{S}{N}$. For small values of $\frac{S}{N}$ we have

$$R_1 = \frac{1}{2} \frac{\overline{H_2\left(\frac{n}{N^{1/2}}\right) y(M^{1/2}n)}}{\overline{y(M^{1/2}n)}} = \frac{1}{2} \frac{MN \overline{y^{[2]}(M^{1/2}n)}}{\overline{y(M^{1/2}n)}} = \frac{1}{2} \frac{\overline{H_2\left(\frac{x}{\sigma}\right) y(x)}}{\overline{y(x)}} = \frac{1}{2} \frac{\overline{\sigma^2 y^{[2]}(x)}}{\overline{y(x)}}$$

$$\frac{S}{N} << 1$$
$$x = M^{1/2}n$$
$$\sigma^2 = MN \tag{95}$$

A4-30

The expression in Eq. (95) does not yield an optimum detector function $y(x)$. A demonstration of the validity of this statement is found in Section IX, in which R_1 is evaluated for different detector functions.

VIII. Signal-to-Noise Ratio--Linear Processors and Non-Square Law Detector

For the purpose of mathematical simplicity, the signal-to-noise performance index R_2 is determined for small values of $\frac{S}{N}$.

Since $x(t)$ is Gaussian Eq. (26) may be applied to yield an expression for the autocorrelation function of the detector output:

$$R_y(\tau) = \overline{y(x)}^2 + \frac{1}{2!}\sigma^4 \overline{y^{[2]}(x)}^2 \rho^2(\tau) + \frac{1}{4!}\sigma^8 \overline{y^{[4]}(x)}^2 \rho^4(\tau) + \dots$$

$$= \sum_{k=0}^{\infty} \frac{1}{(2k)!} \sigma^{4k} \overline{y^{[2k]}(x)}^2 \rho^{2k}(\tau) \tag{96}$$

The first term of Eq. (96) is simply the square of the average array output, and all other terms represent the autocorrelation of the variational component of $y(t)$. Thus, for low values of $\frac{S}{N}$, $R_y'(\tau)$ becomes

$$R_y'(\tau) = \sum_{k=1}^{\infty} \frac{1}{(2k)!} (MN)^{2k} \overline{y^{[2k]}(M^{1/2}n)}^2 \rho^{2k}(\tau) \tag{97}$$

Also

$$\sigma_Z^2 = \omega_F \sum_{k=1}^{\infty} \frac{1}{(2k)!} (MN)^{2k} \overline{y^{[2k]}(M^{1/2}n)}^2 \int_0^{\infty} \rho^{2k}(\tau)\, d\tau \tag{98}$$

For the square-law detector ($y = x^2$), either Eq. (54), in which $K = 1$, or Eq. (98) gives σ_{ZA}^2:

$$\sigma_{ZA}^2 = 2\,\omega_F\, M^2\, N^2 \int_0^{\infty} \rho^2(\tau)\, d\tau \tag{99}$$

The definition of R_2 in Eq. (55) together with the first two terms in Eqs. (88) and (89) and also Eqs. (35), (36), (57), (98), and (99) yield the expression for R_2.

A4-32

$$R_2 = \left[\sum_{k=1}^{\infty} \frac{2}{(2k)!} \, (MN)^{2k-2} \, \frac{\overline{y^{[2k]}(M^{1/2}n)}^2}{\overline{y^{[2]}(M^{1/2}n)}^2} \, \frac{A_{2k}}{A_2} \right]^{-1/2} \qquad \begin{array}{l} \sigma^2 = MN \\[6pt] x = M^{1/2}n \end{array}$$

$$= \left[1 + \frac{2}{4!} \, \sigma^4 \, \frac{\overline{y^{[4]}(x)}^2}{\overline{y^{[2]}(x)}^2} \, \frac{A_4}{A_2} + \frac{2}{6!} \, \sigma^8 \, \frac{\overline{y^{[6]}(x)}^2}{\overline{y^{[2]}(x)}^2} \, \frac{A_6}{A_2} + \ldots \right]^{-1/2} \tag{100}$$

An alternate form of Eq. (100) is

$$R_2 = \left[1 + \frac{2}{4!} \, \frac{\overline{H_4\!\left(\frac{x}{\sigma}\right) y(x)}^2}{\overline{H_2\!\left(\frac{x}{\sigma}\right) y(x)}^2} \, \frac{A_4}{A_2} + \frac{2}{6!} \, \frac{\overline{H_6\!\left(\frac{x}{\sigma}\right) y(x)}^2}{\overline{H_2\!\left(\frac{x}{\sigma}\right) y(x)}^2} \, \frac{A_6}{A_2} + \ldots \right]^{-1/2} \tag{101}$$

$$\frac{S}{N} << \frac{1}{M}$$

For the function $y = x^2$ it is observed that

$$y^{[2k]}(x) = 0 \quad \text{for} \quad k > 1$$

and thus

$$\overline{y^{[2k]}(x)} = 0 \quad \text{for} \quad k > 1$$

For all other functions

$$y^{[2k]}(x) \neq 0 \quad \text{for some } k \text{ and } x$$

and thus

$$\overline{y^{[2k]}(x)} \neq 0 \quad \text{for some } k$$

Since all terms in Eqs. (100) and (101) are positive, $y(x) = Kx^2$ therefore produces a maximum value for R_2, and the square-law detector is optimum with respect to output signal-to-noise ratio.

In the following section, R_1 and R_2 are evaluated for specific detector functions.

A4-33

IX. Evaluation of R_1 and R_2 for Specific Detector Functions

A wide class of detector functions is described by the general power law relation found in Eq. (102). Note that $y(x)$ is an even function of x.

$$y(x) = K|x|^m \qquad (102)$$

Equation (63) is helpful in evaluating $\overline{y^{[2]}(x)}$ and $\overline{y(x)}$:

$$\overline{y(x)} = 2\int_0^\infty Kx^m \frac{1}{\sqrt{2\pi}}\, \varepsilon^{-\frac{x^2}{2\sigma^2}}\, dx = \sqrt{\frac{2}{\pi}}\; K\; \sigma^m\; 2^{\frac{m-1}{2}} \left(\frac{m-1}{2}\right)! \qquad (103)$$

$$\overline{y^{[2]}(x)} = 2\int_0^\infty K\, m(m-1)\, x^{m-2} \frac{1}{\sqrt{2\pi}}\, \varepsilon^{\frac{-x^2}{2\sigma^2}}\, dx = \sqrt{\frac{2}{\pi}}\; K\; \sigma^{m-2}\; m\; 2^{\frac{m-1}{2}} \left(\frac{m-1}{2}\right)! \qquad (104)$$

From Eq. (95) we obtain $R_1(m)$:

$$R_1(m) = \frac{m}{2} \qquad (105)$$

As can be seen from Eq. (105) the signal performance index increases linearly with m.

The higher order average derivatives are computed below.

$$\overline{y^{(4)}(x)} = 2\int_0^\infty K\, m(m-1)(m-2)(m-3)\, x^{m-4} \frac{1}{\sqrt{2\pi}}\, \varepsilon^{-\frac{x^2}{2\sigma^2}}\, dx$$

$$= \sqrt{\frac{2}{\pi}}\; K\; \sigma^{m-4}\; m(m-2)\; 2^{\frac{m-1}{2}} \left(\frac{m-1}{2}\right)! \qquad (106)$$

$$\overline{y^{(6)}(x)} = \sqrt{\frac{2}{\pi}}\; K\; \sigma^{m-6}\; m(m-2)(m-4)\; 2^{\frac{m-1}{2}} \left(\frac{m-1}{2}\right)! \qquad (107)$$

Also from Eq. (71)

$$\frac{A_{2k}}{A_2} = \frac{1}{k}$$

for the low-pass spectrum, and is less than $\frac{1}{k}$ for other spectra.

The signal-to-noise performance index from Eq. (100) becomes

$$R_2(m) = \left[1 + \frac{2}{4!}\frac{1}{2}(m-2)^2 + \frac{2}{6!}\frac{1}{3}(m-2)^2(m-4)^2\right.$$
$$\left. + \frac{2}{8!}\frac{1}{4}(m-2)^2(m-4)^2(m-6)^2 + \ldots\right]^{-1/2} \tag{108}$$

Equation (108) is evaluated and plotted as a function of m in Fig. 6. The optimum detector function from the standpoint of signal-to-noise ratio is, of course, the square-law device, but the maximum is quite broad, as can be seen in Fig. 6.

Another detector function is described in Eq. (109) and shown in Fig. 7.

$$y = \begin{cases} 0 & -x_1 \le x \le x_1 \\ 1 & \text{elsewhere} \end{cases} \tag{109}$$
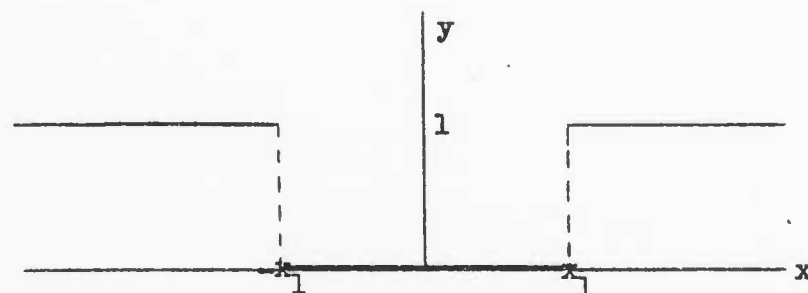

Fig. 7 Detector Function with Dead Band

The following equations yield the results for the averaged function and the averages for the higher order terms found in Eq. (101).

$$\overline{y(x)} = 2\int_{x_1}^{\infty} \frac{1}{\sqrt{2\pi}\,\sigma}\, \varepsilon^{-\frac{x^2}{2\sigma^2}}\, dx = 1 - P\left(\frac{x_1}{\sigma}\right) \tag{110}$$

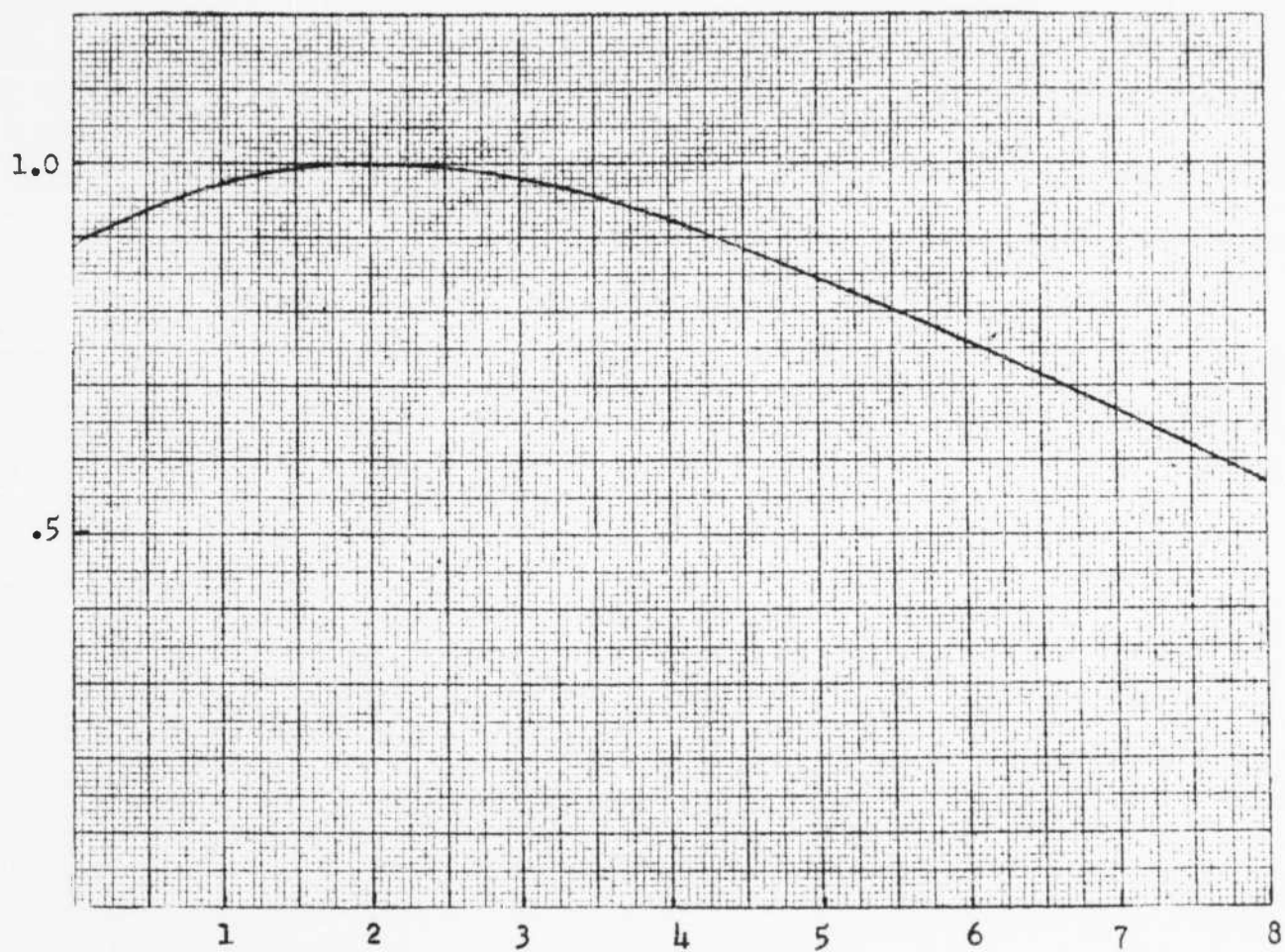where $P\left(\frac{x_1}{\sigma}\right)$ is defined as in Eq. (76). Also,

A4-35

Fig. 6 Signal-to-Noise Index R_2 for Various Power Law Detectors
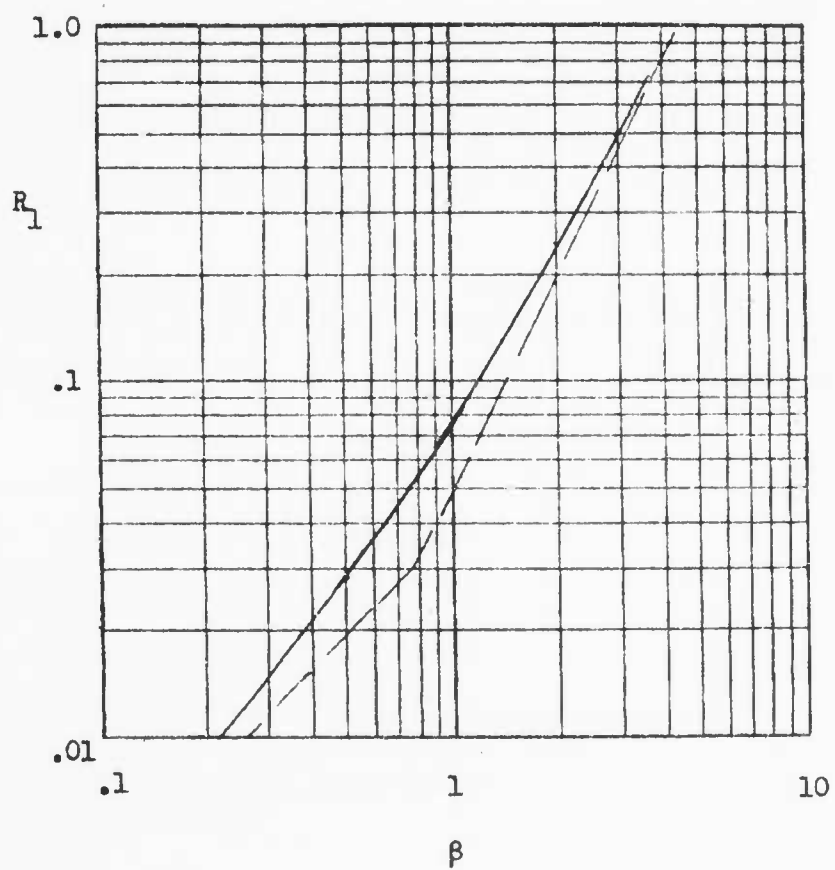
$$y = K|x|^m$$

A4-36

Fig. 8   Signal Performance Index vs. β
for Detector with Dead Band

A4-37

$$\overline{H_{2n}\left(\frac{x}{\sigma}\right) y(x)} = \sqrt{\frac{2}{\pi}} \int_{x_1}^{\infty} H_{2n}\left(\frac{x}{\sigma}\right) \epsilon^{-\frac{x^2}{2\sigma^2}} d\left(\frac{x}{\sigma}\right) = \sqrt{\frac{2}{\pi}} H_{2n-1}\left(\frac{x_1}{\sigma}\right) \epsilon^{-\frac{x_1^2}{2\sigma^2}} \tag{111}$$

If we let $\beta = \frac{x_1}{\sigma}$, the performance index R_1 from Eq. (95) for small $\frac{S}{N}$ becomes

$$R_1 = \frac{1}{\sqrt{2\pi}} \frac{\beta \epsilon^{-\frac{\beta^2}{2}}}{1 - P(\beta)} \cong \begin{cases} \dfrac{1}{\sqrt{2\pi}} \beta & \text{for} \quad \beta << 1 \\[3mm] \dfrac{1}{2} \beta^2 & \text{for} \quad \beta >> 1 \end{cases} \tag{112}$$

The approximation for $\beta >> 1$ is obtained by using the asymptotic expansion for $1 - P(\beta)$ found in Reference 7, p. VIII. Equation (112) is plotted in Fig. 8.

Using the result in Eq. (111) with the general result for R_2 in Eq. (101), we have

$$R_2 = \left[1 + \frac{2}{4!} \frac{1}{2} \frac{H_3^2(\beta)}{\beta^2} + \frac{2}{6!} \frac{1}{3} \frac{H_5^2(\beta)}{\beta^2} + \cdots + \frac{2}{(2n)!} \frac{1}{n} \frac{H_{2n-1}^2(\beta)}{\beta^2} + \cdots \right]^{-1/2} \tag{113}$$

$$\frac{S}{N} << 1$$

Equation (113) has been evaluated with the help of the tables in Reference 8 for six terms of the series. For large values of β the series converges slowly. The results are shown in Fig. 9.

Figures 8 and 9 show that the performance of the detector with dead-band compares favorably with that for the square law device in the region where $1 < \beta < 2$ or $1 < x^2/MN < 4$.
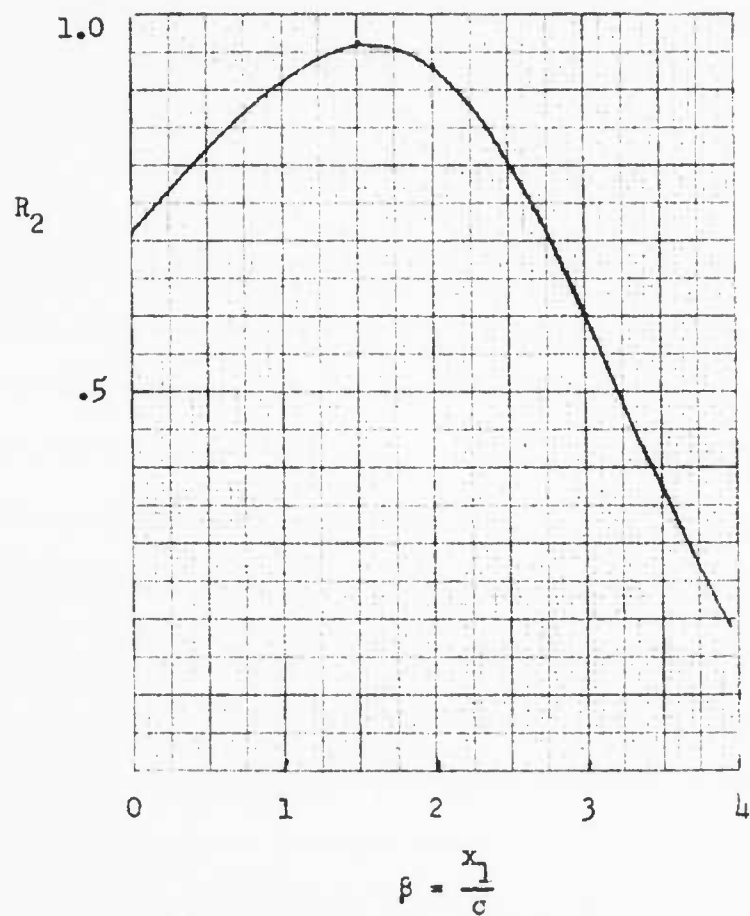
A4-38

Fig. 9 Signal-to-Noise Performance Index vs. β
for Dead Band Detector

A4-39

X. Conclusions

The investigation in Sections IV, V, and VI has shown that the selection of linear processors from a general field of odd-function processors is optimum from the standpoint of both performance indices. It is assumed that a square law detector is used in conjunction with the odd-function processors.

The evaluation of the performance indices in Section VI for specific processors shows, however, that the array performance is not greatly degraded for certain processor functions which deviate significantly from the linear function. For the odd power law device,

$$R_1 \geq .6 \quad \text{and} \quad R_2 \geq .75 \quad \text{for} \quad 0 \leq m \leq 3$$

However, performance was degraded greatly with the infinite clipper with dead band when the rms value of the signal plus noise was equal to or greater than the dead band level of the processor. The examples indicate that significant performance degradation occurs only when the processor has dead space or zero output for a significant range of the input variable.

Thus the use of the infinite clipper $(m = 0)$ as an array processor does not cause significant degradation in performance, particularly in view of the other advantages treated in part in Reference 3.

The investigation in Sections VII, VIII, and IX, which treats an array with linear processors and a general even-function detector, has shown that the square-law detector is optimum from the standpoint of output signal-to-noise ratio. However, other detectors, particularly power law devices with exponents greater than two, yield greater signal detection indices than the square law device. This is a distinct advantage since suppression of the "off-target plateau" in the typical directivity pattern is a desirable result.

As in the investigation with the processors, the optimality of the square law device with respect to the signal-to-noise index is not critical. For example

$$R_2 \geq .75 \quad \text{for} \quad 0 \leq m \leq 6$$

The results for the dead-band detector are interesting in that performance comparable to or somewhat better than that for the square law detector could be obtained if the dead-band level of the detector is adjusted properly. For example

$$R_1 = 2.5 \quad \text{and} \quad R_2 = .93 \quad \text{if} \quad \beta = 2$$

Further work might include investigation of arrays with multipliers as detectors since suppression of the "off-target plateau" in the directivity pattern is certainly desirable for small-signal detection. The inclusion of non-zero correlation between noise inputs for different channels seems necessary, since noise cross-correlation degrades performance in this respect.

A4-41

Appendix A

The terms summed over m in Eq. (22), will be considered a remainder term.

$$F(\Delta) = \sum_{m=1}^{n} \left[\int_C w^{(n-m)} g^{[m-1]}(0) \, \varepsilon^{\frac{\sigma^2 w^2}{2}} \, dw - \int_D w^{(n-m)} g^{[m-1]}(0) \, \varepsilon^{\frac{\sigma^2 w^2}{2}} \, dw \right] \qquad (A-1)$$

For contour C, $w = \Delta + jv$, and for contour D, $w = -\Delta + jv$ where $-\infty < v < \infty$. Rewriting Eq. (A-1) we have

$$F(\Delta) = \sum_{m=1}^{n} g^{[m-1]}(0) \lim_{R \to \infty} \left[\int_{\Delta-jR}^{\Delta+jR} w^{(n-m)} \varepsilon^{\frac{\sigma^2 w^2}{2}} \, dw + \int_{-\Delta+jR}^{-\Delta-jR} w^{(n-m)} \varepsilon^{\frac{\sigma^2 w^2}{2}} \, dw \right] \quad (A-2)$$

Figure A-1 shows a closed rectangular contour defined by Δ and R. The integrals in Eq. (A-2) are taken over the long sides of the rectangle.
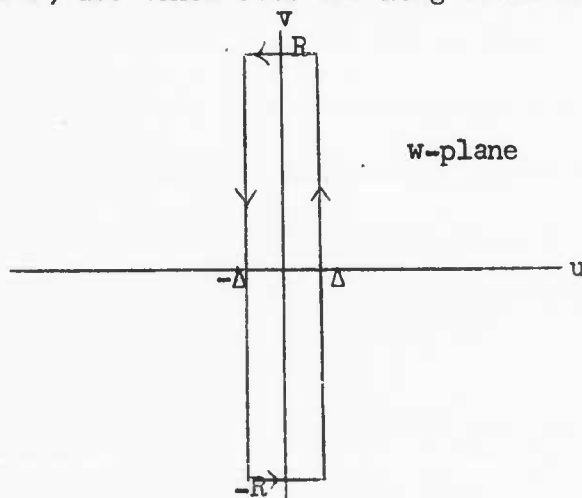

Fig. A-1   Closed Rectangular Contour

Since the integral over the entire closed contour is zero by Cauchy's integral theorem, Eq. (A-2) may be rewritten in terms of the integrals over the short sides of the closed rectangular contour.

A4-42

$$F(\Delta) = \sum_{m=1}^{n} g^{[m-1]}(0) \lim_{R \to \infty} \left[\int_{-\Delta+jR}^{\Delta+jR} w^{(n-m)} \, \varepsilon^{\frac{\sigma^2 w^2}{2}} \, dw + \int_{\Delta-jR}^{-\Delta-jR} w^{(n-m)} \, \varepsilon^{\frac{\sigma^2 w^2}{2}} \, dw \right]$$

$$\cong \sum_{m=1}^{n} g^{[m-1]}(0) \lim_{R \to \infty} \left[\left\{ (jR)^{(n-m)} - (-jR)^{(n-m)} \right\} \varepsilon^{-\frac{\sigma^2 R^2}{2}} (2\Delta) \right] \qquad \text{(A-3)}$$

From the above, $F(\Delta) = 0$, as long as Δ is finite, since

$$\lim_{R \to \infty} R^n \, \varepsilon^{-R^2} = 0$$

A4-43

It is given that

$$\overline{g^{[n]}(e)} \equiv \int_{-\infty}^{\infty} g^{[n]}(e) \; f(e) \; de \tag{B-1}$$

where

$$f(e) = \frac{1}{\sqrt{2\pi} \; \sigma} \; \varepsilon^{-\frac{e^2}{2\sigma^2}} \tag{B-2}$$

Integrating Eq. (B-1) once by parts, we have

$$\overline{g^{[n]}(e)} = g^{[n-1]}(e) \; f(e) \Big|_{-\infty}^{\infty} - \int_{-\infty}^{\infty} g^{[n-1]}(e) \; f^{[1]}(e) \; de$$

$$= 0 - \int_{-\infty}^{\infty} g^{[n-1]}(e) \; f^{[1]}(e) \; de \tag{B-3}$$

In the same fashion, the right hand side of Eq. (B-3) may be integrated by parts another $(n - 1)$ times with the result found in Eq. (B-4).

$$\overline{g^{[n]}(e)} = (-1)^n \int_{-\infty}^{\infty} g(e) \; f^{[n]}(e) \; de \tag{B-4}$$

The product terms of the form $g^{[n-m]}(e) \; f^{[m-1]}(e)$ always disappear because of the exponential nature of $f^{[m-1]}(e)$.

By definition:

$$\frac{d^n}{dx^n}\left\{ e^{-\frac{x^2}{2}} \right\} = (-1)^n \; H_n(x) \; \varepsilon^{-\frac{x^2}{2}} \tag{B-5}$$

where $H_n(x)$ is the Hermite polynomial of order n. Applying the definition in Eq. (B-5) to the probability density function in Eq. (B-2), we have

$$f^{[n]}(e) = (-1)^n \, \sigma^{-n} \, H_n\left(\frac{e}{\sigma}\right) f(e) \qquad (B-6)$$

Combining Eqs. (B-6) and (B-4) we have

$$\overline{g^{[n]}(e)} = \int_{-\infty}^{\infty} g(e) \, \sigma^{-n} \, H_n\left(\frac{e}{\sigma}\right) f(e) \, de$$

$$\overline{g^{[n]}(e)} = \sigma^{-n} \, \overline{H_n\left(\frac{e}{\sigma}\right) g(e)} \qquad (B-7)$$

Given below is a table of the coefficients of the Hermite polynomials up to order 10. Important recursion relations are also given.

10	9	8	7	6	5	4	3	2	1	0	k/n order
										1	0
									1	0	1
								1	0	-1	2
							1	0	-3	0	3
						1	0	-6	0	3	4
					1	0	-10	0	15	0	5
				1	0	-15	0	45	0	-15	6
			1	0	-21	0	105	0	-105	0	7
		1	0	-28	0	210	0	-420	0	105	8
	1	0	-36	0	378	0	-1260	0	945	0	9
1	0	-45	0	630	0	-3150	0	4725	0	-945	10

Table B-1 Coefficients for Hermite Polynomials

$$H_{n+1}(x) = x \, H_n(x) - \frac{dH_n(x)}{dx} \qquad (B-8)$$

$$= x \, H_n(x) - n \, H_{n-1}(x) \qquad (B-9)$$

From Table B-1, for example,

$$H_7(x) = x^7 - 21 \, x^5 + 105 \, x^3 - 105 \, x$$

References

1. Rudnick, P., "Small Signal Detection in the Dimus Array," *J.A.S.A.*, 32, 871, 1960.

2. Faran, J. J., and R. Hills, *The Application of Correlation Techniques to Acoustic Receiving Systems*, Acoustics Research Lab, Tech. Memo. No. 28, Harvard University, Nov. 1, 1952.

3. Usher, T. Jr., *Signal Detection by Arrays in Noise Fields with Local Variations*, Progress Report No. 2, GD/EB Research, Dunham Laboratory, Yale University, March 1963.

4. Davenport, W. B. Jr., and W. L. Root, *An Introduction to the Theory of Random Signals and Noise*, McGraw Hill, 1958.

5. Cramer, H., *Mathematical Methods of Statistics*, Princeton University Press, 1946.

6. Jahnke, E., and F. Emde, *Tables of Functions*, Dover Publications, 1945.

7. *Tables of Normal Probability Functions*, NBS Applied Mathematics Series, 23, 1953.

8. Marcum, J. I., *Tables of Hermite Polynomials and the Derivatives of the Error Function*, Rand Corporation, 1948.

General Dynamics/Electric Boat Research

(53-00-10-0231)

Progress Report No. 5

by

Franz B. Tuteur

Dunham Laboratory
Yale University
New Haven, Connecticut
June 1963

Department of Engineering and Applied Science

Yale University

General Dynamics/Electric Boat Research

(53-00-10-0231)

DETECTION OF WIDE-BAND SIGNALS
MODULATED BY A LOW-FREQUENCY SINUSOID

by

Franz B. Tuteur

June 1963

Summary

The detectability of signals consisting of Gaussian noise modulated by a periodic function of time is considered in this report. It is assumed that the modulation has a precisely known form. Detection is considered in detail for four different examples. These are:

1. The spectrum of both the background noise and the unmodulated signal is white (uniform); the receiving array consists of a single hydrophone.

2. Same as (1) except that the receiving array consists of K hydrophones.

3. The spectrum of the background noise is white, that of the unmodulated signal drops off with the second power of frequency above a certain point. The receiving array consists of K hydrophones.

4. The spectrum of the background noise drops off with the second power of frequency above a certain point, the unmodulated signal spectrum is white, the receiver consists of a single hydrophone.

In all of these cases the improvement in detectability is very modest. In cases 1, 2, and 4 the ratio of detectability index of modulated to unmodulated signal is $1 + \frac{1}{2} b^2$, where b is the modulation index which is less than unity. The results of case 3 are even less favorable. For cases 1 and 2 the structure of the optimum detector has been obtained; it turns out to have essentially the form that is used in practice.

A5-1

I. Introduction

The signals that have been considered in most of the previous studies of underwater detection were assumed to be samples of stationary gaussian noise.[1,2,3,4] However, in practice signals having a certain amount of deterministic structure are occasionally observed. Utilization of this deterministic structure by the detection system should, in general, permit greater detectability. In the present report the type of deterministic structure that is considered is a low-frequency amplitude modulation of the signal power. Such a modulation can be observed quite clearly in the signal produced by a ship with a rotating propeller. The general appearance of such a signal is shown in Fig. 1. The signal appears to be
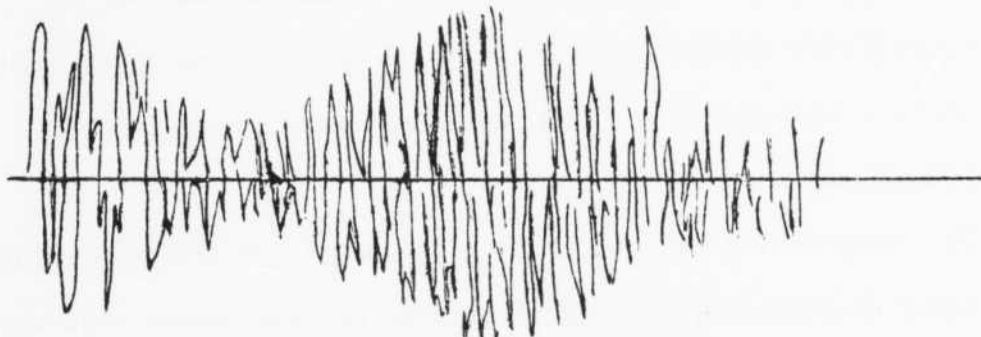

Fig. 1 Amplitude Modulated Noise

a random noise whose power varies at the propeller frequency.

We assume in this analysis that the signal has a gaussian probability distribution with zero mean, and that the variance is a sinusoidal function of time whose amplitude, frequency and phase are known precisely. In practice the modulation is probably not exactly sinusoidal, and even if it were, its amplitude, frequency and phase would be unknown a priori and would have to be estimated from the signal. Thus the situation that-is analyzed is considerably more favorable than the true situation. The analytical results can, however, be considered as providing an upper limit on the attainable detectability - an upper limit which cannot actually be reached in practice.

II. Detection of Gaussian Signals in Gaussian Noise

The problem of detecting gaussian signals in gaussian noise has been studied extensively in the literature.[5,6] The most complete results are probably those of Middleton.[6] Middleton takes the point of view that the received signal is given by

$$x(t) = y(t) + n(t) \tag{1}$$

where $y(t)$ is the signal at the "transmitter" and $n(t)$ is the noise. Although the received signal is usually observed continuously it is convenient to assume that the signal is sampled. In this case Eq. (1) becomes

$$\underline{x} = \underline{y} + \underline{n} \tag{2}$$

where
$$\underline{x} = \begin{bmatrix} x(t_1) \\ x(t_2) \\ \vdots \\ x(t_n) \end{bmatrix}, \qquad \underline{y} = \begin{bmatrix} y(t_1) \\ \\ \vdots \\ y(t_n) \end{bmatrix}, \qquad \underline{n} = \begin{bmatrix} n(t_1) \\ \\ \vdots \\ n(t_n) \end{bmatrix}$$

The samples do not have to be taken at successive time intervals; in fact the idea of signal samples extends directly to the simultaneous observation of several different signals. Thus, if signals received by an array of K hydrophones are to be considered, the signal and noise vectors of Eq. (2) would be of order $n = mxK$, where m is the number of time samples taken on each of the K hydrophones.

In general the samples are not independent. Thus, if $\underline{y}$ is assumed to be a gaussian variable, then the n-fold probability density function of $\underline{y}$ is

$$p(\underline{y}) = \frac{1}{(\sqrt{2\pi})^n |\underline{P}|^{1/2}} e^{-\frac{1}{2} \underline{y}' \underline{P}^{-1} \underline{y}} \qquad (3)$$

where $\underline{P}$ is the covariance matrix of the transmitted signal samples; that is, the ij element of $\underline{P}$ is given by

$$P_{ij} = \overline{y(t_i) \, y(t_j)}$$

$|\underline{P}|$ is the determinant of $\underline{P}$ and $\underline{y}'$ is the transpose of $\underline{y}$. Similarly the n-fold probability density of the noise is given by

$$q(\underline{n}) = \frac{1}{(\sqrt{2\pi})^n |\underline{Q}|^{1/2}} e^{-\frac{1}{2} \underline{n}' \underline{Q}^{-1} \underline{n}} \qquad (4)$$

Hence if signal and noise are independent gaussian processes the probability density function of the received signal $\underline{x}$, given that there is a transmitted signal, is

$$f(\underline{x}/\underline{y}) = \frac{1}{\sqrt{2\pi} \left[\det (\underline{P} + \underline{Q}) \right]^{1/2}} e^{-\frac{1}{2} \underline{x}' (\underline{P}+\underline{Q})^{-1} \underline{x}} \qquad (5)$$

If there is no transmitted signal, the probability density of the received signal is simply that of the noise, i.e.,

$$f(\underline{x}/\underline{0}) = \frac{1}{\sqrt{2\pi} \, (\det \underline{Q})^{1/2}} e^{-\frac{1}{2} \underline{x}' \underline{Q}^{-1} \underline{x}} \qquad (6)$$

Hence the likelihood ratio is

$$\ell(\underline{x}) = \frac{f(\underline{x}/\underline{y})}{f(\underline{x}/\underline{0})} = \left[\frac{\det \underline{Q}}{\det (\underline{P} + \underline{Q})} \right]^{1/2} e^{-\frac{1}{2} \underline{x}' \left[(\underline{P}+\underline{Q})^{-1} - \underline{Q}^{-1} \right] \underline{x}} \qquad (7)$$

In the threshold detection case the signal-to-noise ratio is generally very low, so that the elements of the $\underline{P}$ matrix are all very much smaller than the corresponding elements of the $\underline{Q}$ matrix. In this case Eq. (7) can be simplified as follows:

$$\text{The coefficient} \quad \left[\frac{\det \underline{Q}}{\det (\underline{P} + \underline{Q})} \right]^{1/2} = \left[\frac{1}{\det \left[\underline{I} + \underline{P} \ \underline{Q}^{-1} \right]} \right]^{1/2} \tag{8}$$

It can be shown (Middleton,[6] Chapter 17) that for any arbitrary matrix $\underline{A}$ and arbitrary scalar variable γ

$$\det \left[\underline{I} + \gamma \underline{A} \right] = \exp \sum_{m=1}^{\infty} (-1)^{m+1} \frac{\gamma^m}{m} \ \text{tr} \ \underline{A}^m \tag{9}$$

This expansion is valid so long as for the largest eigenvalue λ_1 of $\underline{A}$ the inequality $\lambda_1 \gamma < 1$ holds. (The "tr" in Eq. (9) means "trace," the sum of the diagonal elements of the matrix.)

Applying Eq. (9) to Eq. (8) we set $\gamma = 1$ and $\underline{A} = \underline{P} \ \underline{Q}^{-1}$. If the signal-to-noise ratio is small all eigenvalues of $\underline{P} \ \underline{Q}^{-1}$ will be less than unity, so that Eq. (9) is valid. Hence the coefficient becomes:

$$\left[\frac{\det \underline{Q}}{\det (\underline{P} + \underline{Q})} \right]^{1/2} = \exp \left\{ -\frac{1}{2} \sum_{m=1}^{\infty} (-1)^{m+1} \frac{\text{tr} \ (\underline{P} \ \underline{Q}^{-1})^m}{m} \right\}$$

$$= e^{-\frac{1}{2} \ \text{tr} \ \underline{P} \ \underline{Q}^{-1} + \frac{1}{4} \ \text{tr}(\underline{P} \ \underline{Q}^{-1})^2 - \dots} \tag{10}$$

The exponent in Eq. (7) may be expanded as follows:

$$-\frac{1}{2}\underline{x}'\left[(\underline{P}+\underline{Q})^{-1}-\underline{Q}^{-1}\right]\underline{x} = -\frac{1}{2}\underline{x}'\underline{Q}^{-1}\left[(\underline{I}+\underline{P}\,\underline{Q}^{-1})^{-1}-\underline{I}\right]\underline{x}$$

$$= -\frac{1}{2}\underline{x}'\underline{Q}^{-1}\left[\underline{I}-\underline{P}\,\underline{Q}^{-1}+(\underline{P}\,\underline{Q}^{-1})^2-\ldots-\underline{I}\right]x$$

$$= \frac{1}{2}\underline{x}'\underline{Q}^{-1}\underline{P}\,\underline{Q}^{-1}x - \frac{1}{2}\underline{x}'\underline{Q}^{-1}\underline{P}\,\underline{Q}^{-1}\underline{P}\,\underline{Q}^{-1}\underline{x} + \ldots \quad (11)$$

For small signal-to-noise ratio the higher-order terms become negligible relative to the first term. However, instead of discarding all the high-order terms completely, it is desirable to retain the second term approximately by replacing it by its average value, where the average is taken for signal absent. Thus

$$\frac{1}{2}\left\langle\underline{x}'\underline{Q}^{-1}\underline{P}\,\underline{Q}^{-1}\underline{P}\,\underline{Q}^{-1}\underline{x}\right\rangle_N = \frac{1}{2}\sum_i\sum_j a_{ij}\left\langle x_i x_j\right\rangle_N = \frac{1}{2}\sum_i\sum_j a_{ij}\,q_{ij}$$

$$= \frac{1}{2}\,\mathrm{tr}\,(\underline{PQ}^{-1})^2 \quad (12)$$

where a_{ij} is the ij element of $\underline{Q}^{-1}\underline{P}\,\underline{Q}^{-1}\underline{P}\,\underline{Q}^{-1}$.

Combining Eqs. (10), (11), and (12) with Eq. (7) yields then the result:

$$\ell(\underline{x}) = \exp\left\{\frac{1}{2}\underline{x}'\underline{Q}^{-1}\underline{P}\,\underline{Q}^{-1}\underline{x} - \frac{1}{2}\,\mathrm{tr}\,\underline{P}\,\underline{Q}^{-1} - \frac{1}{4}\,\mathrm{tr}\,(\underline{P}\,\underline{Q}^{-1})^2 + \ldots\right\} \quad (13)$$

In the standard likelihood-ratio test the likelihood ratio is compared to a threshold K; if the threshold is exceeded it is decided that a signal is present. Hence the conditional false alarm probability α is the probability that $\ell(\underline{x}) > K$ if in fact no signal is present; the conditional miss probability β is the probability that $\ell(\underline{x}) < K$ if a signal is, in fact, present. It is usually more convenient to consider the log $\ell(\underline{x})$; thus:

$$\alpha = \int_{\log K}^{\infty} p_o(u)\, du \quad , \quad \beta = \int_{-\infty}^{\log K} p_1(u)\, du \tag{14}$$

where $u = \log \ell(\underline{x})$, $p_o(u)$ and $p_1(u)$ are the probability densities of the log of the likelihood ratio for signal absent and for signal present, respectively.

For small signal-to-noise ratio, $p_o(u)$ and $p_1(u)$ corresponding to the likelihood ratio of Eq. (13) will be approximately gaussian as a result of the central limit theorem. In this case $p_o(u)$ and $p_1(u)$ are completely determined by the mean and variance of $\log \ell(\underline{x})$. From Eq. (13)

$$\left\langle \log \ell(\underline{x}) \right\rangle_N = \frac{1}{2} \left\langle x'\underline{Q}^{-1}\underline{P}\,\underline{Q}^{-1}x \right\rangle_N - \frac{1}{2}\,\mathrm{tr}\,\underline{P}\,\underline{Q}^{-1} - \frac{1}{4}\,\mathrm{tr}\,(\underline{P}\,\underline{Q}^{-1})^2$$

$$= \frac{1}{2}\,\mathrm{tr}\,\underline{Q}^{-1}\underline{P}\,\underline{Q}^{-1}\underline{Q} - \frac{1}{2}\,\mathrm{tr}\,\underline{P}\,\underline{Q}^{-1} - \frac{1}{4}\,\mathrm{tr}\,(\underline{P}\,\underline{Q}^{-1})^2$$

$$= -\frac{1}{4}\,\mathrm{tr}\,(\underline{P}\,\underline{Q}^{-1})^2 \tag{15}$$

$$\left\langle \left[\log \ell(\underline{x})\right]^2 \right\rangle_N - \left\langle \log \ell(\underline{x}) \right\rangle_N^2 =$$

$$\frac{1}{4} \left\langle (x'\underline{Q}^{-1}\underline{P}\,\underline{Q}^{-1}x')^2 \right\rangle_N - \left[\frac{1}{2}\,\mathrm{tr}\,\underline{P}\,\underline{Q}^{-1} + \frac{1}{4}\,\mathrm{tr}\,(\underline{P}\,\underline{Q}^{-1})^2\right] \left\langle x'\underline{Q}^{-1}\underline{P}\,\underline{Q}^{-1}x \right\rangle_N$$

$$+ \left[\frac{1}{2}\,\mathrm{tr}\,\underline{P}\,\underline{Q}^{-1} + \frac{1}{4}\,\mathrm{tr}\,(\underline{P}\,\underline{Q}^{-1})^2\right]^2 - \left[\frac{1}{4}\,\mathrm{tr}\,(\underline{P}\,\underline{Q}^{-1})^2\right]^2$$

$$= \frac{1}{2}\,\mathrm{tr}\,(\underline{P}\,\underline{Q}^{-1})^2 + \frac{1}{4}\left[\mathrm{tr}\,(\underline{P}\underline{Q}^{-1})\right]^2 - \frac{1}{2}\left[\mathrm{tr}\,(\underline{P}\,\underline{Q}^{-1})\right]^2$$

$$- \frac{1}{4}\,\mathrm{tr}\,(\underline{P}\,\underline{Q}^{-1})\,\mathrm{tr}\,(\underline{P}\,\underline{Q}^{-1})^2 + \left[\frac{1}{2}\,\mathrm{tr}\,\underline{P}\,\underline{Q}^{-1} + \frac{1}{4}\,\mathrm{tr}(\underline{P}\,\underline{Q}^{-1})^2\right]^2$$

$$- \left[\frac{1}{4}\,\mathrm{tr}\,(\underline{P}\,\underline{Q}^{-1})^2\right]^2$$

$$= \frac{1}{2}\,\mathrm{tr}\,(\underline{P}\,\underline{Q}^{-1})^2 \tag{16}$$

Similarly

$$\langle \log \ell(\underline{x}) \rangle_{S+N} = \frac{1}{4} \operatorname{tr} \left(\underline{P}\ \underline{Q}^{-1} \right)^2 \tag{17}$$

$$\left\langle \left[\log \ell(\underline{x}) \right]^2 \right\rangle_{S+N} - \left\langle \log \ell(\underline{x}) \right\rangle_{S+N}^2 = \frac{1}{2} \operatorname{tr} \left(\underline{P}\ \underline{Q}^{-1} \right)^2 \tag{18}$$

Thus $p_o(u)$ and $p_1(u)$ are gaussian distributions having the same variance, and their means are symmetrically located from the origin by a distance $\frac{1}{4} \operatorname{tr} (\underline{P}\ \underline{Q}^{-1})^2$. Substitution into Eq. (14) then yields

$$\begin{matrix} \alpha \\ \\ \beta \end{matrix} = \frac{1}{2} \left[1 - \circledH \left(\frac{1}{4} \sqrt{\operatorname{tr} \left(\underline{P}\ \underline{Q}^{-1} \right)^2} \quad \begin{matrix} + \\ - \end{matrix} \quad \frac{\log K}{\sqrt{\operatorname{tr} \left(\underline{P}\ \underline{Q}^{-1} \right)^2}} \right) \right] \tag{19}$$

where

$$\circledH (x) = \frac{2}{\sqrt{\pi}} \int_0^x e^{-t^2}\, dt$$

It is clear by inspection of this equation (for instance with $K = 1$) that α and β both decrease as $\operatorname{tr} (\underline{P}\ \underline{Q}^{-1})^2$ increases; thus $\operatorname{tr} (\underline{P}\ \underline{Q}^{-1})^2$ can be considered the figure of merit of the detection system.

It is also interesting to note that the "output signal-to-noise ratio" may be defined by

$$\frac{S_o}{N_o} = \frac{\left[\langle \log \ell(\underline{x}) \rangle_{S+N} - \langle \log \ell(\underline{x}) \rangle_N \right]^2}{\left\langle \left[\log \ell(\underline{x}) \right]^2 \right\rangle_N - \left\langle \log \ell(\underline{x}) \right\rangle_N^2} = \frac{1}{2} \operatorname{tr} \left(\underline{P}\ \underline{Q} \right)^2 \tag{20}$$

Thus $\frac{1}{2} \operatorname{tr} (\underline{P}\ \underline{Q}^{-1})^2$ can be identified with a performance index via a suitable definition of signal-to-noise ratio. This index is computed for a number of specific examples in the following section.

III. Detection of Amplitude-Modulated Noise Signals

An amplitude-modulated noise signal of the type pictured in Fig. 1 can be written in the form:

$$y(t) = f(t) \, z(t) \tag{21}$$

where $f(t)$ is a deterministic modulating function and $z(t)$ is a stationary random noise function. Then the general element of the $\underline{P}$ matrix is

$$
\begin{aligned}
P_{ij} &= \left\langle y(t_i) \, y(t_j) \right\rangle \\
&= f(t_i) \, f(t_j) \left\langle z(t_i) \, z(t_j) \right\rangle = f(t_i) \, f(t_j) \, R_z(t_i - t_j)
\end{aligned}
\tag{22}
$$

where $R_z(t_i - t_j)$ is the autocorrelation function of the stationary noise $z(t)$.

Case 1: Single Hydrophone, Uniform Spectra for Signal and Noise

If the noise is white and stationary, the $\underline{Q}$ matrix is a diagonal matrix and can be written in the form

$$\underline{Q} = N \, \underline{I} \tag{23}$$

where $\underline{I}$ is the unit matrix.

Also, if the signal spectrum is uniform, and if one considers only one hydrophone, then

$$R_z(t_i - t_j) = S \, \delta_{ij} \tag{24}$$

where S is the signal power in the unmodulated signal and δ_{ij} is the Kroneker delta; $\delta_{ii} = 1$, $\delta_{ij} = 0$, $i \neq j$. Then the $\underline{P}$ matrix is diagonal, and its general element is

$$P_{ii} = S \, f^2(t_i) \tag{25}$$

A5-9

The matrix $(\underline{P}\ \underline{Q}^{-1})^2$ is then clearly also diagonal, and its general element is

$$\left[(\underline{P}\ \underline{Q}^{-1})^2\right]_{ij} = \frac{S^2}{N^2}\ f^4(t_i) \tag{26}$$

so that

$$\text{tr}\ (\underline{P}\ \underline{Q}^{-1})^2 = \frac{S^2}{N^2}\sum_{i=1}^{n} f^4(t_i) \tag{27}$$

To perform the summation a particular modulating function must be assumed.
In order to provide a fair comparison between detection of modulated and
unmodulated signals, the modulating function should be such that the average
noise power is the same with modulation as without. Hence let

$$f^2(t) = 1 + b\cos\omega t \tag{28}$$

The modulating frequency is assumed to be relatively low so that
$\omega(t_{i+1} - t_i) << 1$. Equation (27) becomes

$$\text{tr}\ (\underline{P}\ \underline{Q}^{-1})^2 = \frac{S^2}{N^2}\sum_{i=1}^{n}(1 + b\cos\omega t_i)^2$$

$$\approx \frac{S^2}{\Delta N^2}\int_0^T (1 + b\cos\omega t)^2\ dt$$

where Δ is the time interval between samples; i.e., $\Delta = t_{i+1} - t_i$.

$$\text{tr}\ (\underline{P}\ \underline{Q}^{-1})^2 \approx \frac{TS^2}{\Delta N^2}\left(1 + \frac{b^2}{2}\right) = n\ \frac{S^2}{N^2}\left(1 + \frac{b^2}{2}\right) \tag{29}$$

if the observation interval $T = n\Delta$ lasts for a large number of cycles of
the modulating function, so that $\omega T >> 1$.

If there were no modulation, $b = 0$. Thus the ratio of detectability index, $\mathrm{tr}(\underline{P}\ \underline{Q}^{-1})^2$, of modulated to unmodulated signal is

$$r = 1 + \frac{b^2}{2} \tag{30}$$

Since b cannot be greater than one, it is seen that the improvement in detectability is rather minor.

This result would appear to violate intuitive concepts, since practical experience with signals of the form shown in Fig. 1 indicates them to be much easier to detect in a noise background than steady noise signals. However, this is true only if the signal-to-noise ratio is quite large. For the threshold situation considered here, where the signal-to-noise ratio is much less than unity, the result given in Eq. (30) will also properly describe the practical detectability.

The Optimum Detector

The optimum detector is a likelihood-ratio detector; i.e., it performs the operations described by Eq. (13). The only term of that equation containing the signal is the first term $\frac{1}{2}\underline{x}'\underline{Q}^{-1}\underline{P}\ \underline{Q}^{-1}\underline{x}$; the other terms are constants. For the white-noise, white-signal-spectrum, single-hydrophone case considered here

$$\frac{1}{2}\underline{x}'\underline{Q}^{-1}\underline{P}\ \underline{Q}^{-1}\underline{x} = \frac{1}{2}\frac{S}{N^2}\sum_{i=1}^{n}(1 + b\cos\omega t_i)\left[x(t_i)\right]^2$$

$$\approx \frac{S}{2N^2\Delta}\int_0^T (1 + b\cos\omega t)\,x^2(t)\,dt \tag{31}$$

Thus the optimum detector squares the signal, multiplies it by the modulating function and then integrates the result. This is shown diagrammatically in Fig. 2.
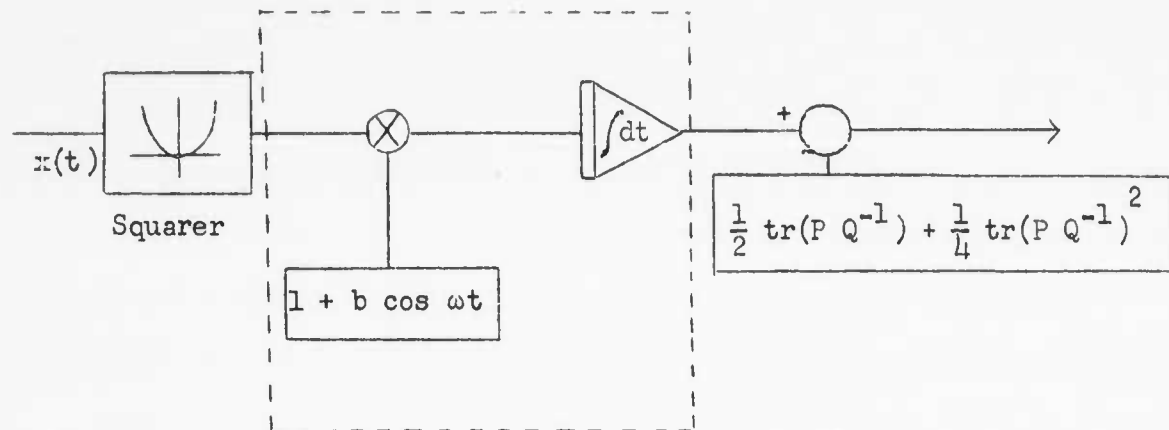
A5-11

Fig. 2 Optimum Detector

The part of the detector shown inside the dashed box can be implemented by a linear filter matched to the modulation envelope.[5] Thus the optimum filter has essentially the form that one would use intuitively on a signal of the form shown in Fig. 1.

Case 2: Uniform Signal and Noise Spectra, Hydrophone Array

Here we assume that there are K hydrophones in a three-dimensional isotropic noise background. For such a background Faran and Hills[7] have shown that the cross-correlation function for noise picked up at elements separated a distance $d = c\tau_s$, where c is the velocity of sound, is

$$R(\tau, \tau_s) = \frac{1}{2\tau_s} \int_{-\tau_s + \tau}^{\tau_s + \tau} R'(\tau') \, d\tau' \qquad (32)$$

where $R'(\tau)$ is the autocorrelation function of the noise at any one hydrophone.

A5-12

For white noise

$$R'(\tau) \approx \frac{N}{2W} \delta(\tau) \tag{33}$$

where N is the noise power and W the band width.

Hence

$$R(\tau,\tau_s) = \frac{N}{4W\tau_s} \int_{-\tau_s+\tau}^{\tau_s+\tau} \delta(\tau') \, d\tau'$$

$$= \begin{cases} \dfrac{N}{4W\tau_s} & \text{for} & -\tau_s < \tau < \tau_s \\[2ex] \dfrac{N}{8W\tau_s} & \text{for} & \tau = \tau_s \quad \text{or} \quad \tau = -\tau_s \\[2ex] 0 & \text{otherwise} \end{cases}$$

$$\tag{34}$$

If white noise of infinite bandwidth but finite power is assumed, $W \to \infty$ so that $R(\tau,\tau_s) = 0$ for all $\tau_s \neq 0$. However

$$R(0,0) = N. \tag{35}$$

Thus $\underline{Q}$ is a diagonal matrix of order $m = K$.

The elements of the $\underline{P}$ matrix are computed under the assumption that the array is steered "on target," since this gives maximum detectability. Under these conditions the general element is

$$P_{ij} = S \, f^2(t_i) \qquad \text{for } |i - j| = m, 2m, 3m \ldots Km$$

$$= 0 \qquad \text{otherwise} \tag{36}$$

where m is the number of observations and K the number of hydrophone elements. Hence the diagonal elements of the matrix $(\underline{P} \, \underline{Q}^{-1})^2$ are

A5-13

$$\left[\left(\underline{P}\ \underline{Q}^{-1}\right)^2 \right]_{ii} = K\ \frac{S^2}{N^2}\ f^4(t_i) \qquad \text{for } 1 \leq i \leq m$$

$$= K\ \frac{S^2}{N^2}\ f^4(t_{i-m}) \qquad \text{for } m+1 \leq i \leq 2m$$

$$= K\ \frac{S^2}{N^2}\ f^4(t_{i-2m}) \qquad \text{for } 2m+1 \leq i \leq 2m$$

$$\vdots$$

$$= K\ \frac{S^2}{N^2}\ f^4(t_{i-(K-1)m}) \qquad \text{for } (K-1)m+1 \leq i \leq Km$$

Therefore

$$\text{tr}\ \left(\underline{P}\ \underline{Q}^{-1}\right)^2 = K^2\ \frac{S^2}{N^2}\ \sum_{i=1}^{m} f^4(t_i) \tag{37}$$

If we again let $f^2(t_i) = 1 + b\cos \omega t_i$ and replace the summation by an integration, we obtain

$$\text{tr}\ \left(\underline{P}\ \underline{Q}^{-1}\right)^2 = K^2\ \frac{S^2}{N^2} \int_0^T (1 + b\cos \omega t)\ dt$$

$$= K^2\ \frac{T}{\Delta}\ \frac{S^2}{N^2} \left(1 + \frac{b^2}{2}\right) = K^2 m\ \frac{S^2}{N^2} \left(1 + \frac{b^2}{2}\right) \tag{38}$$

Thus the ratio of detectability index, $\text{tr}\ \left(\underline{P}\ \underline{Q}^{-1}\right)^2$, of modulated to unmodulated signal is as before

$$r = \left(1 + \frac{b^2}{2}\right) \tag{39}$$

Also it is clear that the optimum detector would consist of a filter of the type shown in Fig. 2 attached to each hydrophone, with the outputs of all the detectors summed to give the total output.

<u>Case 3: Markov-Type Signal Spectrum in White Noise</u>

In this case the power spectrum of the unmodulated signal is

$$G_z(\omega) = \frac{2aS}{a^2 + \omega^2}$$

where S is the signal power. The corresponding autocorrelation function is

$$R_z(\tau) = S\ e^{-a|\tau|} \tag{40}$$

For the moment consider only a single hydrophone. Then, with modulation on the signal the general element of the $\underline{P}$ matrix is given by:

$$P_{ij} = S\ f(t_i)\ f(t_j)\ e^{-a|t_i - t_j|}$$

$$= S\ f(t_i)\ f(t_j)\ \rho^{|i-j|} \tag{41}$$

where $\rho = e^{-a(t_{i+1} - t_i)} = e^{-a\Delta}$ and where Δ is the time interval between samples as before. Also

$$\underline{Q} = N\ \underline{I}$$

as before. Thus the matrix $\underline{P}\ \underline{Q}^{-1}$ is equal to

$$\underline{P}\ \underline{Q}^{-1} = \frac{S}{N} \begin{bmatrix} f_1^2 & \rho f_1 f_2 & \rho^2 f_1 f_3 & \rho^3 f_1 f_4 & \cdots & \rho^{n-1} f_1 f_n \\ \rho f_2 f_1 & f_2^2 & \rho f_2 f_3 & \rho^2 f_2 f_4 & \cdots & \\ \rho^2 f_3 f_1 & \rho f_3 f_2 & f_3^2 & \rho f_3 f_4 & \cdots & \\ \vdots & & & & & \\ \rho^{n-1} f_n f_1 & & \cdots & & & f_n^2 \end{bmatrix}$$

where f_i is shorthand for $f(t_i)$.

Then

$$
(\underline{P}\,\underline{Q}^{-1})^2 = \frac{S^2}{N^2}
\begin{bmatrix}
f_1^2 \displaystyle\sum_{i=1}^{n} f_i^2 \rho^{2(i-1)} & X & X & X \cdots \\[3em]
X & f_2^2 \left[\displaystyle\sum_{i=1}^{2} f_i^2 \rho^{2(2-i)} + \displaystyle\sum_{i=3}^{n} f_i^2 \rho^{2(i-2)} \right] & X & X \cdots \\[3em]
X & X & f_3^3 \left[\displaystyle\sum_{i=1}^{3} f_i^2 \rho^{2(3-i)} + \displaystyle\sum_{i=4}^{n} f_i^2 \rho^{2(i-3)} \right] & \\[3em]
\vdots & & & \circ \\
\vdots & & \circ & \circ
\end{bmatrix}
$$

where only the diagonal terms have been worked out in detail. Thus we obtain

$$
\text{tr}\,(\underline{P}\,\underline{Q}^{-1})^2 = \frac{S^2}{N^2} \sum_{j=1}^{n} \left[f_j^2 \sum_{i=1}^{j} f_i^2\, \rho^{2(j-i)} + f_j^2 \sum_{i=j+1}^{n} f_i^2 \rho^{2(i-j)} \right]
$$

$$
\approx \frac{S^2}{N^2 \Delta^2} \int_0^T f^2(s)\, ds \left[\int_0^s f^2(t)\, \rho^{2(s-t)} dt + \int_s^T f^2(t)\, \rho^{2(t-s)} dt \right]
$$

$$
= \frac{S^2}{N^2 \Delta^2} \int_0^T f^2(s)\, ds \left[\int_0^s f^2(t)\, e^{-2a(s-t)} dt + \int_s^T f^2(t)\, e^{-2a(t-s)} dt \right]
\tag{42}
$$

We again assume that $f^2(t) = 1 + b \cos \omega t$. The integrations involve considerable algebra, but are otherwise straightforward. If all high-frequency terms are ignored – i.e., if we assume as before that $\omega T >> 1$ the result is

$$
\text{tr}\,(\underline{P}\,\underline{Q}^{-1})^2 \approx \frac{S^2 T}{N^2 \Delta^2 a} \left(1 + \frac{2a^2 b^2}{\omega^2 + 4a^2} \right)
\tag{43}
$$

and therefore, the detectability index ratio of modulated to unmodulated signal becomes in this case

$$r = 1 + \frac{2a^2 b^2}{\omega^2 + 4a^2} \tag{44}$$

This result is actually less favorable than the one for a white signal spectrum, which it approaches for $a \to \infty$ or for $\omega \to 0$; in other words, if the modulating frequency is much less than the width of the signal spectrum.

This result extends directly to the multiple array case. As was shown under Case 2, the Q matrix is still diagonal, and if the array is steered on target the P matrix is a K x K array of m x m identical submatrices of the type considered above for one hydrophone. Thus we obtain directly for an array of K elements that

$$\text{tr} \left(\underline{P} \, \underline{Q}^{-1} \right)^2 = K^2 \, \frac{S^2 T}{N^2 \Delta^2 a} \left(1 + \frac{2a^2 b^2}{\omega^2 + 4a^2} \right) \tag{45}$$

The detectability index ratio is then again given by Eq. (44).

Case 4: Uniform Signal Spectrum, Markov-Type Noise Spectrum, Single Hydrophone

This is the only remaining case for which results can be easily obtained. The $\underline{P}$ matrix is diagonal and has the form

$$\underline{P} = S \begin{bmatrix} f_1^2 & & & & \\ & f_2^2 & & & \\ & & \ddots & & \\ & & & f_n^2 \end{bmatrix} \tag{46}$$

The $\underline{Q}$ matrix is

$$\underline{Q} = N \begin{bmatrix} 1 & \rho & \rho^2 & \rho^3 & \rho^4 & \cdots & \rho^{n-1} \\ \rho & 1 & \rho & \rho^2 & \rho^3 & \cdots & \rho^{n-2} \\ \rho^2 & \rho & 1 & \rho & \rho^2 & \cdots & \rho^{n-3} \\ \cdot & & & & & & \\ \cdot & & & & & & \\ \cdot & & & & & & \\ \rho^{n-1} & \rho^{n-2} & & & & \cdots & 1 \end{bmatrix} \qquad (47)$$

where $\rho = e^{-\alpha\Delta}$ as before.

The inversion of the $\underline{Q}$ matrix is fairly easily accomplished; the result is

$$\underline{Q}^{-1} = \frac{1}{N(1-\rho^2)} \begin{bmatrix} 1 & -\rho & & & & \\ -\rho & 1+\rho^2 & -\rho & & & \\ & -\rho & 1+\rho^2 & -\rho & & \\ & & \cdot & \cdot & \cdot & \\ & & & \cdot & \cdot & \cdot & -\rho \\ & & & & -\rho & 1 \end{bmatrix} \qquad (48)$$

Hence

$$\left[PQ^{-1} \right]^2 = \frac{S^2}{N^2(1-\rho^2)^2} \begin{bmatrix} f_1^4 + f_1^2 f_2^2 \rho^2 & & & & \\ & -f_2^2 f_1^2 \rho^2 + f_2^4(1+\rho^2)^2 - f_2^2 f_3^2 \rho^2 & & & \\ & & -f_3^2 f_2^2 \rho^2 + f_3^2(1+\rho^2) - f_3^3 f_4^2 \rho^2 & & \\ & & & \cdot & \\ & & & & \cdot \\ & & & & -f_n^2 f_{n-1}^2 \rho^2 + f_n^2 \end{bmatrix}$$

$$A5-18 \qquad (49)$$

where the off-diagonal terms are not shown. Finally, we obtain

$$tr(\underline{P}\ \underline{Q}^{-1})^2 = \frac{S^2}{N^2(1-\rho^2)^2}\left[f_1^4 + f_n^4 + \sum_{i=2}^{n-1} f_i^4(1+\rho^2)^2 - \rho^2 \sum_{i=1}^{n-1} f_i^2 f_{i+1}^2 \right.$$
$$\left. - \rho^2 \sum_{i=2}^{n} f_i^2 f_{i-1}^2 \right] \qquad (50)$$

This result may be simplified by using

$$f_{i+1}^2 = f_i^2 + \frac{\partial}{\partial t}(f_i^2)\Delta + \frac{1}{2}\frac{\partial^2}{\partial t^2}(f_i^2)\Delta^2 + \cdots$$

$$f_{i-1}^2 = f_i^2 - \frac{\partial}{\partial t}(f_i^2)\Delta + \frac{1}{2}\frac{\partial^2}{\partial t^2}(f_i^2)\Delta^2 - \cdots$$

Then

$$tr(\underline{P}\ \underline{Q}^{-1})^2 = \frac{S^2}{N^2(1-\rho^2)^2}\left[(1+\rho^4)\sum_{i=1}^{n} f_i^4 + \rho^2\Delta^2 \sum_{i=1}^{n} f_i^2 \frac{\partial^2}{\partial t^2}(f_i^2) \right.$$
$$\left. - (f_1^4 + f_n^4)\rho^2(1+\rho^2) + \rho^2\Delta\left[f_n^2 \frac{\partial}{\partial t}(f_n^2) - f_1^2 \frac{\partial}{\partial t}(f_1^2)\right] + \cdots \right]$$
$$(51)$$

For large n, and as Δ becomes very small, the only significant term in this expression is the first summation; thus

$$tr(\underline{P}\ \underline{Q}^{-1})^2 \approx \frac{S^2(1+\rho^4)}{N^2(1-\rho^2)^2}\sum_{i=1}^{n} f_i^4 \qquad (52)$$

A5-19

For $f_i^2 = 1 + b \cos \omega t_i$ this result is identical with that obtained

for case 1, Eq. (27), except for the coefficient multiplying the

summation. Thus for $T = n\Delta$ very large so that $\omega T >> 1$, we find here

that

$$\text{tr } (\underline{P} \; \underline{Q}^{-1})^2 \approx \frac{S^2(1 + \rho^4)}{N^2(1 - \rho^2)^2} \; n \left(1 + \frac{b^2}{2} \right) \tag{53}$$

The ratio of detectability indices of modulated to unmodulated signal is,

as for case 1,

$$r = 1 + \frac{b^2}{2} \tag{54}$$

IV. General Conclusions

The four examples of the effect of modulation on the detectability of

a noise-like signal represent the simplest cases for which results could

easily be obtained. Other examples, such as a Markov signal in a Markov

noise, etc., could also be considered. The computational complexity begins,

however, to grow very rapidly, especially when hydrophone arrays are

considered, and it is unlikely that the results would turn out to be

qualitatively much different from those that have been obtained in the

simpler examples. All these examples show that the improvement in

detectability resulting from modulation of the signal is quite small, with

the maximum increase of detectability index being no more than 50 %. This

value is obtained if the modulation index b is unity and if the modulating

frequency is very much lower than the bandwidth of the signal spectrum.

Also implied in all the computations is that the form of the modulation

envelope be known precisely; this would not normally be true. Thus the

modest improvement in detectability that has been computed is actually a very

optimistic estimate, and the improvement that could be obtained in practice

would be considerably smaller.

If the background noise is white, the results extend directly to multi-element arrays. The case for non-white background noise in a multi-element array has not been completely analyzed, but it is doubtful that it would turn out to be radically different from the cases that have been considered in detail.

Qualitatively, the reason for the poor results that are obtainable is that in spite of the coherent modulation the detection is basically incoherent. This means that the detector is sensitive only to the power in the signal and cannot take into account detailed signal structure. The effect of the amplitude modulation is simply to increase the signal-to-noise ratio above the average at certain times and to decrease it at other times. The detector can take advantage of this by increasing its gain when the signal-to-noise ratio is high, and by decreasing it when it is low. However, even if full advantage is taken of the power fluctuation, the detection cannot actually be as good as that which would be obtainable on an unmodulated signal having a constant signal-to-noise ratio equal to the maximum occurring during the modulation cycle. Thus, since the modulation peak cannot exceed the average value, the maximum improvement in detectability cannot exceed a factor of 2; for sinusoidal modulation it turns out to be a factor of 1.5.

In view of the foregoing discussion it seems clear that major improvements in signal detectability can only be obtained by some form of coherent detection. This would require that the detailed structure of the signal be taken into account. There is some indication that coherent wave patterns resulting from machinery noises, banging of snorkel tubes, etc., might be found at the low end of the signal spectrum. A suggested avenue for further study is, therefore, the investigation of these lower-frequency coherent signals.

List of Symbols

$\underline{A}$ = any matrix

a_{ij} = general matrix element

a = break frequency of first-order Markov spectrum

b = modulation index

c = velocity of sound in water

$f(t_i) = f_i$ = modulating function

$f(\underline{x}/\underline{y})$ = conditional probability density of $\underline{x}$ given $\underline{y}$

$G_z(\omega)$ = power spectrum of unmodulated signal

K = number of hydrophones

K = likelihood-ratio threshold

$\ell(\underline{x})$ = likelihood ratio

m = number of time samples

n = total number of samples

$n(t)$ = noise signal

$\underline{n}$ = noise sample vector

N = noise power

$\underline{P}$ = signal covariance matrix

P_{ij} = general element of $\underline{P}$

$p(\underline{y})$ = probability density of $\underline{y}$

$\underline{Q}$ = noise covariance matrix

$q(\underline{u})$ = noise probability density

$R_z(\tau)$ = autocorrelation function of unmodulated signal

r = ratio of detectability indices

S = signal power

T = length of observation time

W = noise bandwidth

$x(t)$ = received signal

$y(t)$ = transmitted signal

$z(t)$ = unmodulated transmitted signal

$\underline{x}$ = received signal sample vector

$\underline{y}$ = transmitted signal sample vector

Δ = time interval between successive samples

τ_s = time difference between hydrophones

ω = frequency

$\det \underline{A}$ = determinant of $\underline{A}$

$\langle \ \rangle_N$ = conditional averaging operation - noise only present

$\langle \ \rangle_{S+N}$ = conditional averaging operation - signal and noise present

$\mathrm{tr}\ \underline{A}$ = trace of $\underline{A}$ = sum of diagonal elements of $\underline{A}$

$\underline{x}'$ = transpose of $\underline{x}$

List of References

1. Usher, Theron, Jr., "Signal Detection by Arrays in Noise Fields with Local Variations," Progress Report No. 2 of General Dynamics/Electric Boat Research, March 1963.

2. Schultheiss, P. M., "Optimal Detection of Directional Gaussian Signals in an Isotropic Gaussian Noise Field," Progress Report No. 3 of General Dynamics/Electric Boat Research, May 1963.

3. Bryn, Finn, "Optimal Signal Processing of Three-Dimensional Arrays Operating on Gaussian Signals and Noise," <u>Journal of the Acoustical Society of America</u>, vol. 34, No. 3, March 1962.

4. Rudnick, P., "Small Signal Detection in the Dimus Array," <u>J.A.S.A.</u>, 32, 871, (1960).

5. Peterson, W. W. and T. G. Birdsall, "The Theory of Signal Detectibility," Technical Report No. 13, Electronic Defense Group, University of Michigan, 1953.

6. Middleton, D., <u>Introduction to Statistical Communications Theory</u>, McGraw-Hill Book Company, New York, 1960. Chapters 18 to 20.

7. Faran, James J., Jr., and Robert Hills, Jr., "The Application of Correlation Techniques to Acoustic Receiving Systems," Technical Memorandum No. 28, Acoustics Research Laboratory, Division of Applied Science, Harvard University, Cambridge, Mass., Nov. 1, 1952.

General Dynamics/Electric Boat Research

(53.00-10-0231)

Progress Report No. 6

by

Peter M. Schultheiss

Dunham Laboratory

Yale University

New Haven, Connecticut

June 1963

Department of Engineering and Applied Science

Yale University

General Dynamics/Electric Boat Research

(53-00-10-0231)

DEGRADATION OF TARGET DETECTABILITY

DUE TO CLIPPING

by

Peter M. Schultheiss

June 1963

I. Introduction

The object of this investigation is to obtain a realistic estimate of the cost in target detectability of clipping the outputs from an array of hydrophones prior to data processing. The problem is approached by considering the performance of likelihood ratio detectors operating on clipped and on unclipped data. Likelihood ratio detectors are chosen because they are known to be optimal under reasonably general conditions. Data processing is presumably accomplished by digital means so that the hydrophone outputs must be sampled.

Results have been obtained only under the following assumptions:

(1) Signal and noise are both stationary Gaussian processes.

(2) Signal and noise spectra are flat over a frequency band $0 \leq f \leq W$ cps and vanish for $f > W$.

(3) The noise disturbances received at different hydrophones are uncorrelated (hence, because of (1), statistically independent).

(4) The signal to noise ratio at each hydrophone is small.

(5) The array of hydrophones is steered on target.

(6) The sampling period is $\frac{1}{2W}$ seconds for the clipped as well as the unclipped system.

The second of these assumptions is probably the least realistic. It could, in principle, be relaxed, but only at the expense of greatly increased computational complexity. At the present time it does not appear that the additional insight thus gained would justify the effort.

If assumption (2) is satisfied, the disturbance (signal plus noise) received by each hydrophone is completely characterized by a series of samples taken at intervals of $\frac{1}{2W}$ seconds. The continuous signal can be

reconstructed without error from the samples so that use of the samples in place of the continuous signal involves no loss of information. Furthermore, assumption (1) in conjunction with (2) insures that the samples are statistically independent.

If the samples are clipped they remain statistically independent, for functions of independent random variables are independent random variables. It is therefore only necessary to consider the detection problem for a single sample from each hydrophone. Extension to the 2TW samples that will be taken in T seconds is a trivial matter.

In evaluating the results of the present analysis it is necessary to keep in mind that the optimal processor in each case is presented with sampled data. In the unclipped system this represents no loss of information for the reasons indicated above. The clipping operation, on the other hand, changes the original spectrum defined in (2) to one that does not vanish beyond any finite frequency. Sampling at intervals of $\frac{1}{2W}$ seconds (or at any other finite rate) therefore may involve some loss of information. Hence, if one does not regard the sampling at intervals of $\frac{1}{2W}$ seconds as a fixed constraint, the performance of the clipped system might be improved. The price for such improvement is basically the requirement of greater bandwidth (or sampling frequency) in the data processing system.

II.   The Likelihood Ratio Detector

The instantaneous value of the likelihood ratio is the quantity Λ defined by

$$\Lambda = \frac{\left\langle P(V/S) \right\rangle_S}{P(V/0)} \tag{1}$$

A6-2

$P(V/S)$ is the conditional probability that the sample set received by the M hydrophones assumes the value V when the signal component is known to have the value S. V and S are M-dimensional random variables $(V_1, V_2, \ldots V_M)$ and $(S_1, S_2, \ldots S_M)$ respectively. The notation $\langle \ \rangle_S$ indicates an averaging operation with respect to the probability distribution of the signal. $P(V/O)$ is the conditional probability that the received sample set assumes the value V when signal is known to be absent.

The likelihood ratio detector operates by deciding "signal present" if Λ exceeds a certain threshold value and "signal not present" if Λ falls below the threshold. A measure of performance can therefore be obtained by comparing the change in the average value of Λ brought about by the appearance of a signal with the typical fluctuation about the average value. Under assumption (4) the fluctuation is almost entirely due to the noise and one therefore arrives at the following figure of merit.

$$R = \frac{\Delta E(\Lambda)}{D(\Lambda)} \tag{2}$$

$\Delta E(\Lambda)$ is the change in the expectation (mean) of Λ due to the signal and $D(\Lambda)$ is the standard deviation of Λ in the absence of signal.

The quantity R will now be computed for both the clipped and the unclipped instrumentation.

III. Clipped Data

If the hydrophone outputs are clipped and there is no signal, all possible combinations of $(V_1, \ldots V_M)$ have the same probability. Hence

$$P(V/O) = 2^{-M} \tag{3}$$

A6-3

Thus the denominator of $\bigwedge$ is a constant independent of V. Now

$$P(V_1 = \pm 1, V_2 = \pm 1, \ldots V_M = \pm 1) =$$

$$\frac{1}{(2\pi N)^{M/2}} \int_0^\infty dx_1 \cdots \int_0^\infty dx_M \; e^{-\frac{(x_1 \mp s)^2}{2N}} \; e^{-\frac{(x_2 \mp s)^2}{2N}} \cdots e^{-\frac{(x_M \mp s)^2}{2N}} \tag{4}$$

where N is the average noise power at each hydrophone and use has been made of assumption (5), which implies that $S_1 = S_2 = \ldots = S_M = s$. The clipping levels have been written as ± 1, obviously without loss of generality.

Using the Gaussian property of the signal, the numerator of $\bigwedge$ can be written in the following form:

$$\left\langle P(V_1 = \pm 1, V_2 = \pm 1, \ldots V_M = \pm 1) \right\rangle_S =$$

$$\frac{1}{(2\pi N)^{M/2}\sqrt{2\pi S}} \int_0^\infty dx_1 \cdots \int_0^\infty dx_M \int_{-\infty}^\infty ds \; e^{-\frac{s^2}{2S}} \; e^{-\frac{(x_1 \mp s)^2}{2N}} \cdots e^{-\frac{(x_M \mp s)^2}{2N}} \tag{5}$$

S is the average power of the signal whose mean value is taken as zero. The integrations in the various x_i are all identical and can be carried out separately. With the change of variable

$$\frac{(x_1 \mp s)^2}{2N} = y^2 \tag{6}$$

A6-4

one obtains

$$\frac{1}{\sqrt{2\pi N}} \int_0^\infty e^{-\frac{(x_i \mp s)^2}{2N}} dx_i = \frac{1}{\sqrt{\pi}} \int_{\mp\frac{s}{\sqrt{2N}}}^\infty e^{-y^2} dy$$

$$= \frac{1}{2} \pm \frac{1}{\sqrt{\pi}} \int_0^{\frac{s}{\sqrt{2N}}} e^{-y^2} dy$$

$$= \frac{1}{2} \pm \frac{1}{\sqrt{\pi}} \left[\frac{s}{\sqrt{2N}} - \frac{1}{3}\left(\frac{s}{\sqrt{2N}}\right)^3 \cdots \right] \tag{7}$$

Thus Eq. (5) becomes

$$\left\langle P(V_1 = \pm 1, V_2 = \pm 1, \ldots V_M = \pm 1) \right\rangle_S =$$

$$\frac{\pi^{-M/2}}{\sqrt{2\pi S}} \int_{-\infty}^\infty ds \, e^{-\frac{s^2}{2S}} \left[\frac{\sqrt{\pi}}{2} + \frac{s}{\sqrt{2N}} - \frac{1}{3}\left(\frac{s}{\sqrt{2N}}\right)^3 \cdots \right]^K \left[\frac{\sqrt{\pi}}{2} - \frac{s}{\sqrt{2N}} + \frac{1}{3}\left(\frac{s}{\sqrt{2N}}\right)^3 \cdots \right]^{M-K} \tag{8}$$

K is the number of hydrophones having positive outputs. Under the stated assumption it is clearly immaterial which of the hydrophones have positive outputs.

Expanding the two bracketed expressions in the integrand of Eq. (8) according to the Binomial law and retaining only terms up to the power $\left(\frac{s}{\sqrt{2N}}\right)^2$ one obtains[1]

$$\left\langle P(V_1 = \pm 1, V_2 = \pm 1, \ldots V_M = \pm 1) \right\rangle_S =$$

$$\frac{\pi^{-M/2}}{\sqrt{2\pi S}} \int_{-\infty}^\infty ds \, e^{-\frac{s^2}{2S}} \left\{ \left(\frac{\sqrt{\pi}}{2}\right)^M + \left[\frac{K(K-1) + (M-K)(M-K-1)}{2} - K(M-K) \right] \left(\frac{\sqrt{\pi}}{2}\right)^{M-2} \frac{s^2}{2N} \right\}$$

---

[1] Terms in higher powers of $\frac{s}{\sqrt{2N}}$ are ignored because of assumption (4).

$$= 2^{-M}\left\{1 + \frac{4}{\pi}\left[\frac{K(K-1) + (M-K)(M-K-1)}{2} - K(M-K)\right]\frac{S}{2N}\right\} \tag{9}$$

Thus from Eqs. (3) and (9)

$$\bigwedge = 1 + \frac{2}{\pi}\left[\frac{K(K-1) + (M-K)(M-K-1)}{2} - K(M-K)\right]\frac{S}{N} \tag{10}$$

In the absence of signal the probability that K hydrophones have positive outputs is simply $2^{-M}\dfrac{M!}{(M-K)! \, K!}$. In the presence of signal the probability is

$$2^{-M}\frac{M!}{(M-K)! \, K!}\left\{1 + \frac{2}{\pi}\left[\frac{K(K-1) + (M-K)(M-K-1)}{2} - K(M-K)\right]\frac{S}{N}\right\}$$

Hence the quantity $\Delta E(\bigwedge)$ introduced in Eq. (2) is given by

$$\Delta E(\bigwedge) = \sum_{K=0}^{M}{}'\left\{1 + \frac{2}{\pi}\left[\frac{K(K-1) + (M-K)(M-K-1)}{2} - K(M-K)\right]\frac{S}{N}\right\} \times$$

$$2^{-M}\frac{M!}{(M-K)! \, K!}\;\frac{2}{\pi}\left[\frac{K(K-1) + (M-K)(M-K-1)}{2} - K(M-K)\right]\frac{S}{N}$$

$$= 2^{-M}\sum_{K=0}^{M}\frac{M!}{(M-K)! \, K!}\left\{\frac{2}{\pi}\left[\frac{K(K-1) + (M-K)(M-K-1)}{2} - K(M-K)\right]\frac{S}{N}\right.$$

$$\left. + \frac{4}{\pi^2}\left[\frac{K(K-1) + (M-K)(M-K-1)}{2} - K(M-K)\right]^2\left(\frac{S}{N}\right)^2\right\} \tag{11}$$

The K sum can be evaluated without great difficulty if one recognizes [by inspection of the binomial expansion for $(1 + 1)^M$] that

$$\sum_{K=0}^{M}\frac{M!}{(M-K)! \, K!} = 2^M \tag{12}$$

A6-6

Consider first the coefficient of $\frac{S}{N}$ in Eq. (11)

$$2^{-M} \sum_{K=0}^{M} \frac{M!}{(M-K)!\ K!} \left[\frac{K(K-1) + (M-K)(M-K-1)}{2} - K(M-K) \right]$$

$$= \frac{M!\ 2^{-M}}{2} \left[\underbrace{\sum_{K=2}^{M} \frac{1}{(M-K)!\ (K-2)!}}_{①} + \underbrace{\sum_{K=0}^{M-2} \frac{1}{(M-K-2)!\ K!}}_{②} - 2\underbrace{\sum_{K=1}^{M-1} \frac{1}{(M-K-1)!\ (K-1)!}}_{③} \right]$$

$$(13)$$

The three sums will be evaluated separately. In sum ① the change
of variable $K-2 = j$ leads to

$$① = \sum_{j=0}^{M-2} \frac{1}{(M-2-j)!\ j!} = \frac{2^{M-2}}{(M-2)!} \qquad \text{by Eq. (12)} \qquad (14)$$

Again using Eq. (12)

$$② = \sum_{K=0}^{M-2} \frac{1}{(M-2-K)!\ K!} = \frac{2^{M-2}}{(M-2)!} \qquad (15)$$

Finally the change of variable $K-1 = j$ and use of Eq. (12) converts
sum ③ to the form

$$③ = \sum_{j=0}^{M-2} \frac{1}{(M-2-j)!\ j!} = \frac{2^{M-2}}{(M-2)!} \qquad (16)$$

Thus expression (13) vanishes.

A6-7

Next consider the coefficient of $\left(\dfrac{S}{N}\right)^2$ in Eq. (11)

$$2^{-M}\sum_{K=0}^{M}\left[\frac{K(K-1)+(M-K)(M-K-1)}{2}-K(M-K)\right]^2 \frac{M!}{(M-K)!\,K!}$$

$$= 2^{-M}\sum_{K=0}^{M}\frac{1}{4}\left(M^2-4MK+4K^2-M\right)^2 \frac{M!}{(M-K)!\,K!}$$

$$= 2^{-(M+2)}\sum_{K=0}^{M}\left[M(M-1)-4K(M-K)\right]^2 \frac{M!}{(M-K)!\,K!}$$

$$= 2^{-(M+2)}M!\left\{M^2(M-1)^2\underbrace{\sum_{K=0}^{M}\frac{1}{(M-K)!\,K!}}_{④} - 8M(M-1)\underbrace{\sum_{K=1}^{M-1}\frac{1}{(M-K-1)!\,(K-1)!}}_{⑤}\right.$$

$$\left. + 16\underbrace{\sum_{K=1}^{M-1}\frac{K(M-K)}{(M-K-1)!\,(K-1)!}}_{⑥}\right\} \tag{17}$$

Sums ④ and ⑤ can be written down immediately from inspection of Eqs. (12) and (16) respectively:

$$④ = \frac{2^M}{M!} \tag{18}$$

$$⑤ = \frac{2^{M-2}}{(M-2)!} \tag{19}$$

Sum ⑥ requires some further manipulation:

$$⑥ = \sum_{K=1}^{M-1}\frac{[(K-1)+1]\,[(M-K-1)+1]}{(M-K-1)!\,(K-1)!}$$

$$= \sum_{K=2}^{M-2}\frac{1}{(M-K-2)!\,(K-2)!} + (M-1)\sum_{K=1}^{M-1}\frac{1}{(M-K-1)!\,(K-1)!}$$

$$= \sum_{j=0}^{M-4} \frac{1}{(M-4-j)! \; j!} \; + \; (M-1)\sum_{K=1}^{M-1} \frac{1}{(M-K-1)! \; (K-1)!} \tag{20}$$

where $j \equiv K-2$.

Now from Eqs. (12) and (16)

$$\text{(6)} = \frac{2^{M-4}}{(M-4)!} \; + \; \frac{(M-1)\,2^{M-2}}{(M-2)!} \tag{21}$$

Finally, combining Eqs. (17), (18), (19) and (21)

$$2^{-M}\sum_{K=0}^{M} \left[\frac{K(K-1) + (M-K)(M-K-1)}{2} - K(K-1) \right]^2 \frac{M!}{(M-K)! \; K!}$$

$$= \frac{1}{4} M^2(M-1)^2 - \frac{1}{2} M^2(M-1)^2 + \frac{1}{4} M(M-1)(M-2)(M-3) + M(M-1)^2$$

$$= M(M-1)\left[-\frac{1}{4} M(M-1) + \frac{1}{4} (M-2)(M-3) + (M-1) \right]$$

$$= \frac{1}{2} M(M-1) \tag{22}$$

Hence, substituting into Eq. (11):

$$\Delta E(\bigwedge) = \frac{2}{\pi^2} M(M-1) \left(\frac{S}{N} \right)^2 \tag{23}$$

The reader will note that Eq. (23) does not contain terms of the order $\frac{S}{N}$. The question therefore arises whether an error was not introduced when terms of the order $\left(\frac{s}{\sqrt{2N}} \right)^4$ were discarded in Eq. (9), for terms of this form would yield contributions of order $\left(\frac{S}{N} \right)^2$ after integration over the signal distribution. It is a straightforward though tedious matter to demonstrate that the added terms of order $\left(\frac{S}{N} \right)^2$ cancel so that no error arises. The details of this demonstration are carried out in the Appendix.

The next step is the computation of $D(\bigwedge)$

$$D(\bigwedge) = \sqrt{E(\bigwedge^2) - \left[E(\bigwedge)\right]^2} \tag{24}$$

both means being computed in the absence of signal.

From Eq. (10) and the vanishing of (13) it is immediately apparent that

$$E(\bigwedge) = 1 \tag{25}$$

Thus only $E(\bigwedge^2)$ remains to be computed.

$$E(\bigwedge^2) = 2^{-M} \sum_{K=0}^{M} \left\{ 1 + \frac{2}{\pi} \left[\frac{K(K-1) + (M-K)(M-K-1)}{2} - K(M-K) \right] \frac{S}{N} \right\}^2 \frac{M!}{(M-K)! \, K!} \tag{26}$$

By Eq. (12) the term in $\left(\frac{S}{N}\right)^0$ is unity. The term in $\frac{S}{N}$ is identical in form with Eq. (13) and therefore vanishes. The term in $\left(\frac{S}{N}\right)^2$ is identical with the corresponding term in Eq. (11) so that Eq. (26) can be evaluated by inspection of previous results.

$$E(\bigwedge^2) = 1 + \frac{2}{\pi^2} M(M-1) \left(\frac{S}{N}\right)^2 \tag{27}$$

Hence
$$D(\bigwedge) = \frac{\sqrt{2}}{\pi} \sqrt{M(M-1)} \, \frac{S}{N} \tag{28}$$

Again it is necessary to show that no error is introduced by omission of the terms of order $\left(\frac{s}{\sqrt{2N}}\right)^4$ in Eq. (9). This demonstration is carried out in the Appendix.

The figure of merit for a single sample from each of the M hydrophones can now be written down by use of Eqs. (2), (23) and (28):

$$R_{cl} = \frac{\sqrt{2}}{\pi} \sqrt{M(M-1)} \, \frac{S}{N} \tag{29}$$

R_{cl} stands for the single sample figure of merit in the clipped case.

The generalization to the group of 2TWM samples observed in time T follows immediately because of the independence of samples resulting from assumptions (1) and (2). If the figure of merit obtainable by processing clipped samples for T seconds is designated as R_c, one obtains

$$R_c = \sqrt{TW} \ \frac{2}{\pi} \ \sqrt{M(M-1)} \ \frac{S}{N} \tag{30}$$

IV. Unclipped Data

The likelihood ratio detector for operation on unclipped data has been analyzed in Report No. 3. As pointed out previously, no information is lost through sampling under the assumptions of the present analysis. Hence the results of Report No. 3 can be used without modification. Because of assumption (3) the array gain is simply M. Therefore Eq. (30) of Report No. 3 reduces to the simple form

$$\frac{\Delta(DC\ output)}{D(output)} \equiv R_u = \sqrt{\frac{T}{2\pi}} \ \frac{S}{N} \ M \sqrt{\int_0^{2\pi W} d\omega} = \sqrt{TW} \ M \ \frac{S}{N} \tag{31}$$

R_u is the figure of merit for the likelihood ratio detector designed to operate on unclipped data.

By comparing Eqs. (30) and (31), one obtains the desired value for "decrease in detectability" or "cost of clipping"

$$\frac{R_c}{R_u} = \frac{2}{\pi} \ \frac{\sqrt{M(M-1)}}{M} \tag{32}$$

The performance ratio given by Eq. (32) is evidently close to $\frac{2}{\pi}$ for all but very small values of M. The fact that $R_c/R_u = 0$ for M = 1 is due to the definition of "useful output" adopted in the analysis. The quantity

A6-11

$\Delta\ E(\bigwedge)$ is the change in the average value of $\bigwedge$ when a target appears that was not previously present. It is <u>not</u> the difference between the average values of $\bigwedge$ on and off target. Thus a single hydrophone operating on unclipped data is capable of detecting the appearance of a target by noting an increase in received power. A single hydrophone operating on clipped data obviously has no such capability.

V. Conclusion

The figure of approximately $\frac{2}{\pi}$ for the "cost of clipping" defined by Eq. (32) is not unexpected. It was shown in Report No. 3 that the likelihood ratio detector designed for operation on unclipped data is identical in performance with a standard power detector if signal and noise have the properties assumed in the present analysis. It can be shown also (see e.g. Report No. 4) that a standard power detector operating on clipped data derived from an input whose spectral properties satisfy assumption (2) on page 1, has a figure of merit lower than that of a detector operating on unclipped data by a factor of approximately $\frac{2}{\pi}$. What has been demonstrated here is that this degradation must be regarded as an inherent cost of sampling and clipping. No detector operating on clipped samples could exhibit less degradation in performance. On the other hand, a detector operating on a clipped continuous signal (or a signal sampled at a rate above 2W samples per second) might perform somewhat better (see comment in section I). Since any possible improvement is certainly limited to a factor of about $\frac{\pi}{2}$ and the analysis of the continuous case is not simple, no attempt has been made to date to carry it out.

A6-12

Appendix

In Eq. (10) $\bigwedge$ is represented by the first two terms of a power series in $\frac{S'}{N}$. Since $\Delta E(\bigwedge)$ [Eqs. (11), (23)] has a lowest order term proportional to $\left(\frac{S'}{N}\right)^2$ it becomes necessary to investigate whether the omission of terms of order $\left(\frac{S'}{N}\right)^2$ in Eq. (10) causes any error in Eq. (23). Returning to Eq. (8) and carrying terms up to order $\left(\frac{s}{\sqrt{2N}}\right)^4$ one obtains an expression of the form

$$\left\langle P(V_1 = \pm 1, V_2 = \pm 1, \ldots V_M = \pm 1) \right\rangle_S =$$

$$\frac{2^{-M}}{\sqrt{2\pi S'}} \int_{-\infty}^{\infty} ds \; e^{-\frac{s^2}{2S'}} \left[1 + (a_1 s + a_3 s^3) \right]^K \left[1 - (a_1 s + a_3 s^3) \right]^{M-K} \tag{A-1}$$

where a_1, a_3 are numerical constants.

Expanding the bracketed expressions as binomials:

$$\left\langle P(V_1 = \pm 1, V_2 = \pm 1, \ldots V_M = \pm 1) \right\rangle_S =$$

$$\frac{2^{-M}}{\sqrt{2\pi S'}} \int_{-\infty}^{\infty} ds \; e^{-\frac{s^2}{2S'}} \left[1 + K(a_1 s + a_3 s^3) + \frac{K!}{(K-2)! \; 2!} (a_1 s + a_3 s^3)^2 \right.$$

$$\left. + \frac{K!}{(K-3)! \; 3!} (a_1 s + a_3 s^3)^3 + \frac{K!}{(K-4)! \; 4!} (a_1 s + a_3 s^3)^4 \right] \left[1 - (M-K)(a_1 s + a_3 s^3) \right.$$

$$+ \frac{(M-K)!}{(M-K-2)! \; 2!} (a_1 s + a_3 s^3)^2 - \frac{(M-K)!}{(M-K-3)! \; 3!} (a_1 s + a_3 s^3)^3$$

$$\left. + \frac{(M-K)!}{(M-K-4)! \; 4!} (a_1 s + a_3 s^3)^4 \right] \tag{A-2}$$

Only terms of order s^4 in the integrand are of interest for the present purposes. These are

$$\frac{2^{-M}}{\sqrt{2\pi S}} \int_{-\infty}^{\infty} ds \; e^{-\frac{s^2}{2S}} s^4 \left[\frac{(M-K)!}{(M-K-2)!} a_1 a_3 + \frac{(M-K)!}{(M-K-4)! \; 4!} a_1^4 - 2K(M-K) a_1 a_3 \right.$$

$$- \frac{K(M-K)!}{(M-K-3)! \; 3!} a_1^4 + \frac{K! \; (M-K)!}{(K-2)! \; (M-K-2)! \; 4} a_1^4 + \frac{K!}{(K-2)!} a_1 a_3$$

$$\left. - \frac{K! \; (M-K)}{(K-3)! \; 3!} a_1^4 + \frac{K!}{(K-4)! \; 4!} a_1^4 \right]$$

$$= 2^{-M} \cdot 3 \; S^2 \; K! \; (M-K)! \left\{ \left[\frac{1}{(M-K-2)! \; K!} - \frac{2}{(K-1)! \; (M-K-1)!} + \frac{1}{(M-K)! \; (K-2)!} \right] a_1 a_3 \right.$$

$$+ \left[\frac{1}{(M-K-4)! \; K! \; 4!} - \frac{1}{(K-1)! \; (M-K-3)! \; 3!} + \frac{1}{(K-2)! \; (M-K-2)! \; 4} \right.$$

$$\left. \left. - \frac{1}{(M-K-1)! \; (K-3)! \; 3!} + \frac{1}{(K-4)! \; (M-K)! \; 4!} \right] a_1^4 \right\} \tag{A-3}$$

It is apparent from Eq. (11) that the contribution of the above term to $\Delta E(\bigwedge)$ is simply

$$2^{-M} \cdot 3 \; S^2 \; M! \sum_{K=0}^{M} \left\{ \left[\frac{1}{(M-K-2)! \; K!} - \frac{2}{(K-1)! \; (M-K-1)!} + \frac{1}{(M-K)! \; (K-2)!} \right] a_1 a_3 \right.$$

$$+ \left[\frac{1}{(M-K-4)! \; K! \; 4!} - \frac{1}{(K-1)! \; (M-K-3)! \; 3!} + \frac{1}{(K-2)! \; (M-K-2)! \; 4} \right.$$

$$\left. \left. - \frac{1}{(M-K-1)! \; (K-3)! \; 3!} + \frac{1}{(K-4)! \; (M-K)! \; 4!} \right] a_1^4 \right\} \tag{A-4}$$

Where factorials of negative numbers appear in this expression, the term in question is to be interpreted as zero.

It is immediately apparent from Eqs. (13) to (16) that the coefficient of $a_1 a_3$ vanishes. The coefficient of a_1^4 can be rewritten in the form

$$2 \sum_{K=0}^{M-4} \frac{1}{(M-K-4)!\ K!\ 4!} - 2 \sum_{K=0}^{M-4} \frac{1}{(M-K-4)!\ K!\ 3!} + \sum_{K=0}^{M-4} \frac{1}{(M-K-4)!\ K!\ 4}$$

$$- \left(\frac{1}{12} - \frac{1}{3} + \frac{1}{4} \right) \frac{2^{M-4}}{(M-4)!} = 0 \qquad (A-5)$$

Thus $\Delta E(\bigwedge)$ is unchanged by inclusion of the higher order terms. Furthermore, it is clear from Eq. (26) that the additional term of order $\left(\frac{S}{N} \right)^2$ in $E(\bigwedge^2)$ is proportional to Eq. (A-4). Hence there is no change in $E(\bigwedge^2)$.

General Dynamics/Electric Boat Research

(53-00-10-0231)

Progress Report No. 7

by

Richard A. McDonald

Dunham Laboratory

Yale University

New Haven, Connecticut

June 1963

Department of Engineering and Applied Science

Yale University

General Dynamics/Electric Boat Research
(53-00-10-0231)

EVALUATION OF N/S RATIO FOR A CORRELATION DETECTOR

WITH ASSUMED SPECIAL SIGNAL PROPERTIES

by

Richard A. McDonald

June 1963

I. Introduction

An important class of sonar targets has the following two characteristics:

1) The signal emitted by the target contains periodic components in a low frequency band $0 \leq f \leq W_1$. The frequency of these periodic components is not known a priori.

2) The high frequency portion of the signal emitted by the target $(W_1 \leq f \leq W_2)$ has essentially the properties of white Gaussian noise amplitude modulated by the same low frequency periodic component.

Since the ratio of total signal power to total noise power at the receiving array is likely to be low, the question arises whether these special properties of the signal can be used to improve target detectability.

Utilization of the periodic property of the low frequency signal is theoretically attractive but encounters the practical difficulty that self-noise at the receiving array also has periodic components in the same general frequency range. In the absence of a priori knowledge concerning the frequency of the periodic target signal it would be necessary to monitor continuously the periodic components of self noise.

A second possible procedure deals only with the high frequency band $W_1 \leq f \leq W_2$ and attempts to improve detectability by using the fact that the signal is amplitude modulated by the same low frequency periodic component. This possibility was investigated in Progress Report No. 5, which showed that the best possible detector of this type could in general provide only small improvements over a standard power detector.

The present report investigates a scheme that attempts to use the periodic low frequency signal component without requiring knowledge of its frequency or monitoring of the self noise. This is accomplished by demodulating the signal in the high frequency range and employing the detected modulation envelope as a "local oscillator" which can then be cross-correlated with the low frequency component of the signal. The difficulty with this procedure is, of course, that the "local oscillator" signal is extremely noisy.

II. Problem Statement and Assumptions

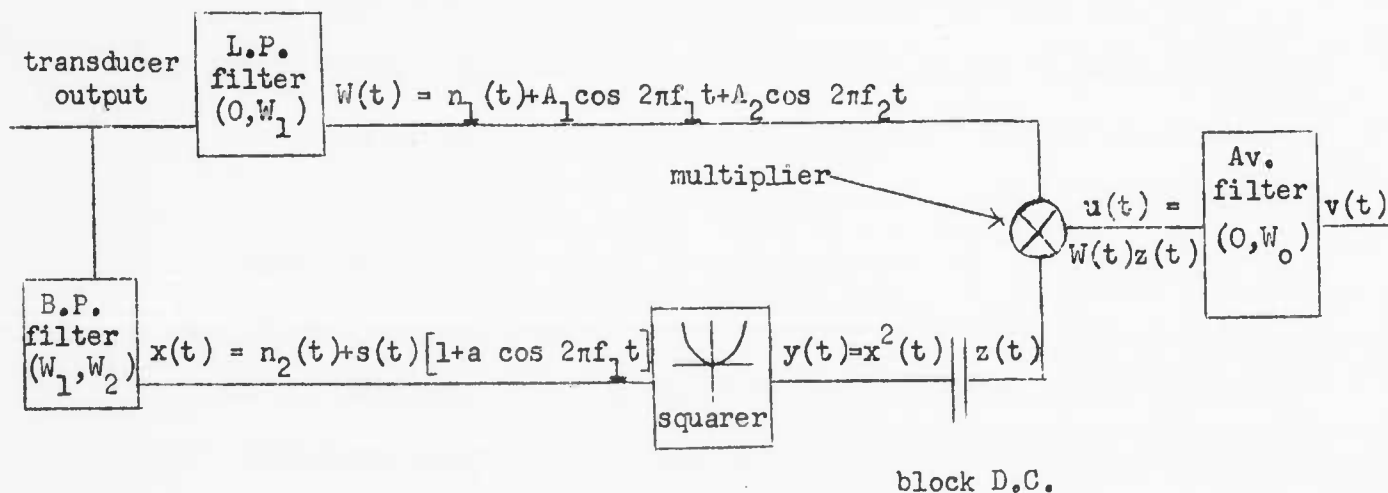A block diagram of the proposed instrumentation is shown in Fig. 1.

Figure 1 Cross-Correlation Detector

The output from the transducer array is split into two parts. The low frequency portion $(0 \leq f \leq W_1)$ is given by

$$W(t) = n_1(t) + A_1 \cos 2\pi f_1 t + A_2 \cos 2\pi f_2 t \qquad (1)$$

$n_1(t)$ has the properties of Gaussian white noise with average power N_1 limited to the band $0 \leq f \leq W_1$. $A_1 \cos 2\pi f_1 t$ is the periodic signal component. $A_2 \cos 2\pi f_2 t$ is a periodic component of self noise.

A7-2

The high frequency portion $(W_1 \leq f \leq W_2)$ of the array output is given by

$$x(t) = n_2(t) + s(t)\left[1 + a \cos 2\pi f_1 t\right] \qquad (2)$$

$n_2(t)$ is the noise component and $s(t)\left[1 + a \cos 2\pi f_1 t\right]$ the signal component. Both $n_2(t)$ and $s(t)$ have the properties of Gaussian white noise bandlimited to $W_1 \leq f \leq W_2$, with average powers N_2 and S respectively. $\underline{a}$ is the modulation index of the sinusoidal amplitude modulation. In most cases of practical interest $a << 1$. The implicit assumption that the modulation envelope and the low frequency sinusoid are in phase is probably not entirely realistic. However, it certainly represents the most favorable situation and will therefore serve the purposes of this study.

The performance of the cross-correlation detector of Fig. 1 will be evaluated by comparison with that of a simple power detector operating on the band $W_1 \leq f \leq W_2$.[1] A block diagram of the latter is shown in Fig. 2.
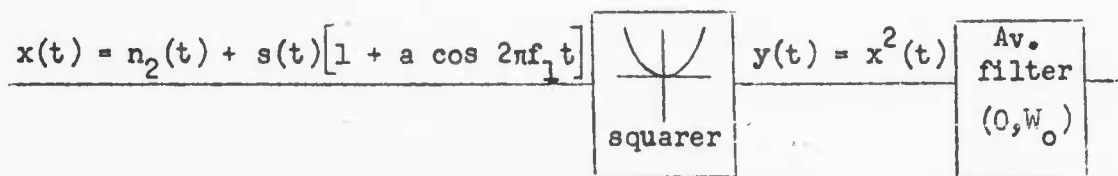

Figure 2   Power Detector

Up to the low pass filter it is clearly identical with the high frequency channel of the cross-correlation detector. The power detector uses the change in average output due to the appearance of a signal for detection purposes. The performance of each instrumentation will be characterized by a noise to signal ratio defined as follows:

$$\frac{N}{S} = \frac{\text{Mean square value of fluctuating component of detector output}}{\text{Square of average signal component of detector output}}$$

$$(3)$$

[1] In practice W_1 would be a relatively low frequency compared to W_2 so that most of the total signal power would be concentrated in the range $W_1 \leq f \leq W_2$.

A7-3

III. Derivation

The mean square fluctuation at the detector output is calculated most readily by integrating the output power spectrum. Since the quantity $y(t)$ is of central importance in each instrumentation, the first task will be the computation of its spectral density $G_y(f)$.[1]

$$y(t) = x^2(t) = \left\{ n_2(t) + s(t)\left[1 + a \cos 2\pi f_1 t\right] \right\}^2$$

$$= n_2^2(t) + 2n_2(t)\, s(t)\left[1 + a \cos 2\pi f_1 t\right] + s^2(t)\left[1 + a \cos 2\pi f_1 t\right]^2 \quad (4)$$

Let

$$n_2'(t) = n_2^2(t) - N_2 \quad (5)$$

$$s'(t) = s^2(t) - S \quad (6)$$

where N_2 and S are average values of $n_2^2(t)$ and $s^2(t)$ respectively. The spectra of $n_2'(t)$ and of $s'(t)$ can then be written down immediately.[2]

$$G_{n_2'}(f) = 2 \int_{-\infty}^{\infty} G_{n_2}(f')\, G_{n_2}(f - f')\, df' \quad (7)$$

$$G_s'(f) = 2 \int_{-\infty}^{\infty} G_s(f')\, G_s(f - f')\, df' \quad (8)$$

Since $n_2(t)$ and $s(t)$ are statistically independent, the spectrum of $n_2(t)s(t)$ can also be written down without difficulty.

$$G_{n_2 s}(f) = \int_{-\infty}^{\infty} G_s(f')\, G_{n_2}(f - f')\, df' \quad (9)$$

---

[1] The notation $G_z(f) \equiv$ spectral density of $z(t)$ will be used throughout. Spectral densities are defined in such a manner that

$$\int_{-\infty}^{\infty} G_z(f)\, df = E\left[z^2\right].$$

[2] W. B. Davenport and W. L. Root, <u>Random Signals and Noise</u>, section 12.2. McGraw-Hill Book Co., 1958.

Before proceeding further it is convenient to rearrange Eq. (4) as follows:

$$y(t) = \underbrace{N_2 + S\left(1 + \frac{a^2}{2}\right)}_{y_1} + \underbrace{n_2{'}(t) + 2n_2(t)\,s(t) + s{'}(t)\left[1 + \frac{a^2}{2}\right]}_{y_2}$$

$$+ \underbrace{2a\left[n_2(t)\,s(t) + s{'}(t)\right]\cos 2\pi f_1 t}_{y_3} + \underbrace{\frac{a^2}{2}\,s{'}(t)\cos 4\pi f_1 t}_{y_4}$$

$$+ \underbrace{2a\,S\cos 2\pi f_1 t}_{y_5} + \underbrace{\frac{a^2}{2}\,S\cos 4\pi f_1 t}_{y_6} \quad\quad (10)$$

Note that y_2 is the only time-dependent term in Eq. (10) that does not vanish as $a \to 0$. If $a << 1$ y_2 will therefore be the dominant component of fluctuation noise. Its three terms are uncorrelated so that its spectrum can be calculated easily from Eqs. (7), (8) and (9). The result is shown in Fig. 3.
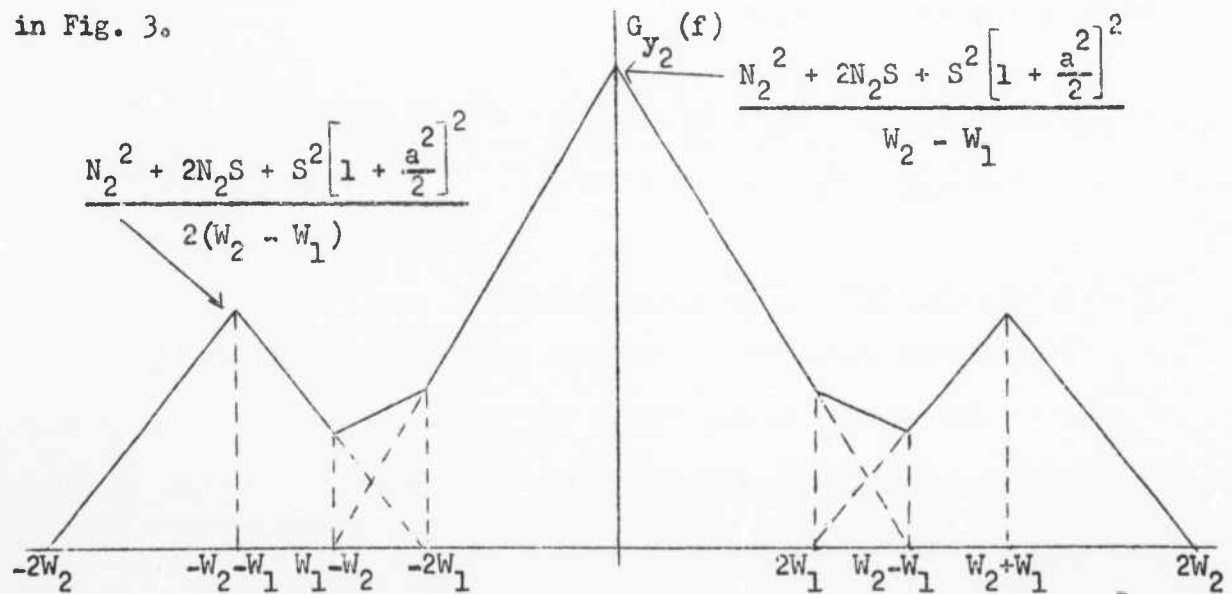

Figure 3 Power Spectral Density for y_2 $\left[\text{see Eq. (10)}\right]$

A7-5

Results for the Power Detector

The change in average output due to signal for the power detector is simply the signal component of y_1. Hence

$$S = S^2 \left(1 + \frac{a^2}{2}\right)^2 \cong S^2 \qquad \text{for} \quad a << 1 \qquad (11)$$

Under the very reasonable assumption $W_o < f_1$ the terms y_5 and y_6 do not appear in the power detector output at all. Furthermore, for $a << 1$ terms y_3 and y_4 are clearly small compared to y_2. In practice the final averaging filter undoubtedly has a bandwidth W_o satisfying $W_o << W_1$. In that case the spectrum of y_2 may be regarded as essentially flat over the band $0 \leq f \leq W_o$ and one obtains

$$N \cong 2 \, G_{y_2}(0) \, W_o \cong 2 \, W_o \, \frac{N_2^2 + 2 \, N_2 S + S^2}{W_2 - W_1} \qquad (12)$$

Equations (11) and (12) immediately yield the desired noise to signal ratio of the power detector

$$\left.\frac{N}{S}\right|_{P.D.} \cong \frac{2W_o}{W_2 - W_1} \, \frac{N_2^2 + 2N_2 S + S^2}{S^2} = \frac{2W_o}{W_2 - W_1} \left(1 + \frac{N_2}{S}\right)^2 \qquad (13)$$

Results for the Cross-Correlation Detector

The blocking capacitor in the high frequency channel of Fig. 1 eliminates the term y_1 in Eq. (10). Its effect on the other components of $y(t)$ will be regarded as negligible. The output $z(t)$ of the blocking capacitor is therefore given by

$$z(t) = y_2(t) + y_3(t) + y_4(t) + y_5(t) + y_6(t) \qquad (14)$$

$z(t)$ is one input into the multiplier. The second input $W(t)$ contains three components. Hence the multiplier output $u(t)$ is

$$u(t) = \sum_{i=1}^{15} u_i(t) \tag{15}$$

where

$$
\begin{array}{lll}
u_1(t) = n_1(t)y_2(t) & u_6(t) = y_2(t)A_1\cos 2\pi f_1 t & u_{11}(t) = y_2(t)A_2\cos 2\pi f_2 t \\
u_2(t) = n_1(t)y_3(t) & u_7(t) = y_3(t)A_1\cos 2\pi f_1 t & u_{12}(t) = y_3(t)A_2\cos 2\pi f_2 t \\
u_3(t) = n_1(t)y_4(t) & u_8(t) = y_4(t)A_1\cos 2\pi f_1 t & u_{13}(t) = y_4(t)A_2\cos 2\pi f_2 t \\
u_4(t) = n_1(t)y_5(t) & u_9(t) = y_5(t)A_1\cos 2\pi f_1 t & u_{14}(t) = y_5(t)A_2\cos 2\pi f_2 t \\
u_5(t) = n_1(t)y_6(t) & u_{10}(t) = y_6(t)A_1\cos 2\pi f_1 t & u_{15}(t) = y_6(t)A_2\cos 2\pi f_2 t
\end{array}
\tag{16}
$$

Inspection of Eqs. (10) and (16) makes it clear that only $u_9(t)$ provides an average component of output. Hence immediately

$$S' = (a\,A_1\,S)^2 \tag{17}$$

The computation of N is simplified by observing that all terms of Eq. (16) except $u_1(t)$, $u_6(t)$ and $u_{11}(t)$ contain factors of $\underline{a}$ or $\underline{a}^2$. Therefore to a first approximation for small $\underline{a}$ only $u_1(t)$, $u_6(t)$ and $u_{11}(t)$ need be considered. As in the case of the power detector, W_o is assumed to be sufficiently small so that only the zero frequency value of $G_u(f)$ is of interest. The two factors of each of the significant $u_1(t)$ are statistically independent so that the corresponding spectra can be written down without difficulty.

$$G_{u_1}(0) = \int_{-W_1}^{W_1} \frac{N_1}{2W_1} G_{y_2}(f)\, df \tag{18}$$

A7-7

or using $G_{y_2}(f)$ as given by Fig. 3

$$G_{u_1}(0) \cong \frac{(N_2 + S)^2}{W_2 - W_1} \frac{N_1}{2} \left(2 - \frac{W_1}{W_2 - W_1}\right) \tag{19}$$

Similarly

$$G_{u_6}(0) = \frac{A_1^2}{4} \left[G_{y_2}(f_1) + G_{y_2}(-f_1)\right] \cong \frac{A_1^2}{2} \left(1 - \frac{f_1}{W_2 - W_1}\right) \frac{(N_2 + S)^2}{W_2 - W_1} \tag{20}$$

and

$$G_{u_{11}}(0) = \frac{A_2^2}{4} \left[G_{y_2}(f_2) + G_{y_2}(-f_2)\right] \cong \frac{A_2^2}{2} \left(1 - \frac{f_2}{W_2 - W_1}\right) \frac{(N_2 + S)^2}{W_2 - W_1} \tag{21}$$

$u_1(t)$, $u_6(t)$ and $u_{11}(t)$ are uncorrelated so that the approximate spectrum of $u(t)$ is simply the sum of the three spectral components. Recalling the previous assumption that $f_1, f_2 < W_1$ and $W_1 << W_2$ one can neglect $\dfrac{W_1}{W_2 - W_1}$, $\dfrac{f_1}{W_2 - W_1}$ and $\dfrac{f_2}{W_2 - W_1}$ compared to unity. Then

$$N \cong 2 W_o \frac{(N_2 + S)^2}{W_2 - W_1} \left(N_1 + \frac{A_1^2}{2} + \frac{A_2^2}{2}\right) \tag{22}$$

Hence the figure of merit for the cross-correlation detector is

$$\left.\frac{N}{S}\right|_{C.D.} \cong \frac{1}{a^2} \frac{2W_o}{W_2 - W_1} \left(1 + \frac{N_2}{S}\right)^2 \left[\frac{1}{2} + \frac{N_1}{A_1^2} + \frac{1}{2}\frac{A_2^2}{A_1^2}\right] \tag{23}$$

IV. Conclusions

The ratio of the two figures of merit $\left[\text{Eqs. (13) and (23)}\right]$ is

$$\left.\frac{N/S}{N/S}\right.\!\!\Big|_{\substack{C.D. \\ P.D.}} = \frac{1}{2a^2} \left[1 + \frac{N_1}{A_1^2/2} + \frac{A_2^2}{A_1^2}\right] \tag{24}$$

A7-8

This ratio can be smaller than unity only if $a > 0.707$ and then only

if the power $\dfrac{A_1^2}{2}$ of the sinusoidal signal component is large compared

to N_1 and to $\dfrac{A_2^2}{2}$. It should be noted that the condition $a > 0.707$

is contrary to the assumption $a < < 1$ repeatedly used in the analysis.

One is therefore forced to the conclusion that the cross-correlation

detector is decidedly inferior to the simple power detector under most

operating conditions of practical interest.

One could, of course, use the cross-correlation detector to

supplement rather than to replace the power detector. However, the

results of the present analysis indicate that the gains to be made by

such a procedure would be slight.

DISTRIBUTION LIST

Armed Services Technical (20)
   Information Agency
Arlington Hall Station
Arlington 12, Virginia

Bureau of Naval Weapons
Navy Department
Washington 25, D. C.
Attn: RUDC-1

Bureau of Ships
Navy Department
Washington 25, D. C.
Attn: Code 525

Bureau of Ships
Navy Department
Washington 25, D. C.
Attn: Code 450

Bureau of Ships
Navy Department
Washington 25, D. C.
Attn: Leroy Roser
      Code 361D

Bureau of Ships
Navy Department
Washington 25, D. C.
Attn: Code 420

Bureau of Ships (3)
Electronics-Electrical Branch
Department of the Navy
Washington 25, D. C.
Attn: N. L. Black
      Code 454E

Bureau of Ships
Navy Department
Washington 25, D. C.
Attn: Code 697

Bureau of Ships
Navy Department
Washington 25, D. C.
Attn: Code 1500

Chief of Naval Operations
Navy Department
Washington 25, D. C.
Attn: OP-311

Chief of Naval Operations
Navy Department
Washington 25, D. C.
Attn: OP-713

Chief of Naval Operations
Navy Department
Washington 25, D. C.
Attn: OP-71

Commandant
Mare Island Naval Shipyard
Vallejo, California
Attn: Design Superintendent

Commandant
Portsmouth Naval Shipyard
Portsmouth, New Hampshire
Attn: Design Superintendent

Commander
Antisubmarine Defense Force
U. S. Pacific Fleet
N. A. S., Navy No. 128
FPO, San Francisco, California

Commander
Submarine Development Group Two
U. S. Naval Submarine Base
Groton, Connecticut

Commander
Submarine Force
U. S. Atlantic Fleet
C/O Fleet Post Office
New York, New York

Commander
Submarine Force
U. S. Pacific Fleet
C/O Fleet Post Office
San Francisco, California

Commanding Officer
U. S. Naval Ordnance Laboratory
White Oak, Silver Spring, Maryland
Attn: Robert Miller

Commanding Officer
Office of Naval Research
Branch Office, Navy 100
C/O Fleet Post Office
New York, New York

Commanding Officer
Submarine School
U. S. Naval Submarine Base
Groton, Connecticut

Commanding Officer
Naval War College
Newport, Rhode Island

Commanding Officer & Director
U. S. Naval Electronics Laboratory
San Diego 52, California
Attn: M. J. Sheehy

Commanding Officer & Director
U. S. Naval Training Device Center
Port Washington, New York
Attn: Technical Library

Director
Aeronautical Instrument Laboratory
Naval Air Development Center
Johnsville, Pennsylvania
Attn: L. S. Guarino

Director
David Taylor Model Basin
Washington 25, D. C.
Attn: Code 533

Director
Naval Research Laboratory
Washington 25, D. C.
Attn: Code 2000

Director
U. S. Navy Underwater Sound
  Laboratory
New London, Connecticut

Director
Special Projects
Department of the Navy
Washington 25, D. C.

Deputy
Comsublant
C/O Fleet Post Office
New York, New York

Naval Air Development Center
ASW Laboratory
Johnsville, Pennsylvania
Attn: ASW System Division

Naval Ordnance Test Station
China Lake, California
Attn: Code 1422

Office of Naval Research   (2)
Navy Department
Washington 25, D. C.
Attn: Code 465
          Cdr. F. R. Haselton, Jr.

Office of Naval Research
Navy Department
Washington 25, D. C.

Office of Naval Research
Navy Department
Washington 25, D. C.
Attn: Code 463

Office, Chief Signal Officer
Department of the Army
Washington 25, D. C.
Attn: Code SIGRD-5
          A. Stombaugh

SACLANT
ASW Research Center
Chief of Naval Operations
(OP 92B3)
Navy Department
Washington 25, D. C.

Technical Library
Room 3E 1065
Pentagon
Washington 25, D. C.

British Joint Naval Staff   (5)
P. O. Box 165
Benjamin Franklin Station
Washington 25, D. C.
via: Director, Naval Research
        Laboratory
     Washington 25, D. C.
     Attn: Code 2000

Canadian Joint Staff   (2)
Washington, D. C.
via: Director, Naval Research
        Laboratory
      Washington 25, D. C.
      Attn: Code 2000

Bell Helicopter Corporation
Highway 183
Fort Worth, Texas
Attn: O. Q. Niehaus

Documentation, Inc.
Man-Machine Information Center
7900 Norfolk Avenue
Bethesda, Maryland
Attn: A. Kreithen

Douglas Aircraft Company, Inc.
Aircraft Division
3855 Lakewood Blvd.
Long Beach 8, California
Attn: Dr. H. L. Wolbers

National Academy of Science
Committee on Undersea Warfare
2101 Constitution Avenue, N. W.
Washington 25, D. C.
Attn: Dr. W. P. Raney
        Executive Secretary

Sperry Gyroscope Company
Surface Armament Division
Great Neck, Long Island, New York
Attn: S. Daunis

Bureau of Naval Weapons
Navy Department
Washington 25, D. C.
Attn: Ree, Dr. A. Miller

Commanding Officer
U. S. Naval Ordnance Test Station
Pasadena, California

Naval Underwater Ordnance Station
Newport, Rhode Island
Attn: John Kelley

University of California
Scripps Institution of Oceanography
La Jolla, California
Attn: Dr. F. N. Spiess
        via - Security Officer

GENERAL DYNAMICS/Electric Boat Division
    Technical Report U417-63-045
Processing of Data from Sonar Systems
Dunham Laboratory, Yale University
September 1, 1963
217 Pages, 27 Illustrations

Work by Dunham Laboratory, Yale University,
is described concerning the detection of a
single target in an isotropic noise field.
In each case studied, the data source was
assumed to be a given array of omnidirec-
tional hydrophones. Problems investigated
involved comparison of optimum detectors
with standard detectors and detectors
operating on clipped and unclipped hydrophone
data.

GENERAL DYNAMICS/Electric Boat Division
    Technical Report U417-63-045
Processing of Data from Sonar Systems
Dunham Laboratory, Yale University
September 1, 1963
217 Pages, 27 Illustrations

Work by Dunham Laboratory, Yale University,
is described concerning the detection of a
single target in an isotropic noise field.
In each case studied, the data source was
assumed to be a given array of omnidirec-
tional hydrophones. Problems investigated
involved comparison of optimum detectors
with standard detectors and detectors
operating on clipped and unclipped hydrophone
data.

GENERAL DYNAMICS/Electric Boat Division
    Technical Report U417-63-045
Processing of Data from Sonar Systems
Dunham Laboratory, Yale University
September 1, 1963
217 Pages, 27 Illustrations

Work by Dunham Laboratory, Yale University,
is described concerning the detection of a
single target in an isotropic noise field.
In each case studied, the data source was
assumed to be a given array of omnidirec-
tional hydrophones. Problems investigated
involved comparison of optimum detectors
with standard detectors and detectors
operating on clipped and unclipped hydrophone
data.

GENERAL DYNAMICS/Electric Boat Division
    Technical Report U417-63-045
Processing of Data from Sonar Systems
Dunham Laboratory, Yale University
September 1, 1963
217 Pages, 27 Illustrations

Work by Dunham Laboratory, Yale University
is described concerning the detection of a
single target in an isotropic noise field.
In each case studied, the data source was
assumed to be a given array of omnidirec-
tional hydrophones. Problems investigated
involved comparison of optimum detectors
with standard detectors and detectors
operating on clipped and unclipped hydrophone
data.